EMBRYONIC DEVELOPMENT OF THE PLATYFISH (*PLATYPOECILUS*), THE SWORDTAIL (*XIPHOPHORUS*), AND THEIR HYBRIDS

WILLIAM N. TAVOLGA

BULLETIN
OF THE
AMERICAN MUSEUM OF NATURAL HISTORY
VOLUME 94 : ARTICLE 4 NEW YORK : 1949

EMBRYONIC DEVELOPMENT OF THE PLATYFISH (*PLATYPOECILUS*), THE SWORDTAIL (*XIPHOPHORUS*), AND THEIR HYBRIDS

EMBRYONIC DEVELOPMENT OF THE PLATYFISH (*PLATYPOECILUS*), THE SWORDTAIL (*XIPHOPHORUS*), AND THEIR HYBRIDS

WILLIAM N. TAVOLGA

The American Museum of Natural History
New York University

A DISSERTATION SUBMITTED TO THE FACULTY OF THE GRADUATE SCHOOL OF ARTS AND SCIENCE OF NEW YORK UNIVERSITY IN PARTIAL FULFILLMENT OF THE REQUIREMENTS FOR THE DEGREE OF DOCTOR OF PHILOSOPHY

BULLETIN
OF THE
AMERICAN MUSEUM OF NATURAL HISTORY
VOLUME 94 : ARTICLE 4 NEW YORK : 1949

BULLETIN OF THE AMERICAN MUSEUM OF NATURAL HISTORY
Volume 94, article 4, pages 161–230, text
figures 1–48, tables 1–7

Issued November 1, 1949

Price: $.85 a copy

CONTENTS

INTRODUCTION

IN A PRELIMINARY PAPER, Tavolga and Rugh (1947) described the normal embryonic stages of *Platypoecilus maculatus* in terms of gross morphology. Based upon the stages previously defined, the present work describes the development of organ systems, pigment differentiation, and embryonic growth.

As described by Gordon (1948 and earlier papers), the related swordtail (*Xiphophorus hellerii*) can be hybridized readily in the laboratory with *P. maculatus*. Peculiar effects of heterosis and gene reassortment are produced, particularly with regard to the development of spontaneous melanomas in the hybrids. Consequently, a comparison is made between *Platypoecilus* development and that of *Xiphophorus* and the *Platypoecilus-Xiphophorus* hybrids, with special emphasis on the effects of hybridization on embryonic growth.

The previous paper (Tavolga and Rugh, 1947) represented the first phase of the problem, i.e., the definition of normal stages. The present work describes the second and third phases, namely, a detailed account of developmental morphology and a comparison of this account with the prenatal development of hybrids possessing potentialities for atypical pigment cell growths.

ACKNOWLEDGMENTS

The writer is indebted to Dr. Charles M. Breder, Jr., Chairman of the Department of Fishes and Aquatic Biology, of the American Museum of Natural History, and of New York University for his encouragement and sponsorship of this work and for his reading and criticism of the paper. Thanks are extended to Dr. Roberts Rugh of the Radiological Laboratory of the College of Physicians and Surgeons and of New York University, and to Dr. Myron Gordon, of New York University and the New York Aquarium, New York Zoological Society, for their comments and criticisms.

The laboratory facilities were made available through the courtesy of Dr. Lester R. Aronson of the Department of Animal Behavior, the American Museum of Natural History. The fishes used here were supplied by Dr. Myron Gordon from the stocks in the Genetics Laboratory of the New York Zoological Society. This laboratory is supported in part by grants from the National Cancer Institute, United States Public Health Service.

MATERIALS AND METHODS

METHOD OF OBTAINING EMBRYOS

Because of the viviparous nature of reproduction in the xiphophorin fishes, it was necessary to dissect the embryonic broods from the ovaries of gravid females. The method of obtaining broods of various ages was that described by Hopper (1943) and Tavolga and Rugh (1947), in which the date of birth of the previous brood was considered as the starting point for the development of the next complement of eggs. The interval between broods in all the species used here averaged 28 to 30 days, and this period is somewhat longer than the actual gestation period, since, as reported by Hopper (1943), fertilization occurs at about seven days after the birth of a brood. By dissecting females at various times during the brood interval, an estimate of the developmental stage of the embryonic brood at a given time could thus be determined.

SPECIES AND STRAINS OF FISH USED

The animals used here were viviparous teleost fishes of the tribe Xiphophorini, family Poeciliidae, Order Cyprinodontes (Order Haplomi according to older classifications). These forms, represented only by the two genera *Platypoecilus* and *Xiphophorus*, are commonly kept in home aquaria and popularly referred to as platyfishes and swordtails, respectively.

Members of this group have frequently been used in the study of genetics, sex determination, and speciation. In two recent papers, Gordon (1947b, 1948) reviewed the work on the Xiphophorini with respect to population genetics and genetic control of tumor formation.

The original stock fishes were collected from several east Mexican rivers, and the localities mentioned below may be found on maps figured by Gordon (1947b).

Platypoecilus maculatus GUNTHER

The majority of the *P. maculatus* used were obtained from an inbred stock originally collected from Plaza de Agua at el Tejar, Rio Jamapa, Mexico, by Gordon and Gordon in 1939, and cultured at the Genetics Laboratory of the New York Zoological Society. The number of wild stock females used was 89, which yielded by inbreeding a total of 2425 embryos.

Several pattern strains were included. Most of the adults possessed one or two of the autosomal allelic series of genes producing the several tail patterns of micromelanophores described by Gordon (1947b). In addition, some of the strains carried sex-linked genes for macromelanophores (Gordon, 1948). The distinction between the two types of melanophores is important, since it is only the macromelanophore type that, by hybridization, can be intensified into a melanotic or melanomatous condition (Gordon, 1927, 1936).

In addition to the above wild stock of *P. maculatus*, 10 females of an inbred domesticated strain of golden platyfish were examined. The golden color is produced by a great reduction in the number of micromelanophores and an apparent increase in the number of xanthophores. This effect is the result of an autosomal recessive gene "*st*," which appeared as a mutant during laboratory culture (Gordon, 1935).

OTHER SPECIES OF *Platypoecilus*

Embryonic broods were obtained from females of the following species, the strains all being of the inbred wild type, originally collected at the localities given:

Platypoecilus variatus Meek (15 females), collected at El Nilo in the Rio Panuco system, Mexico, in 1940, by the New York Aquarium Expedition.

Platypoecilus couchianus Girard (five females), collected at Rio Santa Catarina in the Rio Grande system, Mexico, in 1939, by Gordon and Gordon.

Platypoecilus xiphidium Hubbs and Gordon (five females), collected at Rio Purification in the Rio Soto la Marina system, Mexico, in 1939, by Gordon and Gordon.

The genetic relationships of these species to *P. maculatus* were discussed by Gordon (1946a, 1946b, 1947) and Gordon and Smith (1938b).

Xiphophorus hellerii HAECKEL

Twenty-three females of a ninth generation inbred stock of the wild type of *X. hellerii* were used to obtain embryonic broods. These were descendants of a group originally collected in 1939 by Gordon and Gordon at Arroyo Zacatispan, in the Rio Papaloapan system. Four of these females were mated to litter-mate males.

The remaining 19 females were mated to males of another strain. The latter group of males was the result of a cross between a female of the Zacatispan strain and a male *X. hellerii* from a population at Cordova, on the Rio Blanco, originally collected in 1939 by C. L. Turner.

An additional group of gravid female swordtails was obtained in preserved state from a 1948 collection taken at L'Encero, near Jalapa, in the Rio Jamapa system by M. Gordon, J. W. Atz, and F. G. Wood. Since none of these was available alive, no determinations of gestation period or embryonic age were possible, but some data on the embryos of this strain are included in a later section.

Xiphophorus-Platypoecilus HYBRIDS

The original mating producing all the F_1 hybrid fishes used in this work was that of a *X. hellerii* male (Zacatispan strain) and a *P. maculatus* female (Jamapa strain), both of wild stock, and the latter possessed a gene for macromelanophores on each of its X-chromosomes. The two genes were *Sp* (spots on the sides) and *Sd* (spots on the dorsal fin). Twelve such females were dissected for F_1 embryonic broods. This cross was first described by Gordon in 1948, who gave preliminary results on the sex ratios of the hybrids.

TABLE 1

Strain or Species	Number of Females	Number of Embryos
Pure species		
P. maculatus, wild stock, inbred	89	2425
P. maculatus, golden strain	10	108
P. variatus	15	412
P. couchianus	5	132
P. xiphidium	5	110
X. hellerii, laboratory bred, Zacatispan strain	23	650
X. hellerii, field bred, L'Encero strain	20	370
Platypoecilus-Xiphophorus hybrids		
P. maculatus ♀ × *X. hellerii* ♂ (female with sex chromosomes $X_{Sp}X_{Sd}$)	12	317
F_1 *Sp* ♀ × F_1 *Sp* ♂	10	196
F_1 *Sp* ♀ × F_1 *Sd* ♂	4	82
F_1 *Sp* ♀ × *P. maculatus* ♂	7	132
F_1 *Sp* ♀ × *X. hellerii* ♂	12	225
F_1 *Sd* ♀ × F_1 *Sp* ♂	11	97
F_1 *Sd* ♀ × F_1 *Sd* ♂	6	38
F_1 *Sd* ♀ × *P. maculatus* ♂	8	36
F_1 *Sd* ♀ × *X. hellerii* ♂	9	87
P. maculatus ♀ × F_1 *Sd* ♂	5	177
Total	251	5594

Mature F_1 hybrids possessed one of the two pattern genes (a 1:1 ratio of *Sp* to *Sd*), as a result of Mendelian segregation. Most of these animals were females, and a total of 67 of them were mated in various combinations for the purpose of obtaining embryos.

Table 1 summarizes all the strains and matings used here, the number of females in each case, and the total number of embryos examined.

MAINTENANCE OF FISH

The female fish were isolated in two- or five-gallon aquaria which were maintained at a temperature of 75° to 80° F. in the greenhouse of the Department of Animal Behavior at the American Museum of Natural History. Males were introduced for a long enough period to permit insemination and development and birth of an initial brood, then were removed and re-introduced into tanks with other females. Removal of males after initial insemination did not interrupt the production of future broods, since sperm were stored by the female in sufficient quantities for the fertilization of several successive complements of ova. Thus a small number of active males known to be fertile could be utilized most efficiently.

The fishes were fed daily on a diet of dried, powdered shrimp mash, alternated with living *Daphnia*.

TREATMENT OF EMBRYOS

In general, the entire ovary was removed, since the embryos develop within the ovarian follicles. The follicles were dissected and the embryos removed in a .9 per cent saline solution. The embryos were then examined while living and allocated to the various developmental stages. Most of the embryos were preserved in 10 per cent formalin for future study. A number of embryos of each stage, representing each of the several strains of fishes, were fixed in Bouin's picro-formol and dehydrated in dioxan. Some of the latter group were used for total mounts both in an unstained condition and stained with Harris' haematoxylin. The remainder were sectioned serially at 8 microns and stained with Harris' haematoxylin and eosin or a modification of the Masson trichrome stain. In many cases the embryos were removed from the yolk either before or after fixation and then sectioned after being embedded in paraffin. In order to leave the embryo-yolk relationship undisturbed, it was found necessary to section some of the embryos with the entire yolk attached. A modification of the Peterfi method of double-embedding was used here, in which the celloidin was dissolved in dioxan.

Representative embryos of all stages possessing an actively beating heart were injected with India ink for the study of the circulatory system. Because of the peculiar position of the embryonic heart in these forms, the sinus venosus was exposed and could be penetrated by a capillary pipet. India ink, diluted with saline solution, was then allowed to flow into the vascular system, being pumped through by heart action. This was stopped at the desired point by flooding the embryo with hot Bouin's solution. The injected specimens were cleared and mounted in Clarite.

The reconstruction drawings were made from combined observations on living and preserved specimens, both total mounts and serial cross sections.

EMBRYOLOGY OF *PLATYPOECILUS*

DESCRIPTION OF NORMAL STAGES IN THE EMBRYONIC DEVELOPMENT OF *PLATYPOECILUS*

THE FOLLOWING DESCRIPTIONS of embryological development of *Platypoecilus* were based primarily on the *P. maculatus* material. However, observations on *Platypoecilus variatus*, *P. couchianus*, and *P. xiphidium* are included, since no distinctions could be found in either gross or microscopic morphology in the development of the four species. This was determined on the basis of the somewhat smaller amount of material representing the three latter species (see Materials and Methods section).

The diagnoses of the morphological stages are essentially the same as those described by Tavolga and Rugh (1947) with the addition of observations on internal anatomy and organogenesis. The average dimensions given here are to be considered more accurate since they are based on a much larger sample. Estimated ages given for each stage are based on the determinations described in a later section.

CONDITION OF OVARY AFTER BIRTH OF A BROOD AND PRIOR TO FERTILIZATION

The average size of the ovocytes two to three days after the birth of a brood is 0.7 mm. Some yolk is present in the cytoplasm, and the follicular epithelium is cuboidal and vacuolated. The material in these vacuoles has the same staining properties as the yolk. The vacuoles are frequently seen partially extruded into the follicular cavity and in contact with the egg cytoplasm.

The nuclei are central in position in ovocytes up to 0.9 mm in diameter. Above that size, yolk deposition is completed and the nucleus moves to the periphery, where maturation divisions take place. These observations are in agreement with those of Hopper (1943).

STAGE 1

This stage is to be considered as representing 0 time of embryonic development.

The mature ova, just prior to or during fertilization, average 1.6 mm. in diameter. They are of a clear yellow color with peripherally arranged fat globules of various sizes. When the egg is damaged, the globules are found to remain embedded in a more gelatinous cortical region. The globules are composed of a colorless oil of apparently lower viscosity.

Unfertilized, degenerating eggs are of frequent occurrence, particularly in virgin females, and can be identified easily by the aggregation of oil globules at one pole and the presence of irregular strands of coagulated cytoplasm on and below the egg surface, usually near the polar cap of oil globules. A similar condition characterizes degenerate, early gastrula stages, but these can be distinguished by the presence of coagulated cytoplasm on the egg surface only.

STAGE 2

Age, 0.3 day.

This stage is defined as representing the period of cleavage and early blastula formation. It is not readily distinguishable without sectioning, since the cleavage cells are broad, flat, and extremely thin and transparent. Hopper (1943) showed figures and photographs of sections of cleavage stages, and his observations on these were confirmed in the present work.

STAGE 3

Figure 1A, B

Age, 0.5 day.

The compact blastula is very flat, not more than 30 to 50 microns thick in the center, and averages 0.4 mm. in diameter (fig. 1A). The center is composed of two layers of irregular polyhedral cells 15 to 20 microns in diameter. The cells are smaller and more numerous peripherally, averaging 5 to 10 microns, and are arranged in three or four layers. Around the rim of the blastula there is a narrow zone of junction. A very thin, flat, segmentation cavity can be discerned between the blastula and the yolk surface (fig. 1B).

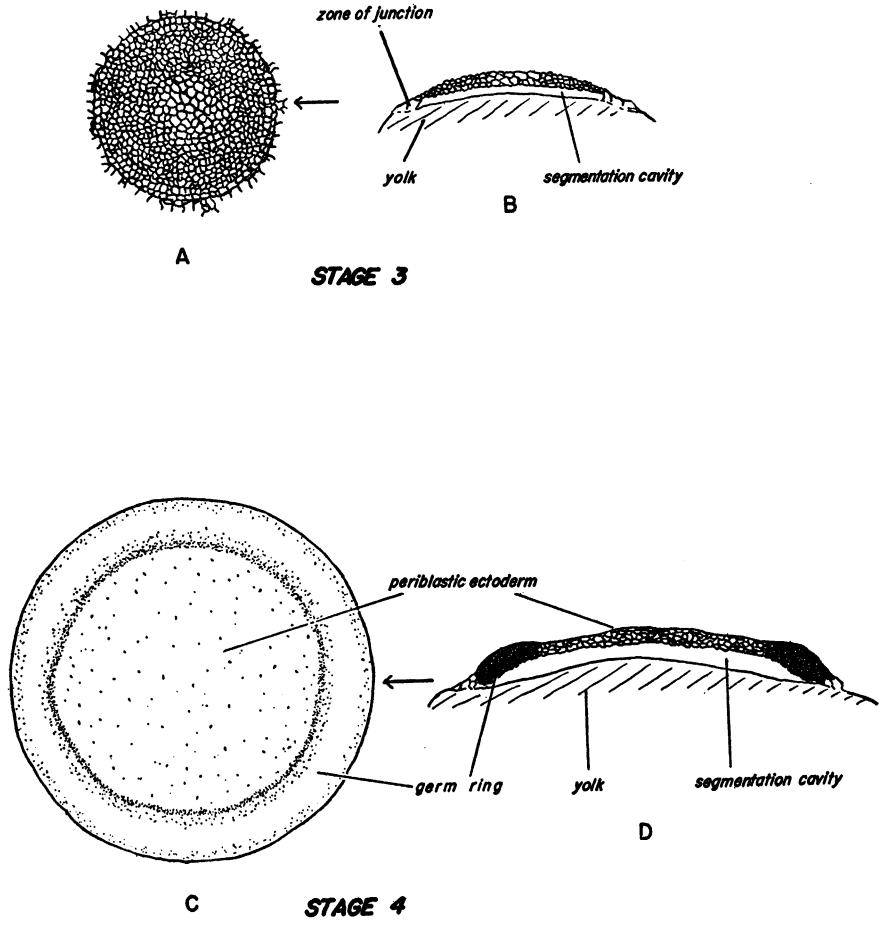

FIG. 1. A. Stage 3, top view. B. Stage 3, cross section at level indicated by arrow. C. Stage 4, top view. D. Stage 4, cross section at level indicated. ×60.

STAGE 4
Figure 1C, D

Age, 0.8 day.

The diameter of this later blastula or germ ring is 0.8 mm. (fig. 1C). The thickness at the center is 30 microns. This region is composed of three to four layers of cells averaging 10 to 15 microns in size. The peripheral germ ring region is 0.06 mm. thick, 0.1 mm. broad, and consists of 10 to 15 layers of very small, rapidly dividing cells (fig. 1D). The thinner central region has few mitotic figures and forms a syncytium. It may therefore be termed the periblastic ectoderm, since there is some doubt as to whether its origin is the same as that of the periblast described by Wilson (1889). The segmentation cavity is still very thin, with the under surface of the blastula often in contact with the underlying yolk (fig. 1D). A narrow and incomplete zone of junction is present.

STAGE 5
Figure 2A, B, C

Age, 0.9 day.

At this stage, the periblastic ectoderm covers approximately one-quarter of the surface of the yolk (fig. 2A). One segment of the germ ring has expanded and thickened to form the embryonic shield (or germinal shield) which will form the embryo proper (fig. 2A). The caudal lip of the germinal shield is thickened and may be considered homologous to the dorsal lip of the blasto-

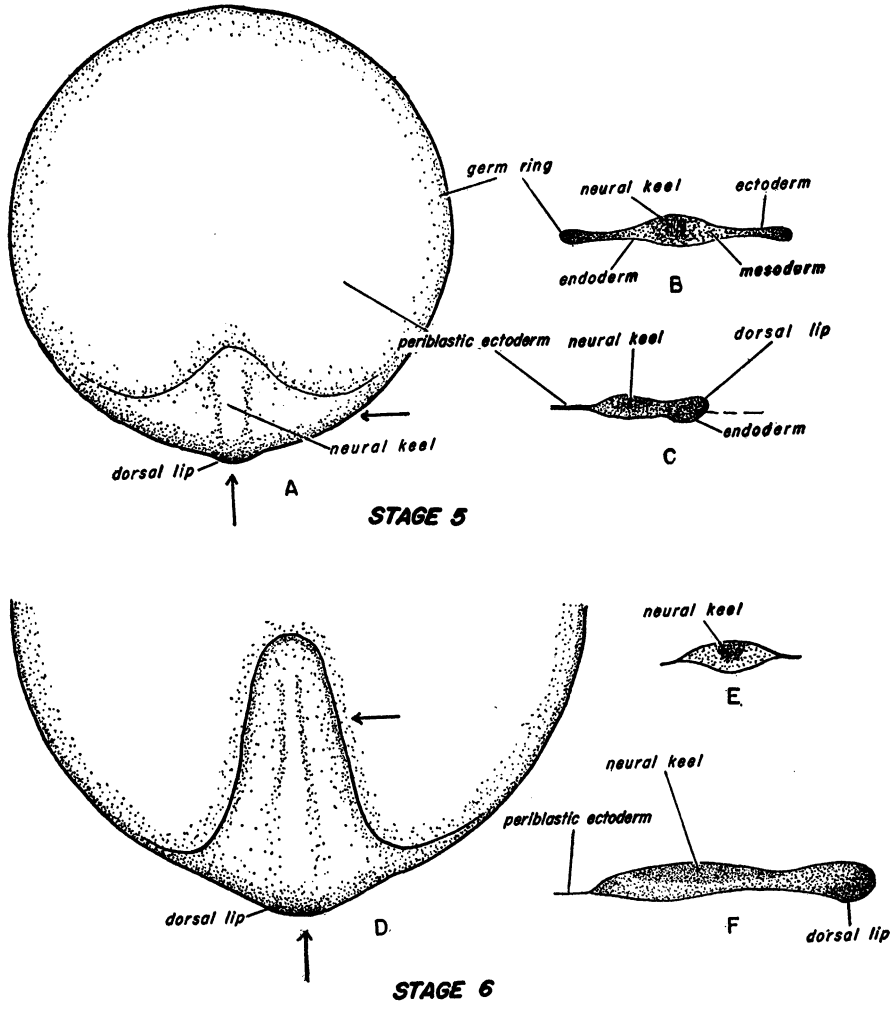

FIG. 2. A. Stage 5, top view. B. Stage 5, cross section at level indicated by arrow. C. Stage 5, sagittal section at level indicated. D. Stage 6, top view of embryonic shield. E. Stage 6, cross section at level indicated. F. Stage 6, sagittal section at level indicated. ×60.

pore in other animals (fig. 2C). The length of the germinal shield is 0.35 mm. It possesses a thickened central region which results from the proliferation and invagination of cells to form the neural keel (fig. 2B).

STAGE 6

Figure 2D, E, F

Age, 1.7 days.

The germ ring has now taken an almost equatorial position on the surface of the yolk, i.e., about one-half of the yolk surface is covered by periblastic ectoderm. The embryonic shield is 0.6 mm. long and 0.25 mm. broad at the middle (fig. 2D). The neural keel is formed in the anterior two-thirds of the shield (fig. 2E, F).

STAGE 7

Figure 3

Age, 1.9 days.

The length of the embryonal area is about 0.82 mm. The entire embryo appears to consist of the neural keel, which is slightly broader at the cephalic end (fig. 3E, F). Serial cross sections show the presence of a second cord of cells extending cephalad

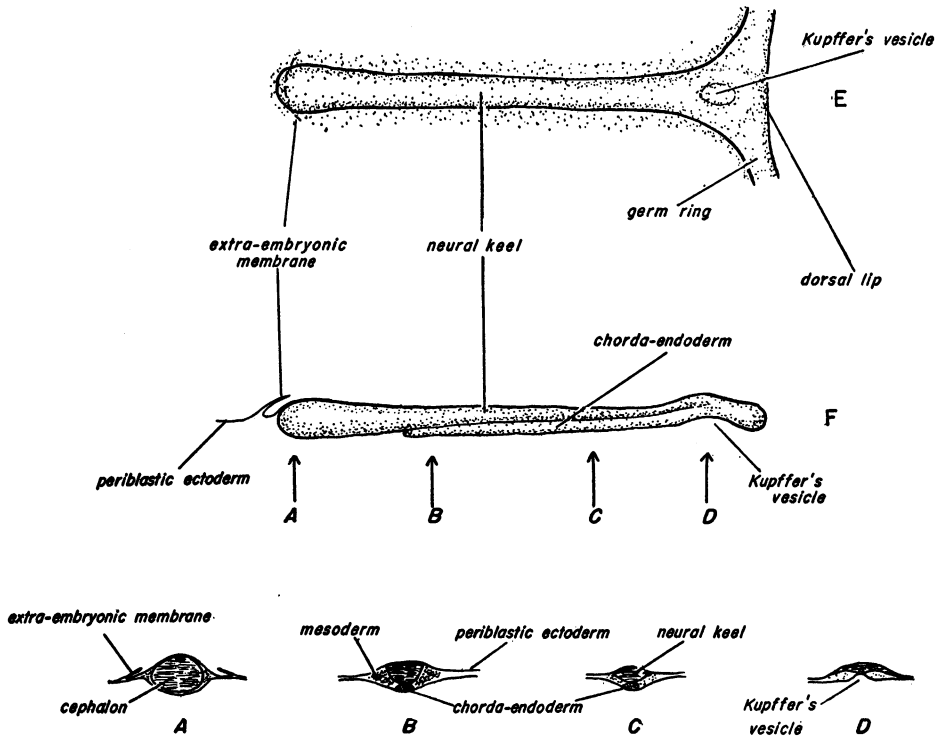

FIG. 3. Stage 7. A–D. Cross sections at levels indicated. E. Dorsal view. F. Lateral view. ×90.

from the region of the dorsal lip of the blastopore about two-thirds the length of the embryo (fig. 3B, C, F). The cord of cells, situated ventral to the neural keel and contiguous with it, is provisionally called the chorda-endoderm (see description of stage 8).

A small cavity is formed on the under surface of the caudal region of the germinal shield and is identified as Kupffer's vesicle (fig. 3D, F). A fold of periblastic ectoderm covers the anterior tip of the cephalon (fig. 3A, E, F). This two-layered fold is the primordium of the extra-embryonic pericardial membranes. In subsequent stages, the fold is invaded by mesenchyme, and forms two double-layered somatopleural membranes, i.e. pericardial amnion and pericardial serosa (described by Tavolga and Rugh, 1947).

STAGE 8

Figure 4

Age, 2.3 days.

The total length of the embryo at this stage averages 1.06 mm.

The nerve cord extends for the entire length except for a short undifferentiated region at the caudal end (fig. 4E). The anterior half of the nerve cord possesses a cavity which is widest in the region of the prosencephalon (fig. 4A, E). A pair of lateral outgrowths, optic buds, are present. These are solid at first, but quickly develop small cavities (fig. 4A, E, F).

The ectoderm of the head is folded ventrad, forming a head fold with an underlying subcephalic pocket (fig. 4A, F). The head region is enclosed in a thin, double-layered sac of periblastic ectoderm.

The auditory placode is present at this stage (fig. 4B, E, F). Mesenchyme is aggregated on either side of the neural keel in the midbody region where the first somites will form (fig. 4C, E, F).

The chorda-endoderm appears to split

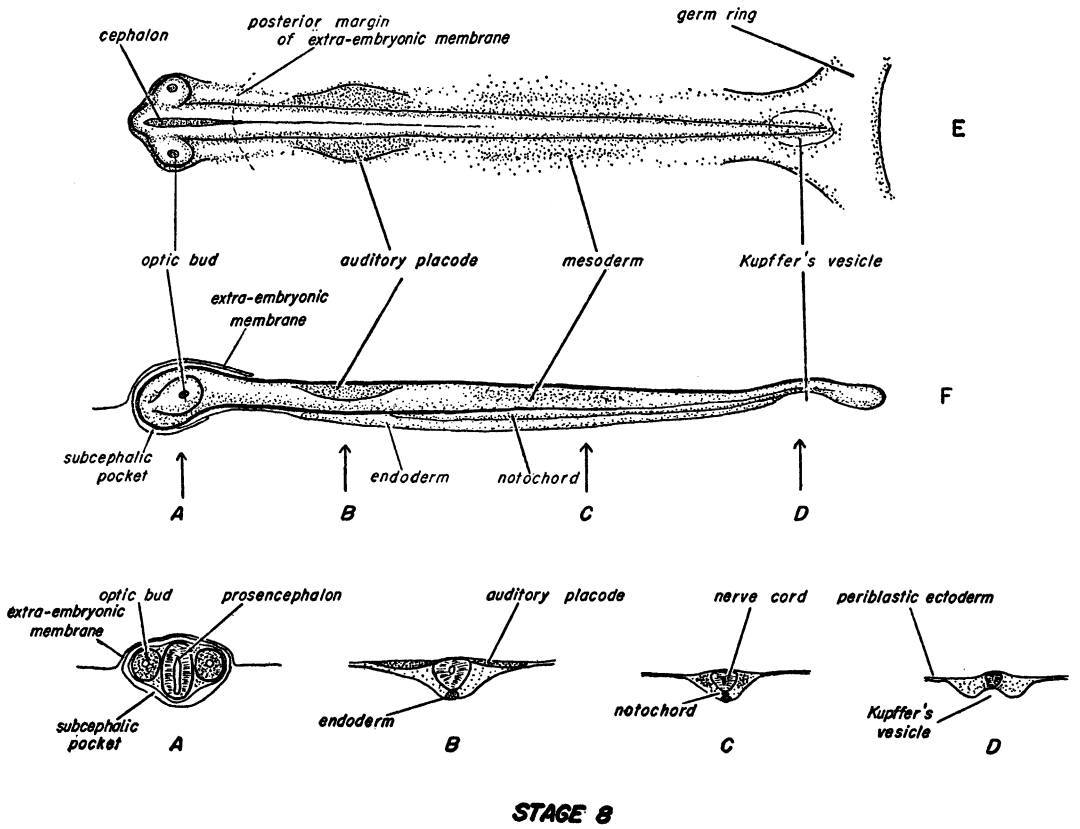

FIG. 4. Stage 8. A–D. Cross sections at levels indicated. E. Dorsal view. F. Lateral view. ×90.

longitudinally, with the ventral cord of cells being the solid primordium of the gut and the dorsal cord forming the notochord (fig. 4C, F). The shallow Kupffer's vesicle marks the posterior limit of the chorda-endoderm (fig. 4D, F).

The germ ring, by this stage, has advanced considerably, leaving about one-fifth of the yolk surface uncovered by periblast. This cap of uncovered yolk may be considered homologous to the yolk plug of amphibian eggs.

STAGE 9

Figure 5

Age, 3.0 days.

The total length of the early tail bud stage is 1.23 mm. The head has expanded considerably, primarily as a result of the growth of the optic vesicles (fig. 5A, G). The width of the mesencephalon region is 0.08 mm. The extra-embryonic periblastic membrane encloses the head to the level of the auditory placodes (fig. 5H). The blastopore is elliptical in shape, about 0.5 mm. in its longest axis. A small tail bud, 0.05 mm. in length, is present, overhanging the anterior lip of the blastopore (fig. 5G, H).

The nerve cord is tubular throughout, except in the relatively undifferentiated tail bud region. The neurocoele is widest in the head region, where primary divisions into prosencephalon, mesencephalon, and rhombencephalon can be distinguished (fig. 5G). The optic vesicles are large, hollow, and connected to the prosencephalon by solid optic stalks (fig. 5A, G, H). In cross section, lens placodes are shown (fig. 5A). The first cranial placode of neural crest (anlage of the fifth cranial nerve) is present (fig. 5B, G, H).

The gut endoderm is a cylindrical cord of cells extending from Kupffer's vesicle (post-anal gut) anteriorly to the level of the first cranial placode where the pharyngeal re-

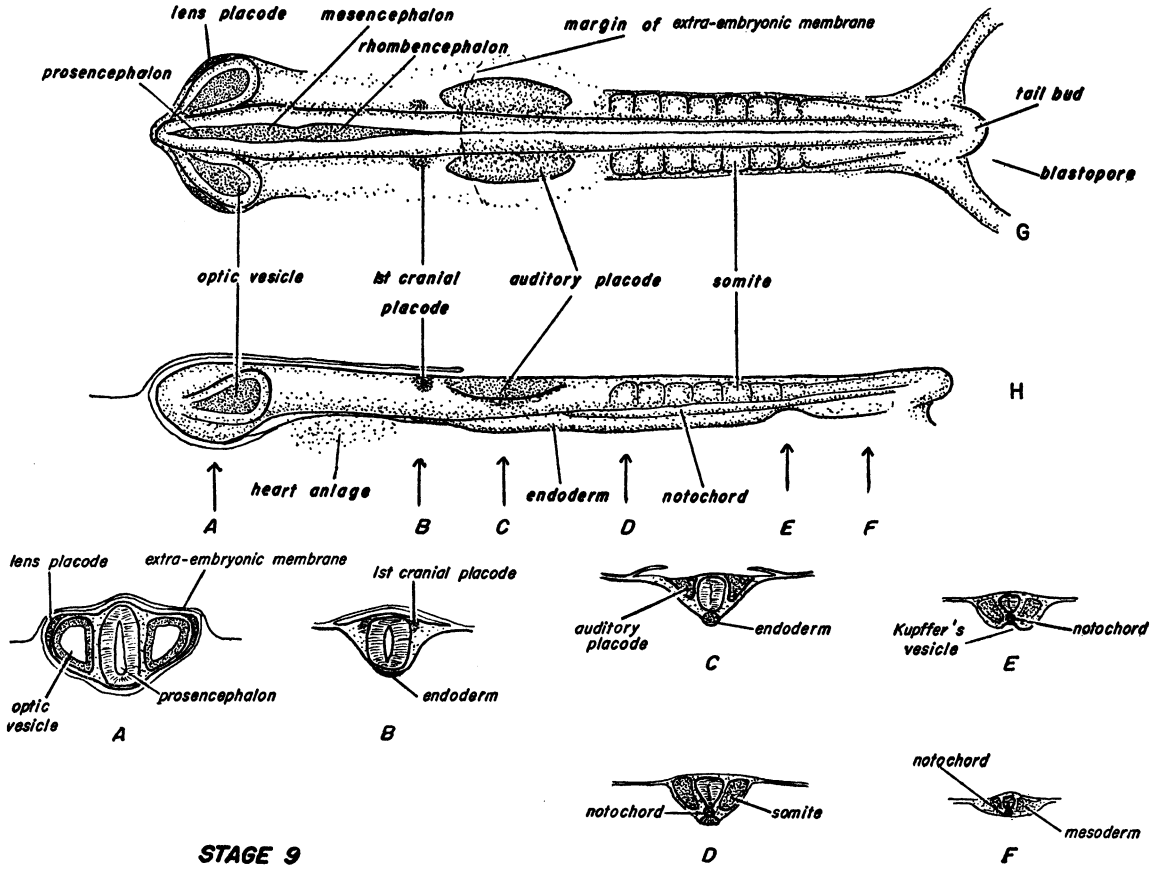

FIG. 5. Stage 9. A–F. Cross sections at levels indicated. G. Dorsal view. H. Lateral view. ×90.

gion becomes flattened (fig. 5B, C, D, H). The notochord can be traced from the blastopore lip region to the level of the auditory placode (fig. 5D, E, F, H).

Five to seven pairs of somites may be present in this stage (fig. 5G, H). Occasionally somites appear as early as stage 8. An aggregation of mesenchyme may frequently be found ventral to the nerve cord, anterior to the first cranial placode. This is interpreted as the anlage of the endocardium.

STAGE 10

Figures 6 and 7

Age, 3.4 days.

The total length at this stage is 1.45 mm., and the width at the mesencephalon is 0.13 mm. A bluntly rounded tail bud, 0.20 mm. long, overhangs the still open blastopore (fig. 6A, B). The extra-embryonic membrane encloses the head as far back as the auditory vesicle (figs. 6A, B, 7A–F). The subcephalic pocket extends to about the middle of the mesencephalon.

The three primary divisions of the brain are easily seen, with the mesencephalic portion possessing the thickest walls (fig. 6A). The telencephalic portion of the prosencephalon is small and acuminate (figs. 6A, 7A). The diencephalic region is relatively long and deep. The deepest point represents the site of the infundibulum (fig. 6B).

The optic vesicles are folded into optic cups with a thickened sensory layer (figs. 6A, 7A). The optic stalks are hollow at this stage. The lens placodes are partially invaginated (figs. 6A, 7B). Small olfactory placodes are present (figs. 6A, 7A). The auditory placode has invaginated as a solid mass and, at this stage, has formed a small

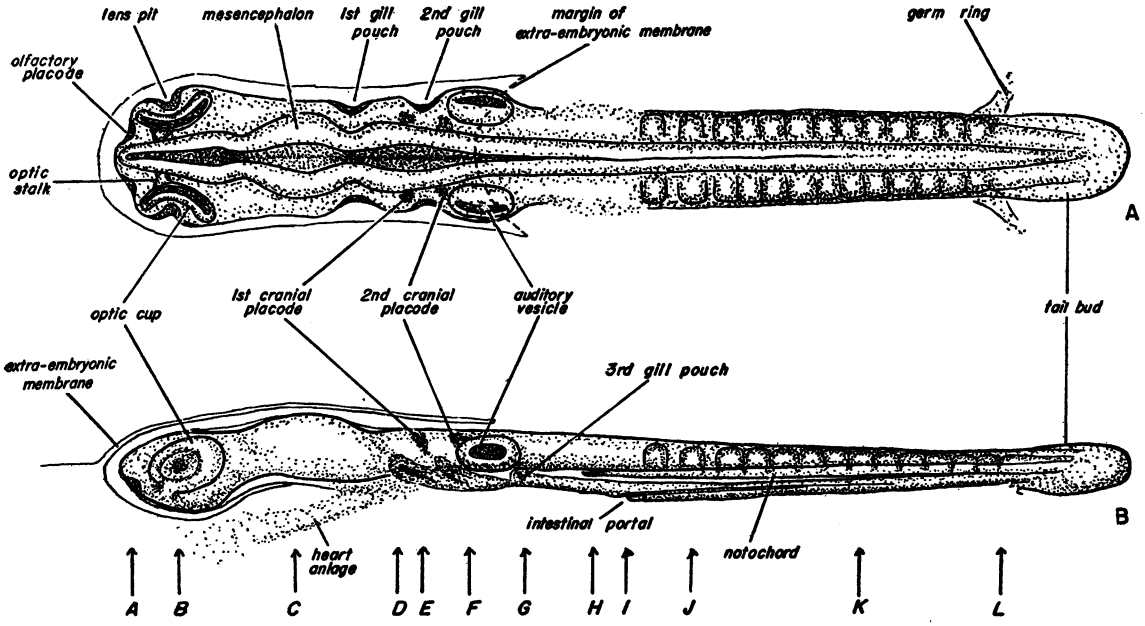

STAGE 10

FIG. 6. Stage 10. A. Dorsal view. B. Lateral view. ×90.

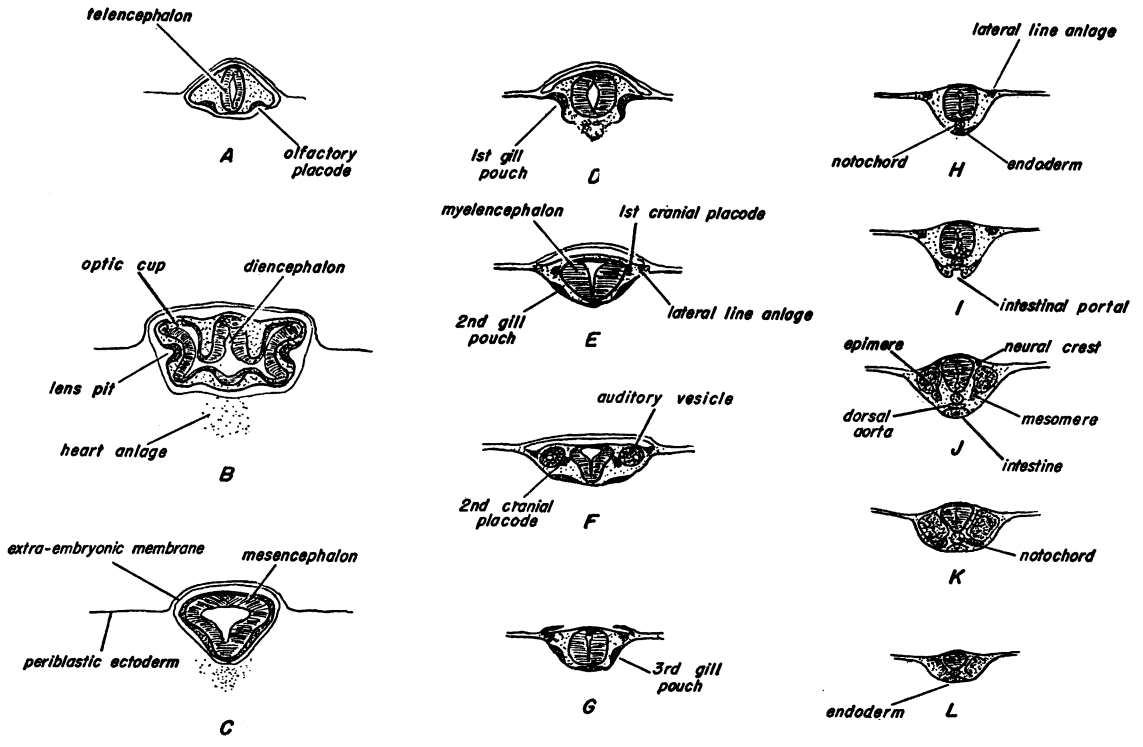

STAGE 10

FIG. 7. Stage 10. A–L. Cross sections at levels indicated in figure 6B. ×90.

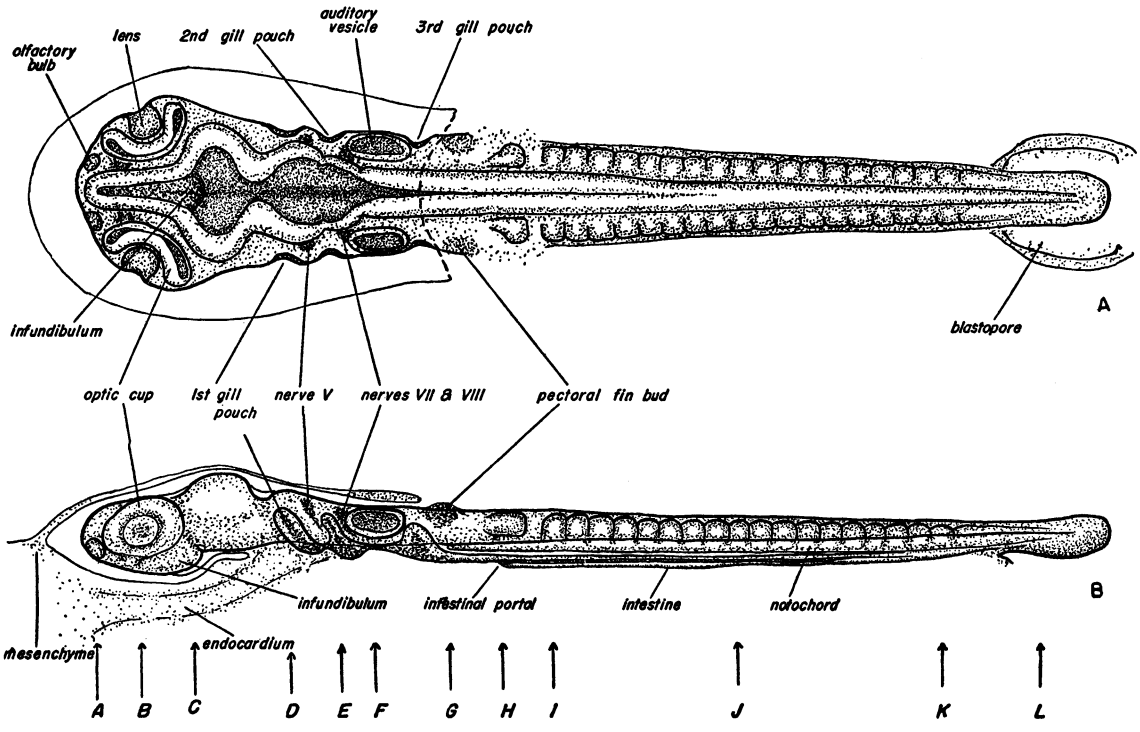

STAGE II

FIG. 8. Stage 11. A. Dorsal view. B. Lateral view. ×90.

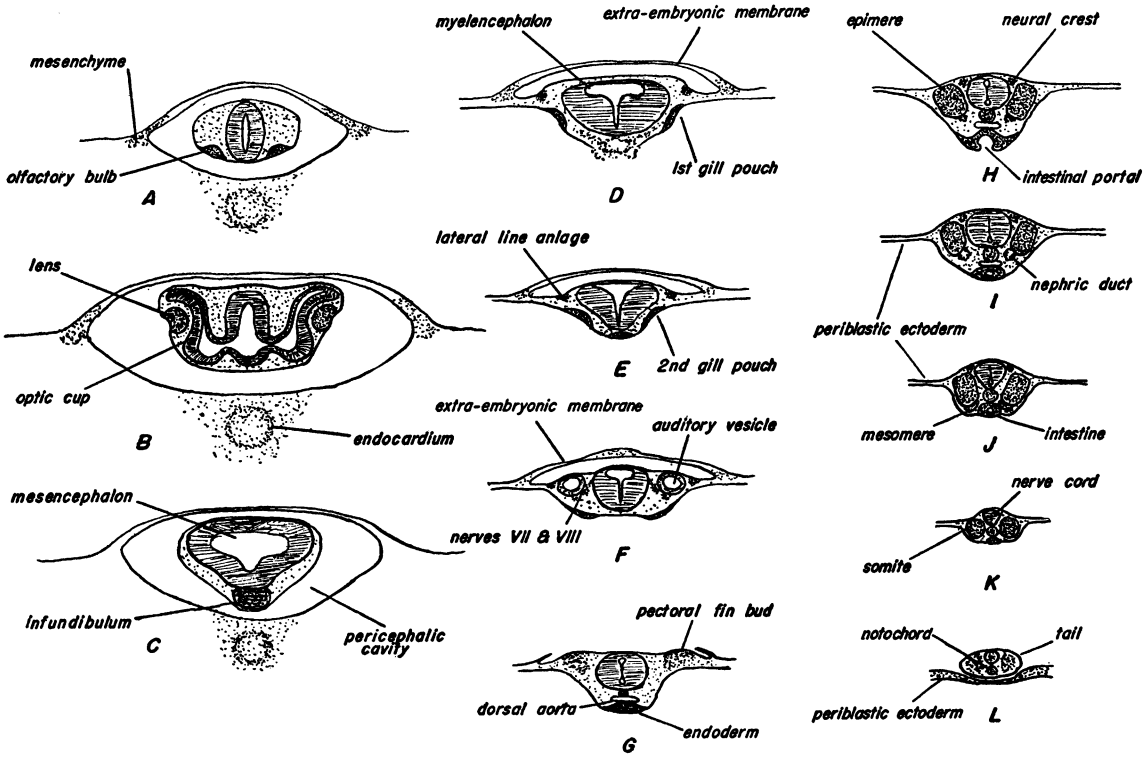

STAGE II

FIG. 9. Stage 11. A–L. Cross sections at levels indicated in figure 8B. ×90.

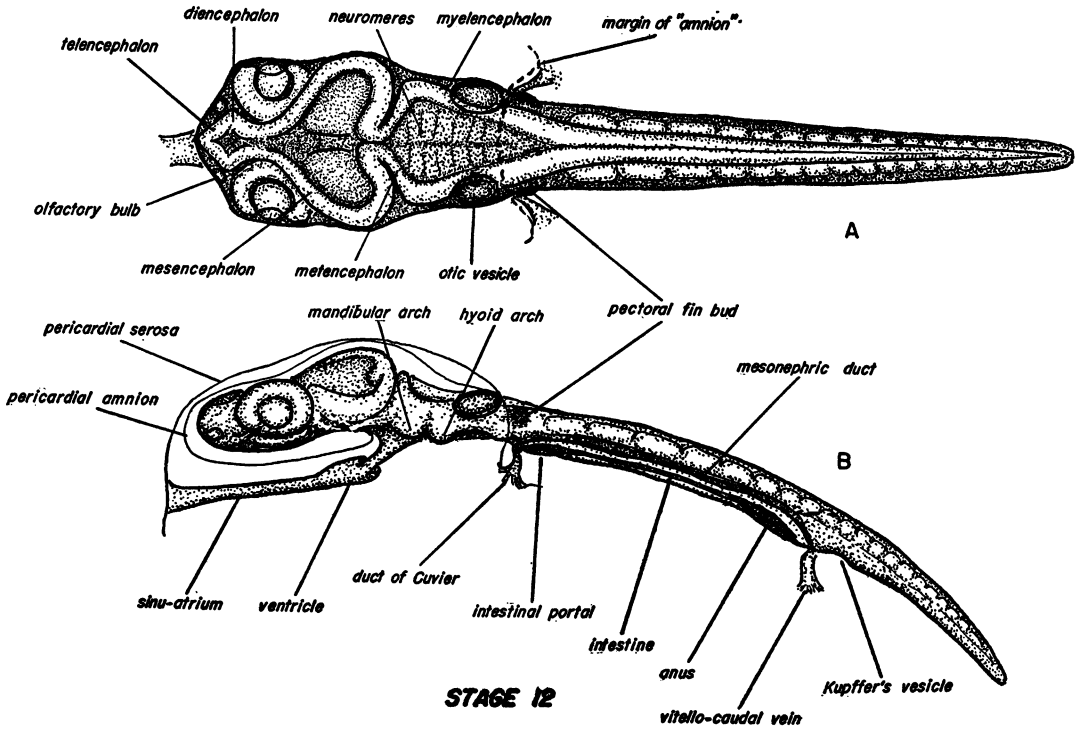

FIG. 10. Stage 12. A. Dorsal view. B. Lateral view. ×60.

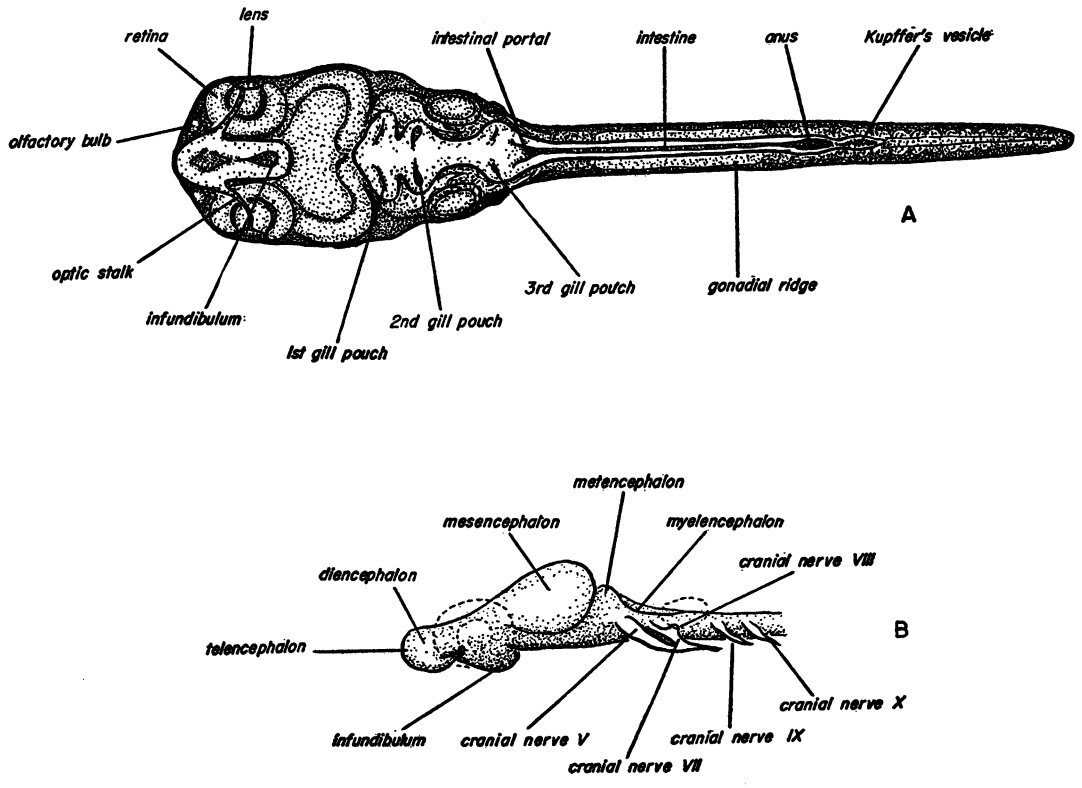

FIG. 11. Stage 12. A. Ventral view. B. Lateral view of brain and cranial nerves. ×60.

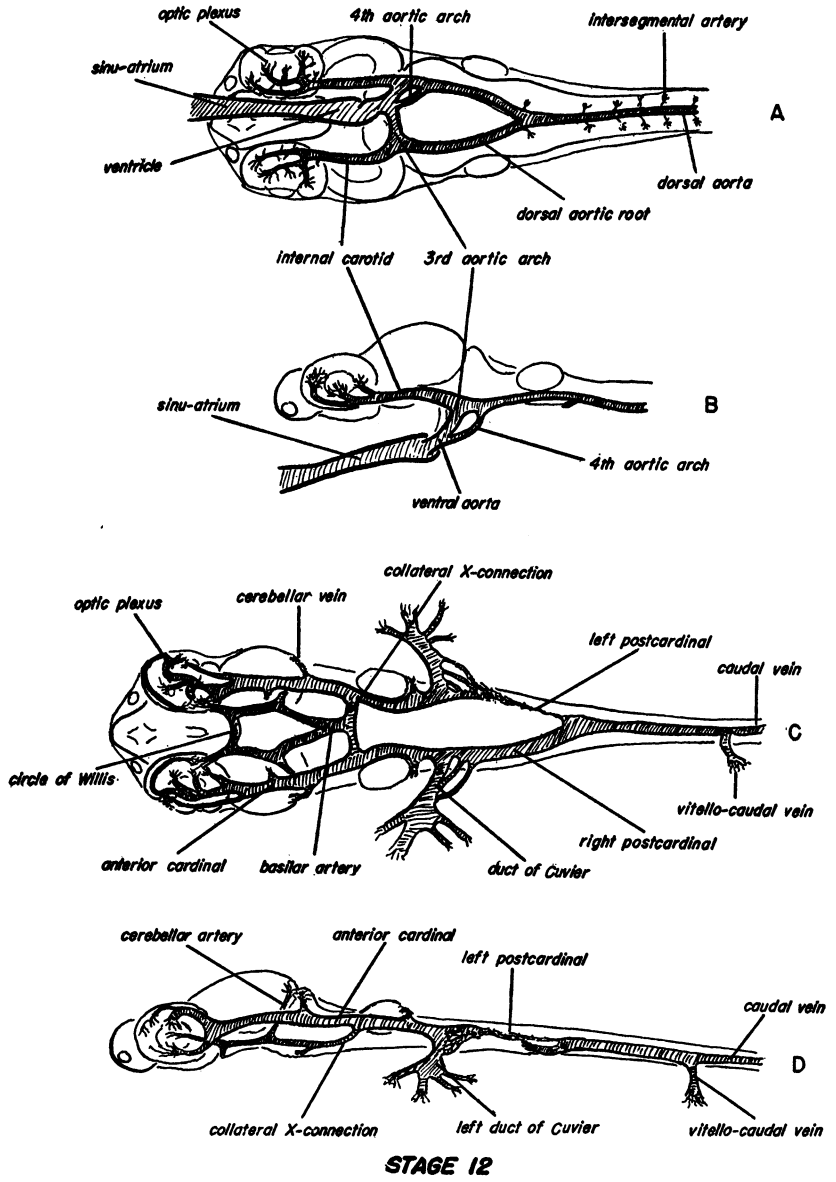

FIG. 12. Stage 12. A. Ventral view of arterial system. B. Lateral view of arterial system. C. Ventral view of venous system. D. Lateral view of venous system. ×60.

cavity (figs. 6A, B, 7F). No endolymphatic duct or vestige of it is ever present. Two aggregations of neural crest cells are visible in the cross sections and are shown in figure 6A and B. The anterior of these is the first cranial placode (fig. 7E), and the other is the second cranial placode (fig. 7F), primordium of the seventh and eighth cranial nerves. Three or four of the first spinal nerve primordia are also present in the form of neural crest (fig. 7J).

The cranial portion of the endoderm is flattened and extended dorso-laterad to form the first evidences of the first three gill pouches, which are thickened grooves at this stage (figs. 6B, 7D, E, G). Just anterior to

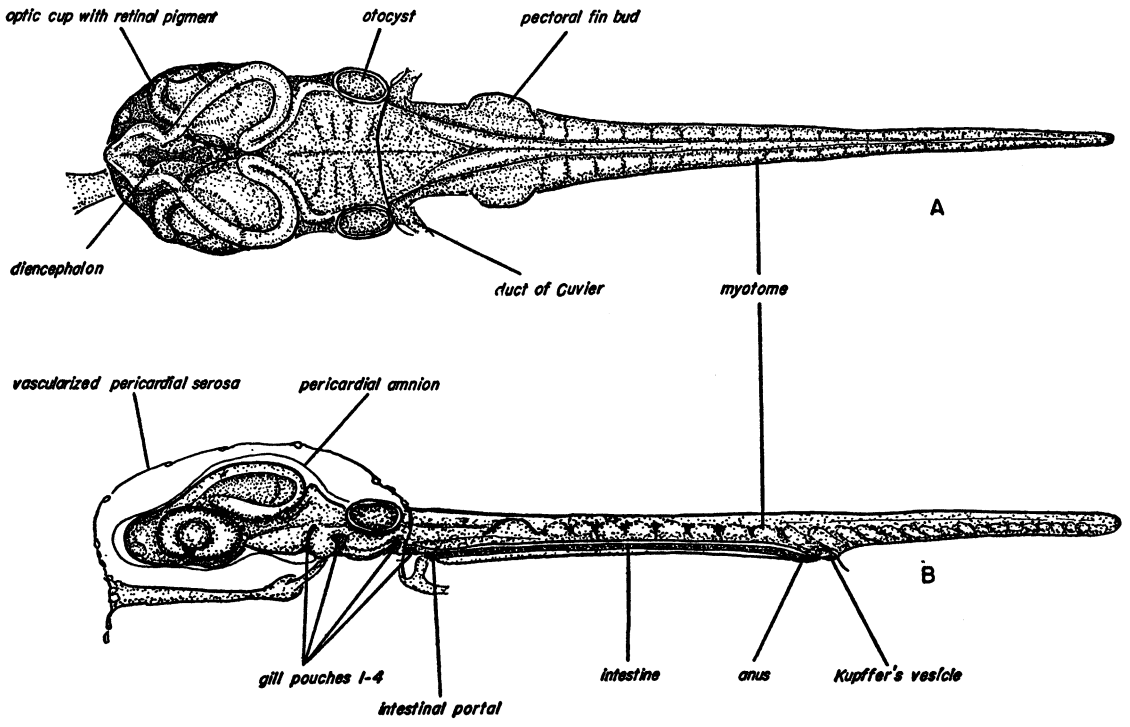

STAGE 13

FIG. 13. Stage 13. A. Dorsal view. B. Lateral view. ×60.

the level of the first somite, there is an intestinal portal opening into a small tubular cavity which extends posteriorly from that point to about the level of the sixth somite (figs. 6B, 7I, J). Caudad, the endodermal cord is solid (figs. 6B, 7K, L), and Kupffer's vesicle is greatly reduced.

Twelve or 13 pairs of somites are present (fig. 6). From the second somite to the ninth or tenth, a mesomeric region (nephrogenic cord) can be distinguished (fig. 7J). The heart anlage is still a diffuse mass of mesenchyme (figs. 6B, 7B, C, D). The dorsal aorta may be found as a thin-walled, flattened tube lying between the notochord and the endoderm in the region of the first four or five somites (fig. 7J). Blood-cell anlagen are found inside and around the dorsal aorta.

A pair of thickened grooves of ectoderm are present along the lateral limiting sulci, extending from the level of the first cranial placode up to about the first somite (fig. 7E). These structures are believed to be the primordia of the rather reduced lateral line system typical of the Poeciliidae.

STAGE 11

Figures 8 and 9

Age, 3.9 days.

Total length, 1.67 mm.

Width of mesencephalon, 0.25 mm.

The tail bud, approximately 0.37 mm. in length, covers most of the area of the blastopore (fig. 8A). The latter is small and elliptical or slit shaped. Occasional embryos have been found with much larger blastopores at this stage. The head lies free within a pericephalic (amnionic) cavity only as far back as the beginning of the rhombencephalon (figs. 8B, 9A, B, C). The extra-embryonic membrane is thicker and possesses some mesenchyme at its margins (figs. 8B, 9A–F). This is the first step in the transformation of the periblastic-ectodermal extra-embryonic membranes into the definitive inner pericardial amnion and outer pericardial serosa,

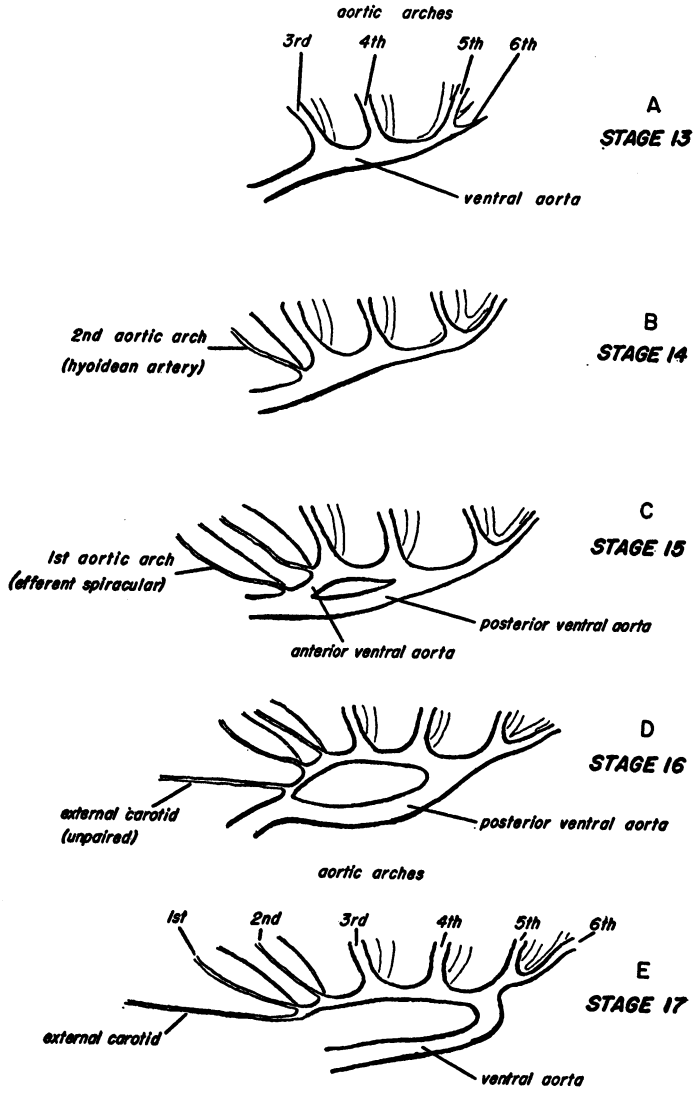

FIG. 14. Left lateral views of aortic arches and ventral aortae of stages 13 to 17.

each a somatopleural membrane.

The mesencephalon is widened, and the rhombencephalon less so. The infundibular region is deep and distinct (fig. 8B). The rhombencephalon, in the region of the cranial placodes, possesses a thin roof, i.e., the characteristic tela choroidea of the myelencephalon (fig. 9D). The lens placode is fully invaginated, solid, but not yet separated from the superficial ectoderm (figs. 8A, 9B). The olfactory organs appear as a pair of small solid masses of invaginated ectodermal tissue (figs. 8A, 9B). The lateral-line anlagen extend from the level of the first gill pouch to the pectoral fin bud (fig. 9D, E, F).

The endoderm shows little change from the condition in stage 10. The intestinal portion possesses a cavity extending back to the fifteenth somite (figs. 8B, 9H–K). The three gill pouch primordia are more sharply defined (figs. 8A, B, 9D, E).

Nineteen to 20 somites are present at this stage (fig. 8). A pair of pectoral fin buds make their appearance just anterior and

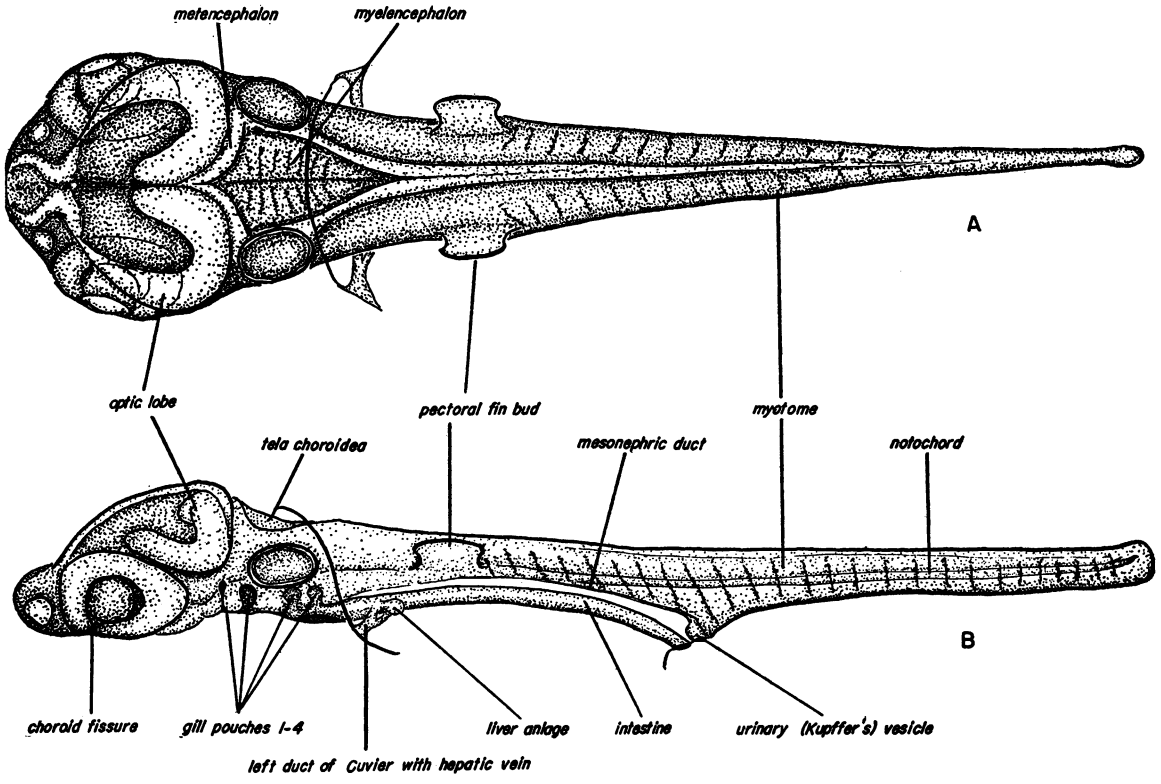

FIG. 15. Stage 14. A. Dorsal view. B. Lateral view. ×60.

lateral to the first somite (figs. 8A, B, 9G). The mesomere is distinguishable from the first to the thirteenth somites. At the level of the second to fourth somites, the mesomere is organized into a nephric duct (fig. 9I). The circulatory system consists of only a rather diffuse heart anlage and a single vessel, the dorsal aorta (figs. 8B, 9A–D, H, I).

STAGE 12

Figures 10–12

Age, 4.2 days.
Total length, 1.81 mm.
Tail length, posterior to anus, 0.48 mm.
Width of mesencephalon, 0.38 mm.

When embryos at this stage are freed from their membranes, they exhibit slow twitching movements of the body and tail. The extra-embryonic membranes are complete, forming a two-layered sac and enclosing the head of the embryo, including, posteriorly, the auditory vesicles. These membranes, namely, the pericardial amnion and pericardial serosa, are indicated in figure 10B. The blastopore is usually closed at this stage, but a faint raphe, marking the closure of the lips, may be distinguished. This raphe is located postanally and underlies the tail bud.

The mesencephalon is considerably widened and possesses thickened sides and floor (fig. 10A). The metencephalon is small and relatively poorly distinguishable from the following myelencephalon, the latter possessing its characteristic tela choroidea and visible neuromeres (fig. 10A). The optic stalks are thin (fig. 11A, B). The infundibular region of the diencephalon is large and deep (fig. 11A, B).

Five pairs of cranial nerves can be identified and traced in serial cross sections reconstructed in figure 10B. The trigeminal is the largest and most anterior, running ventrally and posteriorly to fuse with the facial (VII). The facial and auditory nerves arise at the

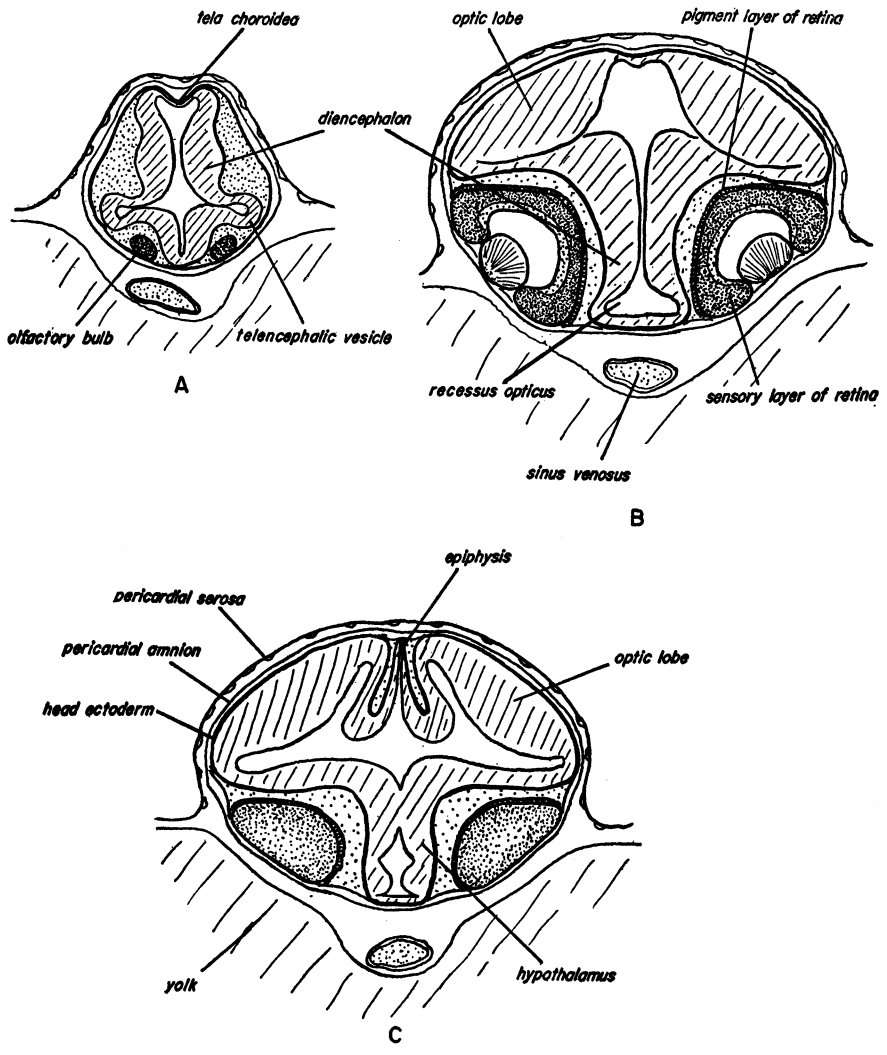

FIG. 16. Stage 14. A. Cross section at level of olfactory bulbs. B. Cross section at level of lenses. C. Cross section at level of epiphysis. ×90.

same point, just anterior to the auditory vesicle. The auditory (VIII) branches off and fuses with the otocyst tissue. The facial (VII) continues ventrally and posteriorly to fuse with the trigeminal (V). The glossopharyngeal (IX) and vagus (X) arise separately and can be traced for a short distance postero-ventrad.

The pharyngeal portion of the gut is flat, with three pairs of flanges extending laterad and dorsad (fig. 11A). These are the primordia of the first three pairs of gill pouches. The first and third possess small grooves, and the second a small, shallow pouch. The second pouch will become the first true gill cleft. Posterior to the third pouch is the intestinal portal leading into the straight intestine and ending in a groove-shaped anus. Posterior to the anus is the shallow postanal gut (Kupffer's vesicle) (figs. 10B, 11A).

Twenty-one to 22 compact somites may be discerned, the anus being at the level of the

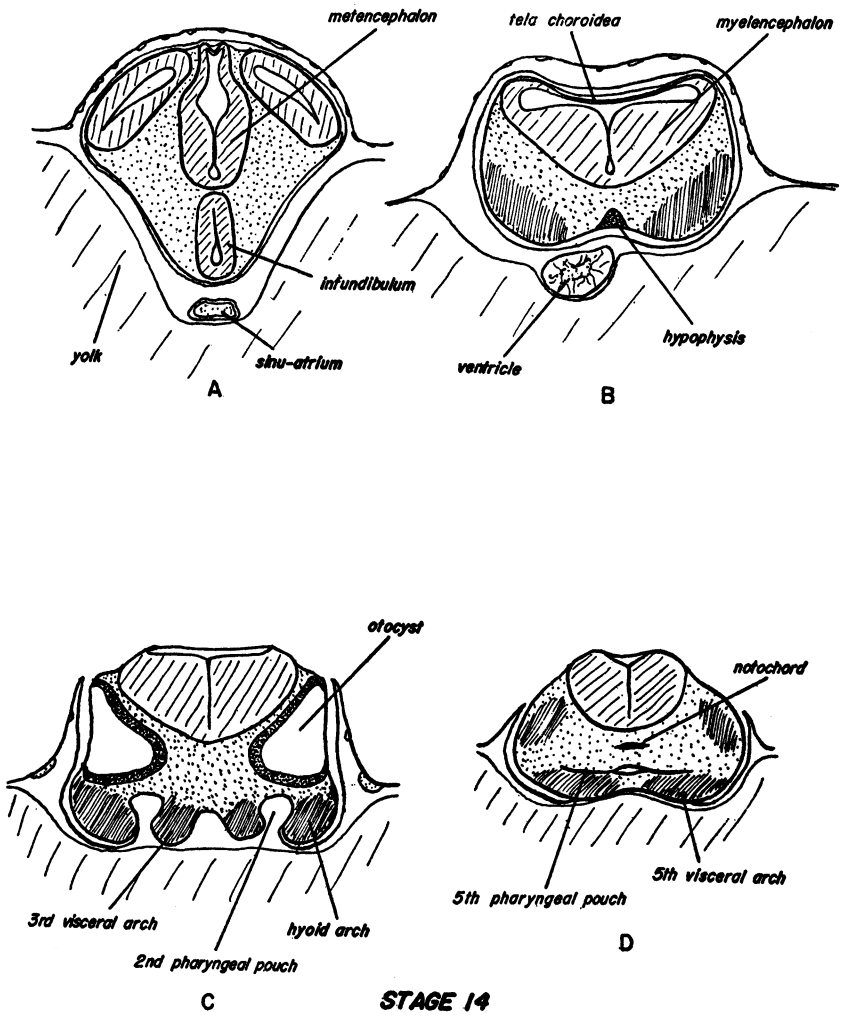

FIG. 17. Stage 14. A. Cross section at level of infundibulum. B. Cross section at level of hypophysis. C. Cross section at level of otocysts. D. Cross section at posterior pharyngeal level. ×90.

eighth (fig. 10A, B). The mesomeric region is relatively undifferentiated at the level of the pectoral fin bud and the first somite. Posteriorly, a pair of nephric ducts extend to the level of the seventh somite where they taper off into a solid cord of cells (fig. 10B). A pair of cords of primordial germ cells are aggregated into gonadial ridges in the region of the second to fifth pairs of somites. The position of these is indicated in figure 11A.

The circulatory system at this stage is a complete circuit, but little visible blood is present. The heart beat is irregular. The blood circuit can be traced in this stage both in serial cross sections and in India ink injected specimens (fig. 12A–D). The blood enters the elongate sinu-atrial region of the heart in front of the tip of the head. A pulsating ventricular region bulges slightly towards the right side, and empties into a short conus and ventral aorta (fig. 12A, B). The third aortic arches (first to develop) are well formed, and a single fourth arch is usually present on the left side (fig. 12A, B). Leading forward from the third arches are a pair of internal carotid arteries supplying the extensive optic plexi. Running caudad, the two radices aortae fuse into a single dorsal

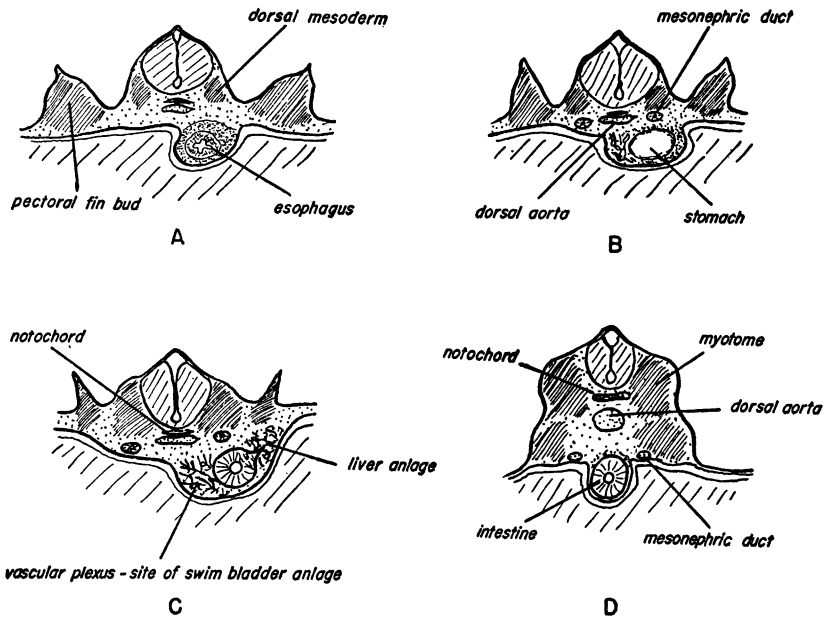

STAGE 14

FIG. 18. Stage 14. A. Cross section at level of esophagus. B. Cross section at level of gastric region. C. Cross section at level of liver anlage. D. Cross section at midbody level. ×90.

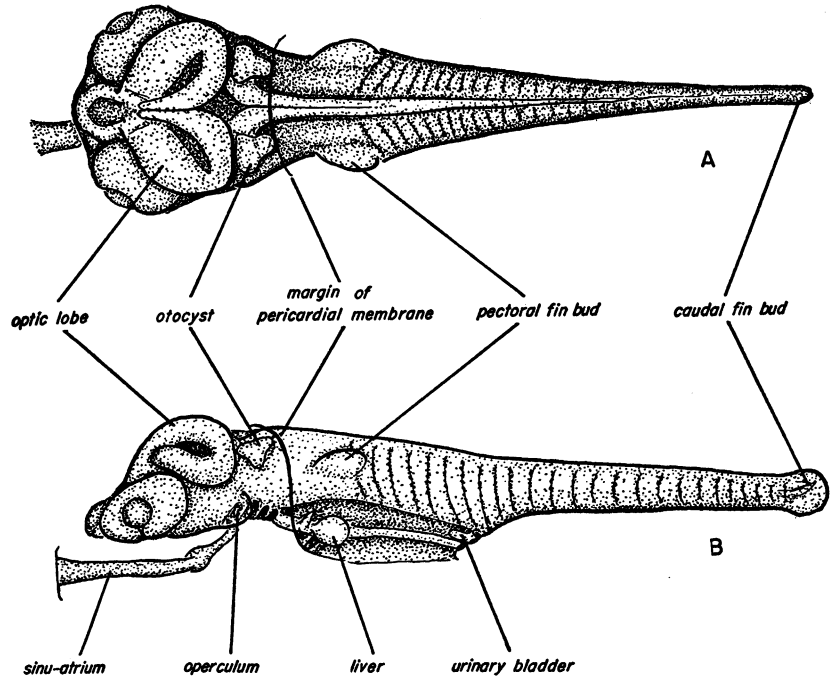

STAGE 15

FIG. 19. Stage 15. A. Dorsal view. B. Lateral view. ×30.

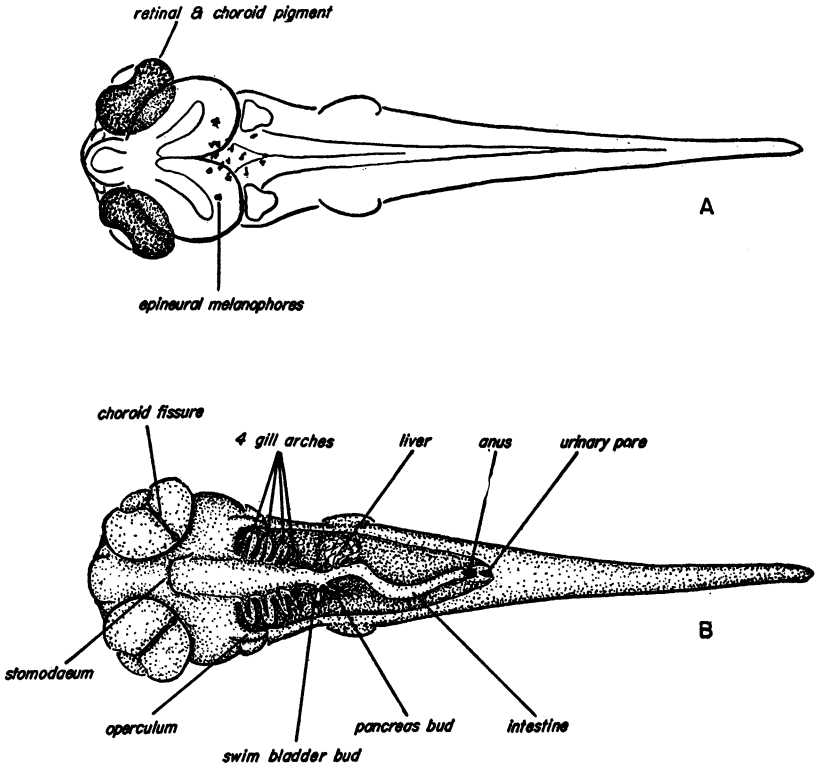

STAGE 15

FIG. 20. Stage 15. A. Dorsal view, showing distribution of melanophores. B. Ventral view, showing viscera and gills. ×30.

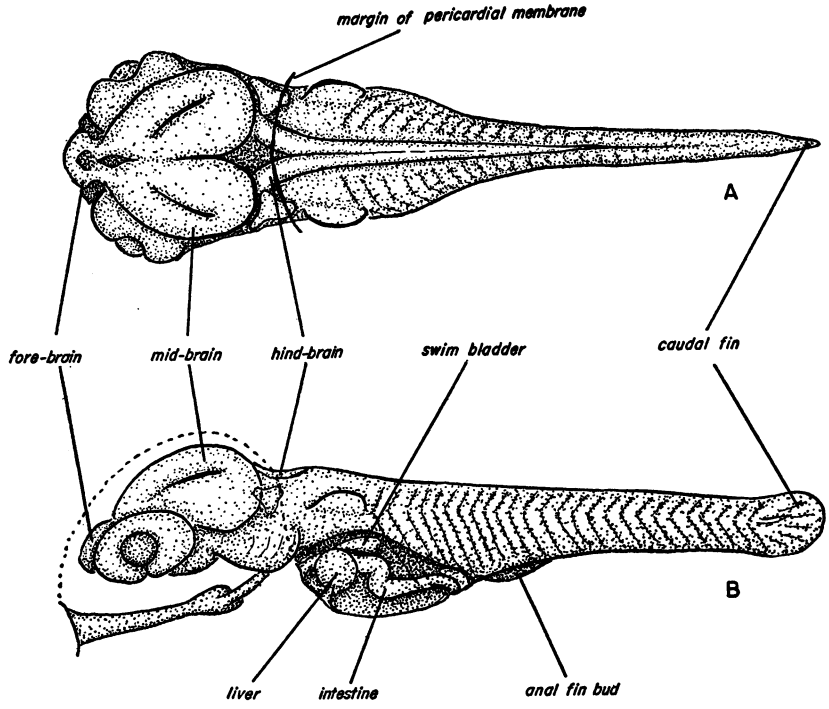

STAGE 16

FIG. 21. Stage 16. A. Dorsal view. B. Lateral view. ×30.

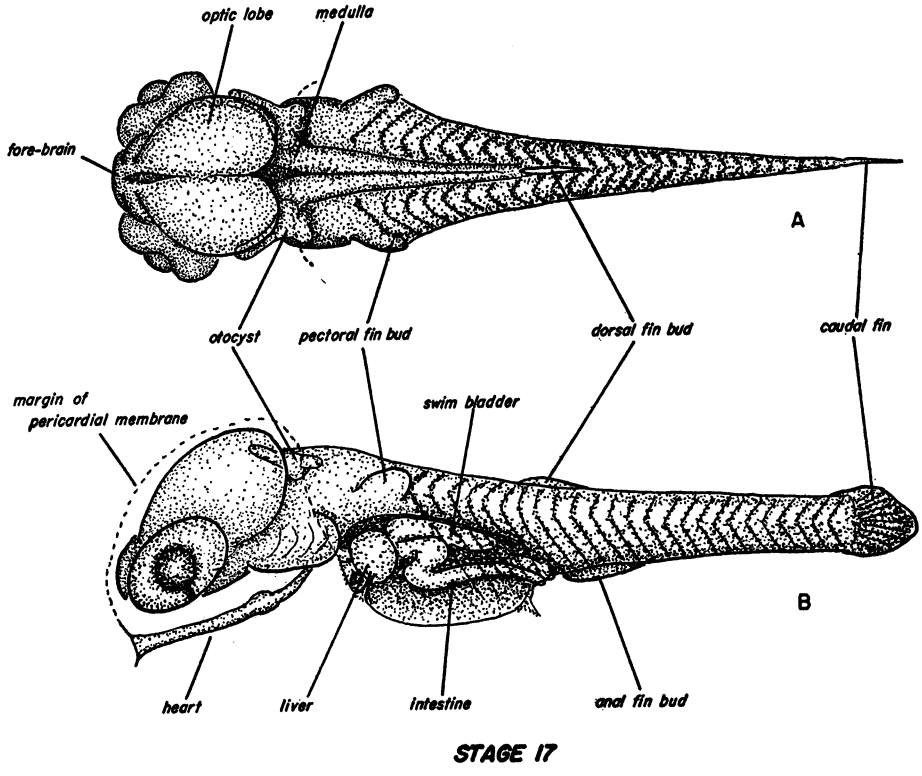

FIG. 22. Stage 17. A. Dorsal view. B. Lateral view. ×30.

aorta just posterior to the level of the auditory vesicles. At that point, a pair of small subclavian arteries are given off. The dorsal aorta extends into the tail region as the caudal artery, giving off numerous intersegmentals along the way (fig. 12A, B).

A pair of large anterior cardinal veins lead from the optic plexi to the ducts of Cuvier (fig. 12C, D). The caudal vein is drained by the vitello-caudal vessel emptying into the yolk sac circulation at a level just posterior to the anus. The caudal vein is also drained by the postcardinals. The left postcardinal is a vestigial structure, whereas the right is well developed (fig. 12C, D). A circle of small arterial vessels is present beneath the mesencephalon, posterior to the infundibulum (fig. 12C). These blood vessels arise from the internal carotid plexus in the eye, give off a pair of cerebellar arteries, and fuse into a single median basilar artery. The basilar artery is short and, at this stage, is connected by a collateral cross connection to the anterior cardinals (fig. 12C). This circle of blood vessels, as will be shown later, comes to surround the infundibulum and consequently may be considered comparable to the circle of Willis, present in birds and mammals.

The ducts of Cuvier lead into the extensive vascular yolk sac (fig. 12C, D).

STAGE 13

Figure 13

Age, 4.8 days.
Total length, 2.02 mm.
Tail length, 0.62 mm.
Mesencephalon width, 0.42 mm.

At this stage the blastopore is completely closed. Usually a thin streak is visible extending for about 0.4 mm. on the surface of the yolk membrane underlying the tail, marking the site of closure of the blastopore.

Aside from a general difference in size, the most prominent feature distinguishing this stage from stage 12 is the presence of the first indications of visible pigment (fig. 13A). This

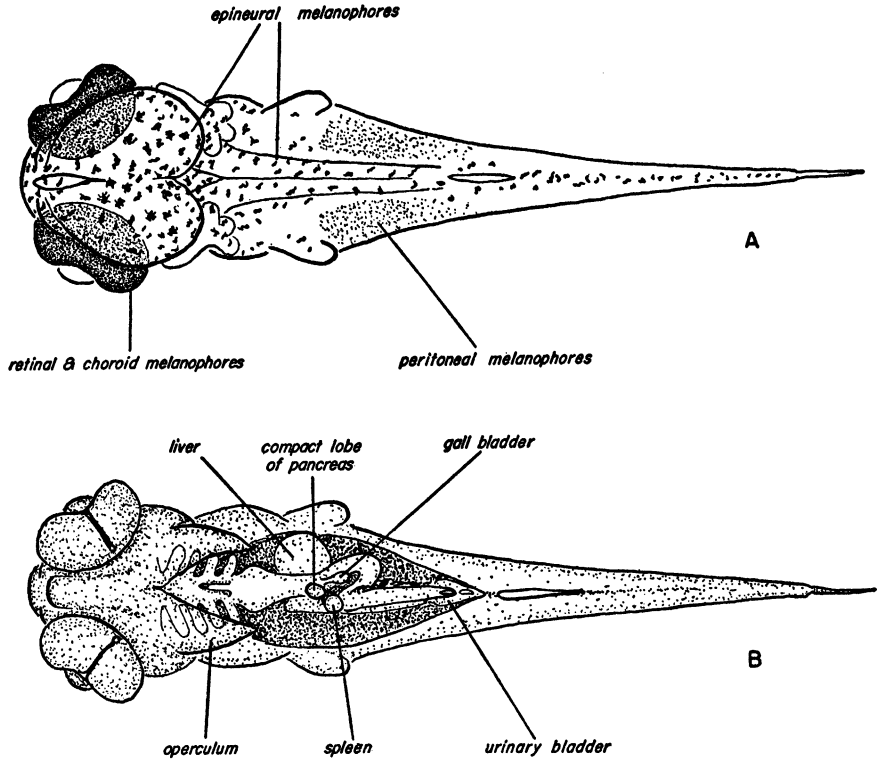

FIG. 23. Stage 17. A. Dorsal view, showing distribution of melanophores. B. Ventral view, showing viscera and gills. ×30.

appears in the outer retinal layer, delineating the eyes of living specimens with a thin dark margin.

In the pharyngeal region, four pairs of gill pouches are present, with the first (spiracular or pseudobranchial) somewhat constricted (fig. 13B). The development of the postanal gut (Kupffer's vesicle) into the urinary bladder (or vesicle) is indicated by an enlargement and invagination of the former (fig. 13B).

Considerable changes have taken place in the circulatory system. There are usually four pairs of aortic arches present, i.e., the third fourth, fifth, and sixth (fig. 14A). Occasionally the fourth or the sixth pairs are incompletely formed. The ventral aorta posterior to the fourth arches is double, and it is noteworthy that the ventricular end of the ventral aorta is anterior to the third aortic arch. The blood flow in the ventral aorta, then, is caudad.

The circle of Willis partially surrounds the infundibulum, and the collateral cross connection of the basilar and the anterior cardinals is greatly reduced or absent. The basilar runs caudad and splits into a pair of vertebral arteries at about the level of the pectoral fin buds.

The pericardial serosa is partially vascularized by branches of the common cardinal veins, and is drained by the sinus venosus.

STAGE 14

Figures 15–18

Age, 5.0 days.
Total length, 2.31 mm.
Tail length, 0.84 mm.
Mesencephalon width, 0.56 mm.

The pericardial serosa is well vascularized and is continuous with the extensive yolk sac membrane (fig. 16C). Pigment is limited to the retinal layer but is more evident and darker than in stage 13 (fig. 16B).

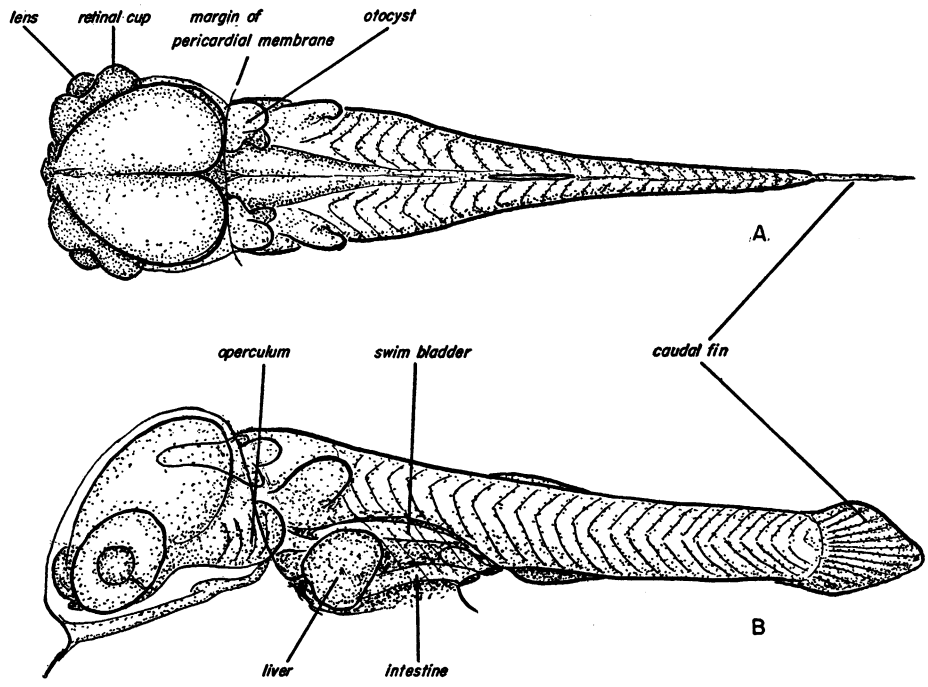

FIG. 24. Stage 18. A. Dorsal view. B. Lateral view. ×30.

The telencephalon is short, extending somewhat ventrad between two small olfactory bulbs (fig. 16A). A pair of small, flattened telencephalic vesicles are present. In the same transverse section (fig. 16A), the anterior region of the diencephalon is visible, with a thin dorsal roof (anterior tela choroidea). The mesencephalic (optic) lobes are large and thick walled, encroaching anteriorly over the diencephalon (figs. 15A, B, 16C, D). The optic stalks are vestigial or absent, originating from a broadly flattened optic recess in the floor of the diencephalon. Extending dorsad between the optic lobes is a narrow conical projection of diencephalic origin, i.e., the epiphysis (fig. 16C). The infundibulum projects posteriorly from a somewhat larger hypothalamic region (figs. 16C, 17A), and just posterior to the level of the infundibulum is a solid midventral mass of cells growing from the superficial ectoderm, i.e., the hypophysis (fig. 17B). The metencephalon is short and poorly distinguishable from the myelencephalon (fig. 17A, B), the latter being recognizable by the position of the cranial nerves and the presence of a posterior tela choroidea. The neurocoele is narrow in the spinal cord region and constricted to form a dorsal and a ventral canal (fig. 18A).

The retina exhibits three layers (fig. 16B). The outermost is the thin pigment layer. The sensory layer is divided into an outer nuclear layer and a paler staining, inner, nerve fiber layer.

The otocyst is ellipsoidal in shape (fig. 15), with the lateral walls thin and the median and ventral walls considerably thickened and fused with the fibers of the eighth nerve (fig. 17C).

The pharyngeal region possesses four pairs of gill pouches (figs. 15B, 17C). The first is greatly constricted, and the third and fourth pairs are shallow, dorsolateral evaginations of the broad, flat pharynx. The intestinal portal has moved forward to a position ventral to the third pair of pouches. Primordia of the fifth pouches are visible in sections as flat, solid outgrowths of the pharynx (fig. 17D).

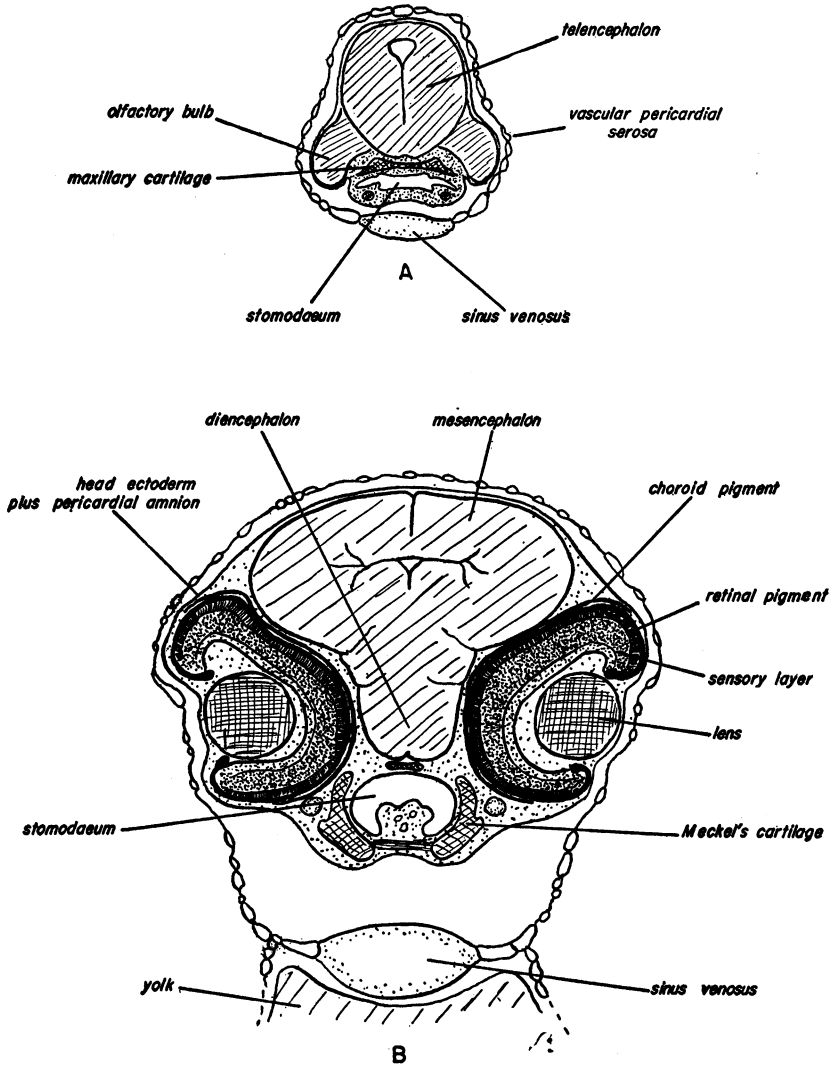

FIG. 25. Stage 18. A. Cross section at level of telencephalon. B. Cross section at level of lenses. ×60.

Posterior to the fifth pouch primordia, the short esophagus may be identified (fig. 18A). It possesses an irregular lumen lined by a single layer of cuboidal cells with basophilic cytoplasm. Immediately in front of the liver anlage (figs. 15B, 18C) is a widened region of the gut, about 30 microns in length and possessing a squamous type of epithelium arranged in three or four layers (fig. 18B). This widened region is presumed to be a vestigial stomach, absent in all subsequent stages.

The liver primordium, projecting to the left side of the intestine with a plexus of hepatic blood vessels, is a solid mass of undifferentiated cells (figs. 15B, 18C). The swim bladder primordium is not yet visible, but its site of future development is marked by a plexus of blood vessels on the right side of the intestine at the level of the vestigial stomach (fig. 18B, C).

The intestine is a straight tube, identifiable from the level of the liver primordium by its columnar, vacuolated epithelium and small

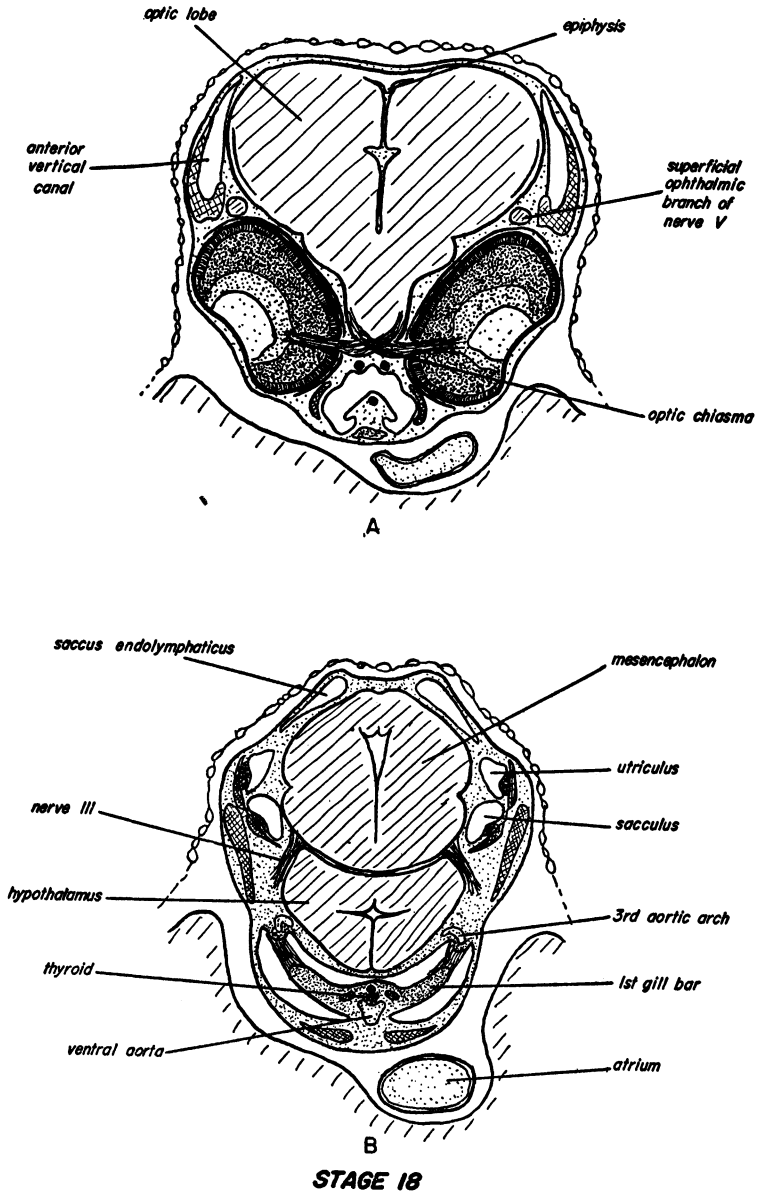

FIG. 26. Stage 18. A. Cross section at level of optic chiasma. B. Cross section at level of first gill bar. ×60.

circular lumen (figs. 15B, 18C, D). The intestine ends in a slit-shaped anus (fig. 15B).

Twenty-four to 25 myotomes are present at this stage (fig. 15), and striated muscle fibers can easily be identified in the sections. The mandibular arch is large, and the hyoid, third, fourth, and fifth arches are progressively smaller. The pectoral fin buds are broad at the base and have a thin distal margin (figs. 15A, B, 18A, B, C).

The notochord is dorsoventrally flattened, originating at a level posterior to the otocysts (figs. 17D, 18A–D), extending into the tail, where it becomes more rounded. The posterior end is curved dorsad (fig. 15B).

The ventral aorta runs caudad, giving off five pairs of aortic arches (fig. 14B). The second arch (afferent spiracular artery or

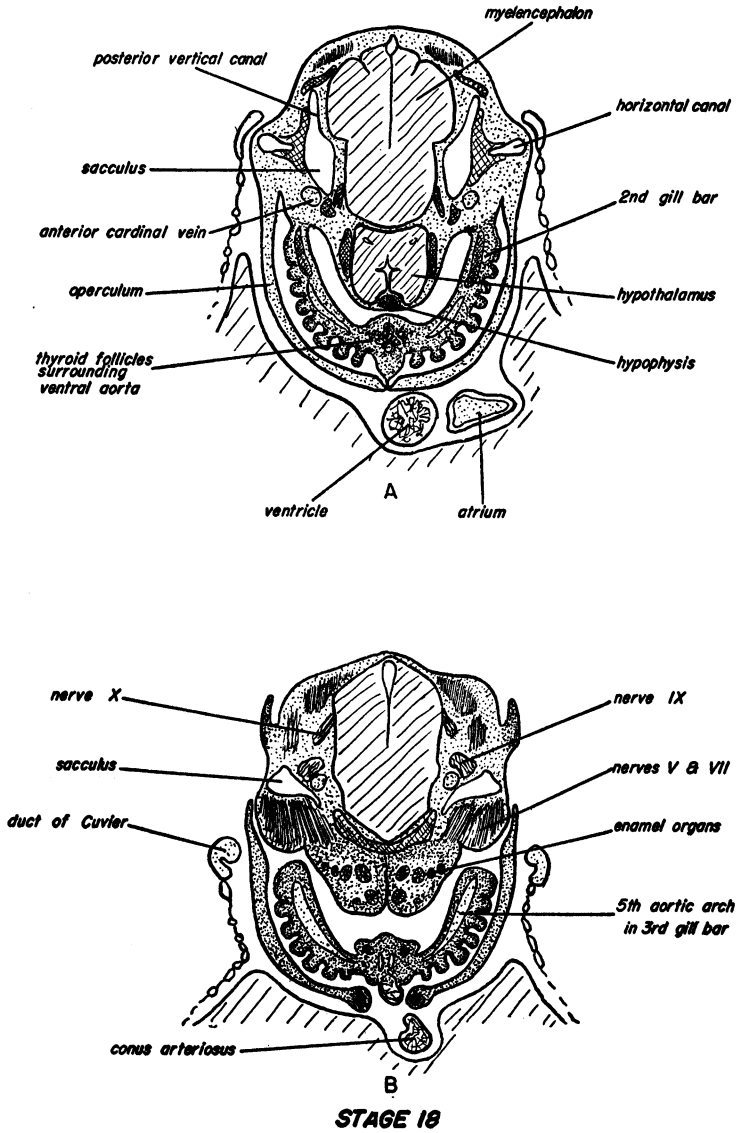

FIG. 27. Stage 18. A. Cross section at level of hypophysis. B. Cross section at level of third gill bar. ×60.

hyoidean artery) is thin and slender. The third arch is the largest, and the fourth, fifth, and sixth are progressively smaller, with the sixth arch appearing as a branch of the fourth (fig. 14B). A hepatic plexus is formed around the liver primordium, drained by a short hepatic vein, which, in turn, empties into the left common cardinal vein.

The urinary vesicle (formed from the post-anal gut) has invaginated more deeply than in stage 13 and possesses a slit-shaped opening (fig. 15B). The nephric ducts become evident at the level of the esophagus, possess a lumen, and extend caudad to about the sixth or seventh somite, becoming solid at about the fourth. No tubules are present at this stage.

STAGE 15

Figures 19, 20

Age, 5.5 days.
Standard length, 2.52 mm.

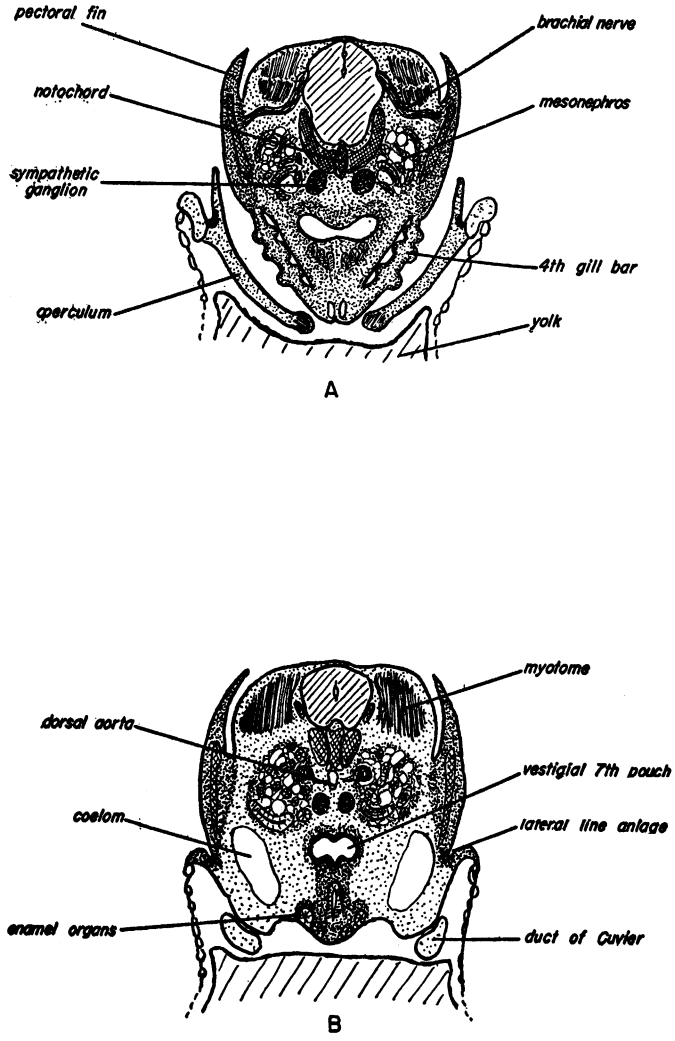

FIG. 28. Stage 18. A–B. Cross sections at level of mesonephroi. ×60.

Length of caudal fin bud, 0.09 mm.

Mesencephalon width, 0.68 mm.

This stage is characterized by the appearance of melanophores other than retinal. The retinal melanophores are obscured by pigment in the choroid layer, the latter containing numerous iridiocytes in addition to melanophores (fig. 20A). About 10 to 20 small, stellate epineural melanophores appear in the dorsal region above the metencephalon and myelencephalon (fig. 20A).

The optic lobes of the mesencephalon are greatly widened and thickened, forcing the eyes into an almost frontal position, and these lobes overlie the metencephalon and diencephalon (fig. 19A, B). The choroid fissure of the retina is distinct and possesses numerous fibers of the optic nerve (fig. 20B). The hypothalamic region of the diencephalon has enlarged so that it partially overlies the hypophysis and has pushed the infundibulum into a slightly more posterior position. Three bluntly rounded lobes can be distinguished as constituting the otocyst (fig. 19A, B): a

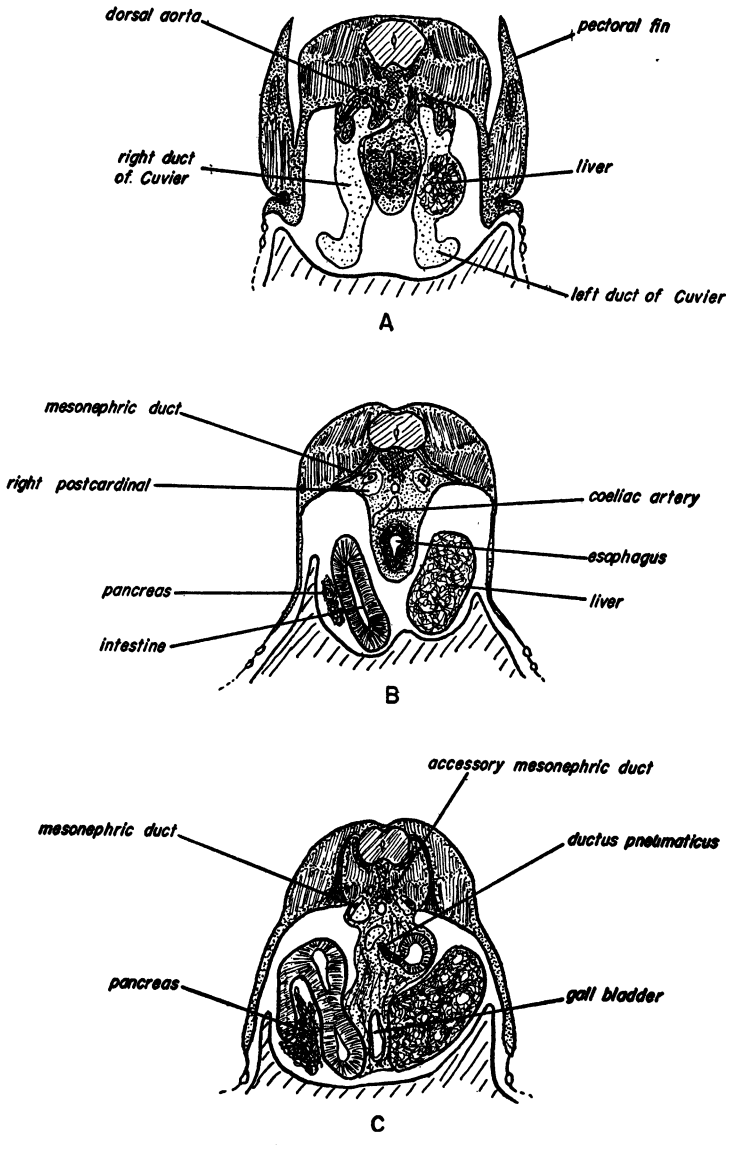

FIG. 29. Stage 18. A. Cross section at level of ducts of Cuvier. B. Cross section at level of esophagus. C. Cross section at level of gall bladder. ×60.

ventral, saccular portion; an anterior, medial portion possessing a single large otolith; and a posterior portion with a single small otolith.

Lateral extensions of the mandibular and hyoid arches forming opercula are present here. The opercula are short and blunt, concealing only the first of four pairs of gill arches. Twenty-five somites are present, this number being only one fewer than the full complement (fig. 19). A caudal fin bud is present (fig. 19B).

The esophagus is short and distinct. The gastric region, described for stage 14, is absent. From the anteriormost intestinal region three primordia may be traced (fig. 20B). To the right is the short, tubular

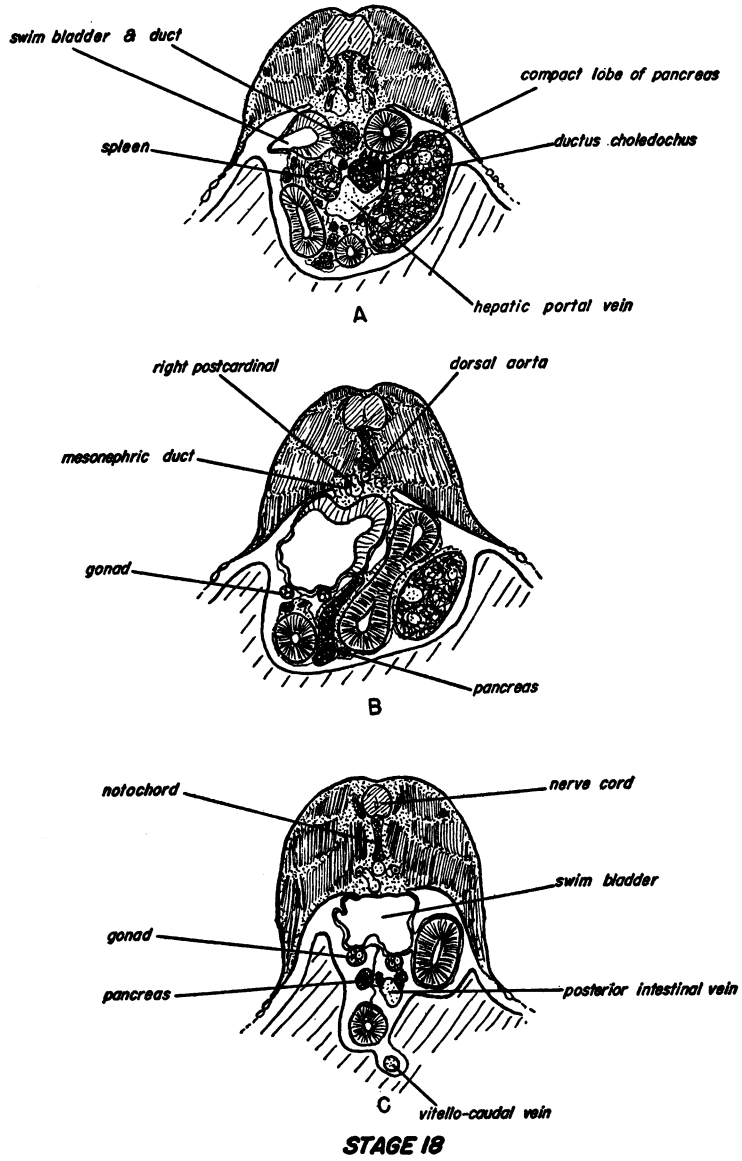

FIG. 30. Stage 18. A. Cross section at level of spleen. B–C. Cross sections at midbody level. ×60.

primordium of the swim bladder, surrounded by a plexus of blood vessels. Just posterior to the above and also extending to the right is a solid endodermal outgrowth in which pancreatic cells and ductules can be distinguished. At the same level, to the left of the intestine, is the liver (figs. 19B, 20B). The intestine is somewhat S-shaped in ventral view and ends in the anus at about the level of the sixth somite (figs. 19B, 20B).

The most important development in the circulatory system is in the region of the ventral aorta. At this stage, the ventral aorta is split into two vessels (fig. 14C). The anterior of these drains a pair of small, efferent, spiracular arteries (first aortic arches), and supplies a pair of small efferent spiraculars (second aortic arches), and the third and

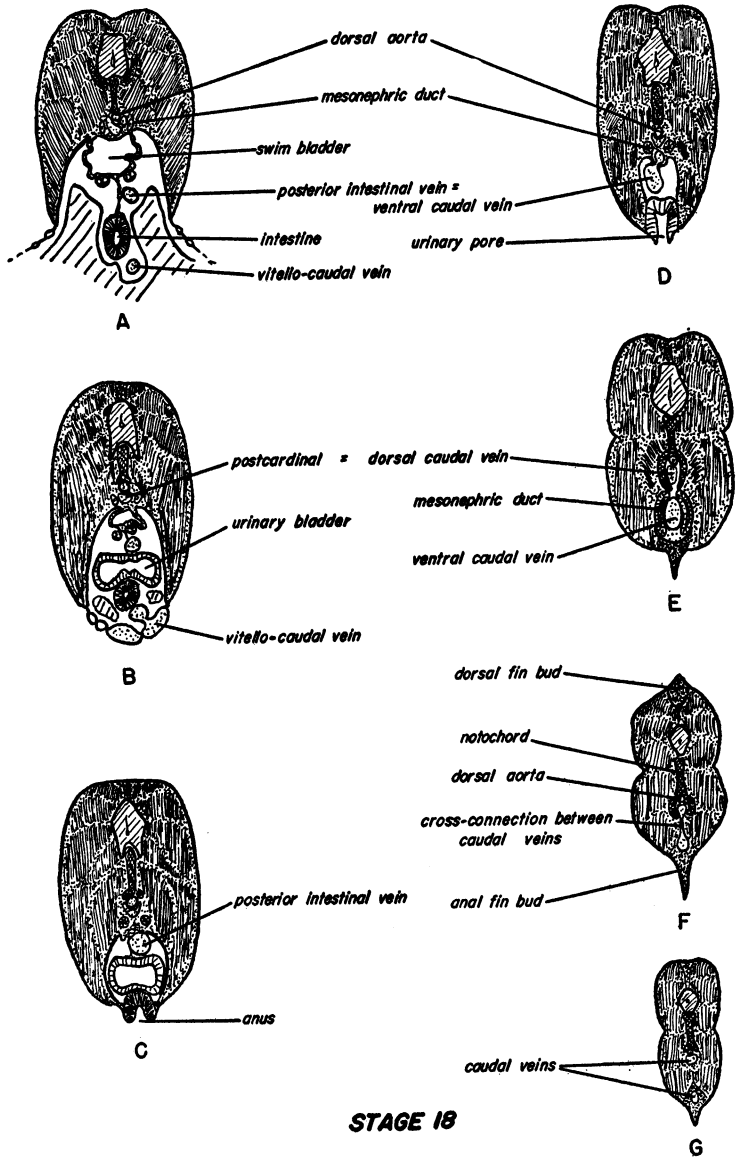

FIG. 31. Stage 18. A–C. Cross sections at posterior body level. D–G. Cross sections at post-anal levels. ×60.

fourth pairs of aortic arches. The posterior ventral aorta is connected to the common base of the fifth and sixth aortic arches and also supplies the fourth arch in part (fig. 14C).

At a level just anterior to that of the pectoral fin buds, a few mesonephric tubules have developed in the mesomere region dorsal to the mesonephric duct. The mesonephric ducts possess short extensions 50 to 100 microns anterior to the above region. These extensions may be vestigial homologues of the pronephric ducts. Posteriorly, the mesonephric duct can be traced up to the base of the urinary vesicle. The latter structure has invaginated considerably and lies in a position dorsal to the anal portion of the intestine, its distal (or cephalic) end being slightly bilobed (figs. 19B, 20B).

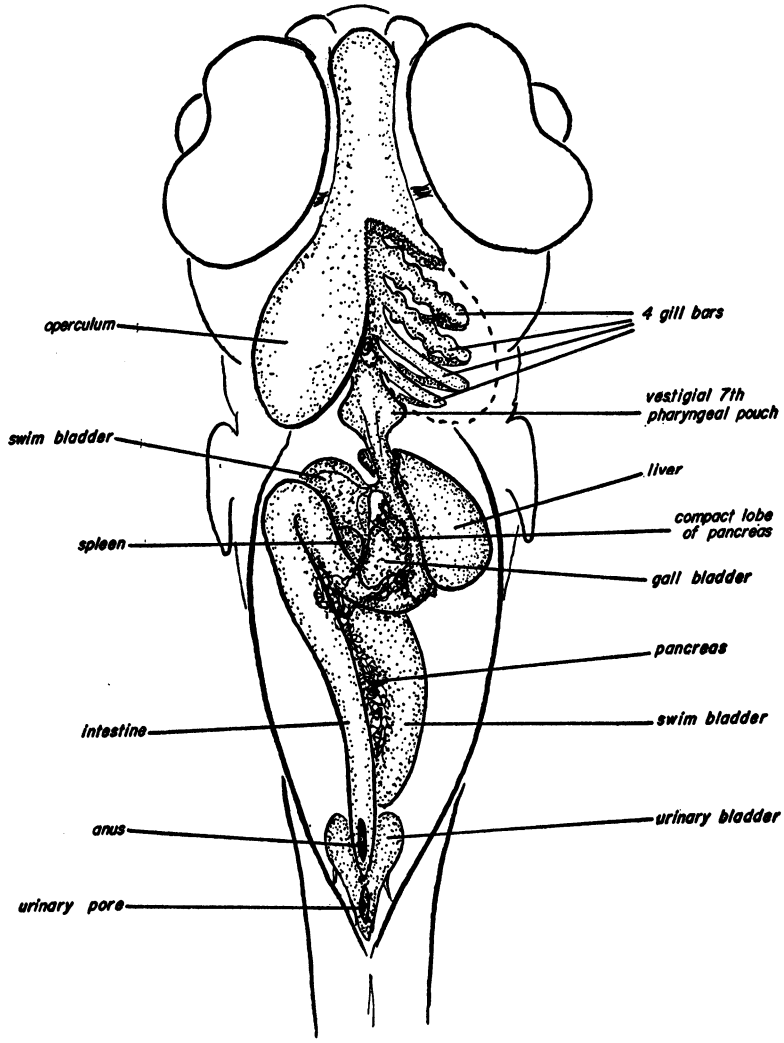

FIG. 32. Stage 18. Ventral view, showing viscera and gills. ×60.

STAGE 16

Figure 21

Age, 6.9 days.

Standard length, 2.80 mm.

Length of caudal fin, 0.12 mm.

Mesencephalon width, 0.79 mm.

The small, stellate, epineural melanophores are more numerous and scattered over the brain region, extending along the dorsal midline slightly beyond the pectoral fin buds.

The opercula are larger, covering the first three pairs of gill arches (fig. 21B).

The full complement of 26 myomeres is present (fig. 21A, B). Beyond the last myomere and the upturned tip of the notochord is the compressed caudal fin bud with primordia of six fin rays (fig. 21B). An anal fin primordium is present (fig. 21B).

The intestine is S-shaped in ventral view. At the anterior end of the intestine, near where it gradates from the esophagus, is the liver, connected to the left side of the intestine by means of a bile duct (fig. 21B). At the same level is the pancreas, extending

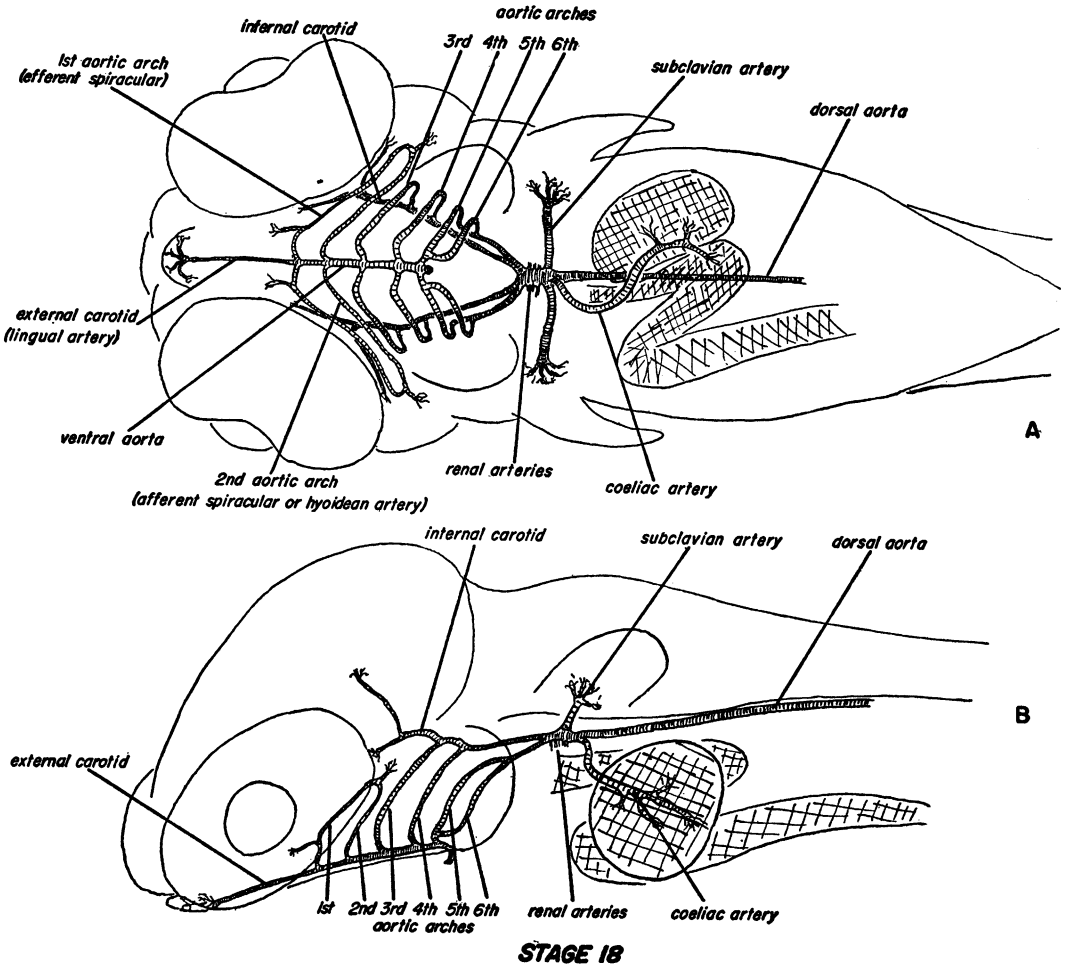

FIG. 33. Stage 18. A. Ventral view of arterial system. B. Lateral view of arterial system. ×60.

ventrally and to the right of the intestine in a series of nests of cells embedded in the mesentery. The anteriormost end of the pancreas consists of a more compact lobe of relatively undifferentiated tissue. Connected to the right side of the intestine, at this level, is the ductus pneumaticus, characterized by a columnar epithelium and a fine circular lumen. The swim bladder is small, about the width of the intestine, flattened, and in a position dorsal to the intestine. Its epithelium is high columnar and highly vacuolated. The swim bladder extends retroperitoneally and caudad to about the level of the first myomere (fig. 21B). This structure is described in greater detail in stage 18.

The gonadial ridges originate near the base of the swim bladder and are attached to the dorsal peritoneum. They extend caudad to the level of the fourth or fifth myomeres. The mesonephric ducts possess a lumen throughout their length and empty into the base of the urinary vesicle. Mesonephric tubules are numerous at the level of the pectoral fin buds, and a few renal capsules and glomeruli are visible.

The ventral aorta is still double, but the anterior branch is reduced in size. A fine, unpaired external carotid (or lingual) artery branches off the base of the anterior branch of the ventral aorta (fig. 14D).

STAGE 17

Figures 22, 23

Age, 7.7 days.
Standard length, 3.29 mm.

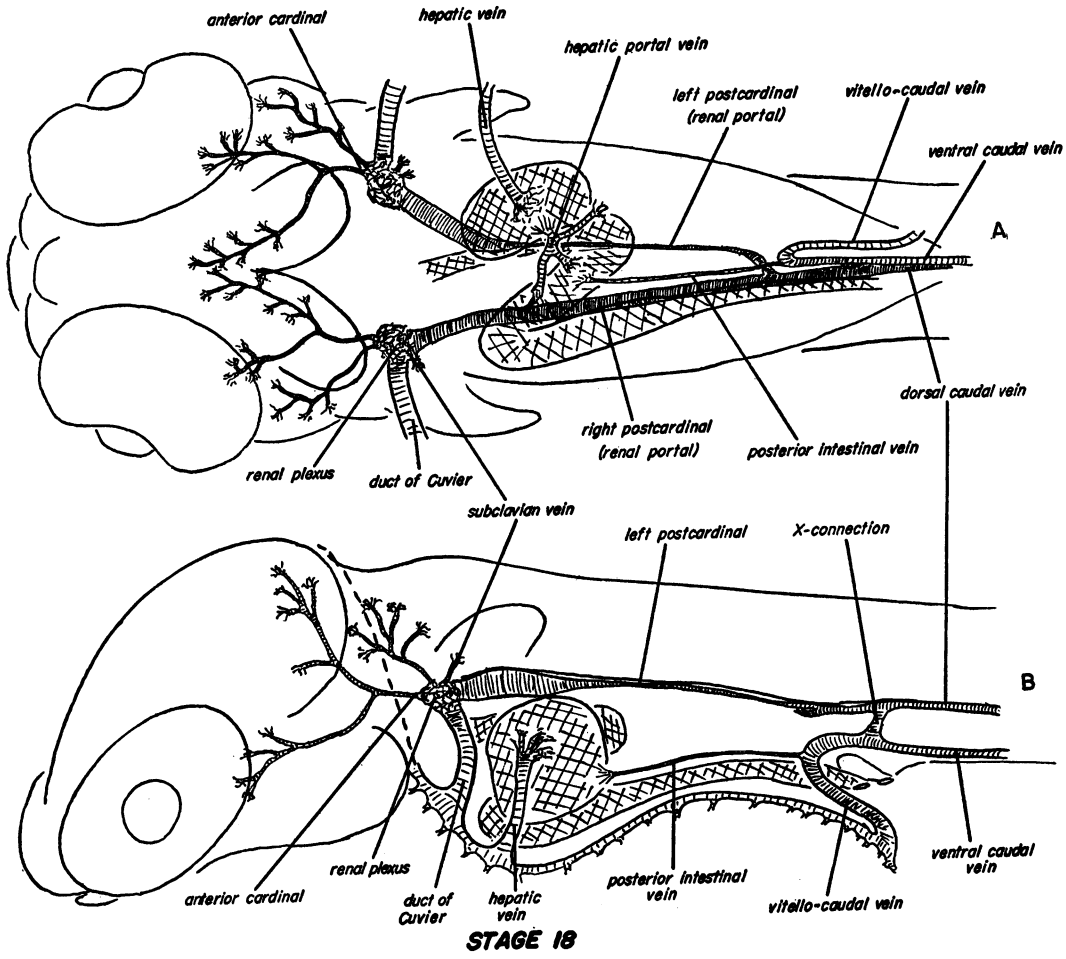

FIG. 34. Stage 18. A. Ventral view of venous system. B. Lateral view of venous system. ×60.

Length of caudal fin, 0.23 mm.

Mesencephalon width, 0.84 mm.

Small, stellate epineural and cutaneous melanophores are thinly scattered over the entire head and along the middorsal region of the body and tail. The melanophores over the mesencephalon are somewhat larger. Fine, dot-like melanophores appear in the lateral peritoneal lining (fig. 23A).

Both a dorsal and an anal fin bud are present, and the caudal fin possesses at least 10 rays (fig. 22B). The operculum, arising from the mandibular and hyoid gill arches, covers the four remaining gill arches (fig. 23B). Posterior to the last branchial arch (sixth visceral arch), the pharynx possesses a pair of shallow lateral evaginations. The latter are the vestigial seventh visceral pouches.

At the entrance of the ductus choledochus into the intestine, a ventral saccular outgrowth representing the gall bladder is present (fig. 23B). The diffuse pancreas also originates at this point and extends caudad, scattered in small lobules in the mesentery and the enteric serosa. The compact cephalic lobe of the pancreas possesses no crypts or ducts, and its cells are strongly basophilic (fig. 23B). On the basis of its origin, position, and morphology, it is possible that it represents the homologue of islets of Langerhans tissue of the pancreas. The spleen, a highly

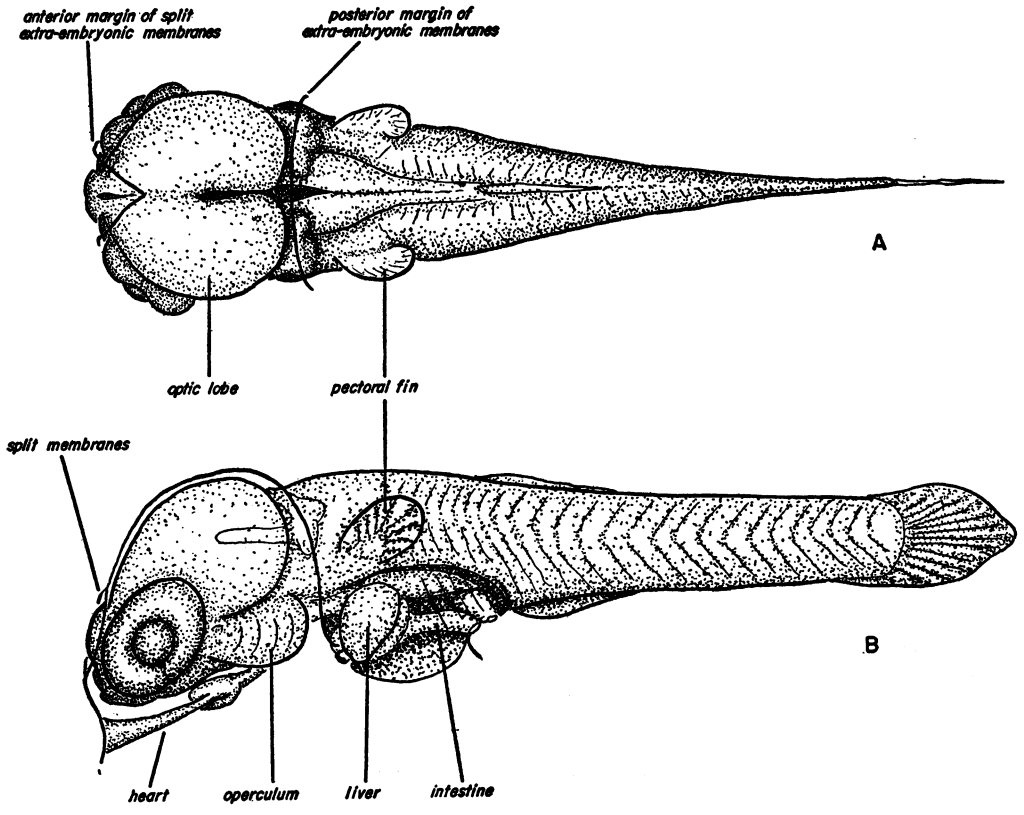

FIG. 35. Stage 19. A. Dorsal view. B. Lateral view. ×30.

vascular lymphoid structure, is present at this level to the right of the pancreas (fig. 23B).

The swim bladder has enlarged laterally (to the right side) and posteriorly (figs. 22B, 23B). This new portion, however, possesses a squamous epithelium, in contrast to the basal and left regions which possess a vacuolated columnar epithelium as described for stage 16.

The anterior branch of the ventral aorta has completely degenerated (fig. 14E). The posterior branch curves dorsally to supply the sixth, fifth, fourth, and third aortic arches in that order. The hyoidean (second) and efferent spiracular (first) arteries are smaller. The ventral aorta continues craniad as an unpaired external carotid artery (fig. 14E).

STAGE 18

Figures 24–34

Age, 8.4 days.
Standard length, 3.57 mm.
Length of caudal fin, 0.30 mm.
Mesencephalon width, 0.89 mm.
Yolk depth, 1.45 mm.

The anatomy of this stage is described more fully than that of other stages for the reason that, in terms of organogenesis, development here may be considered completed. Descriptions of subsequent stages will be limited, for the most part, to gross morphology and measurements.

A cephalic flexure is present here, with the telencephalon underlying the diencephalon in part (fig. 24A). The head is tightly enclosed within the pericardial extra-embryonic membranes (figs. 24B, 25A, B). The muscular and

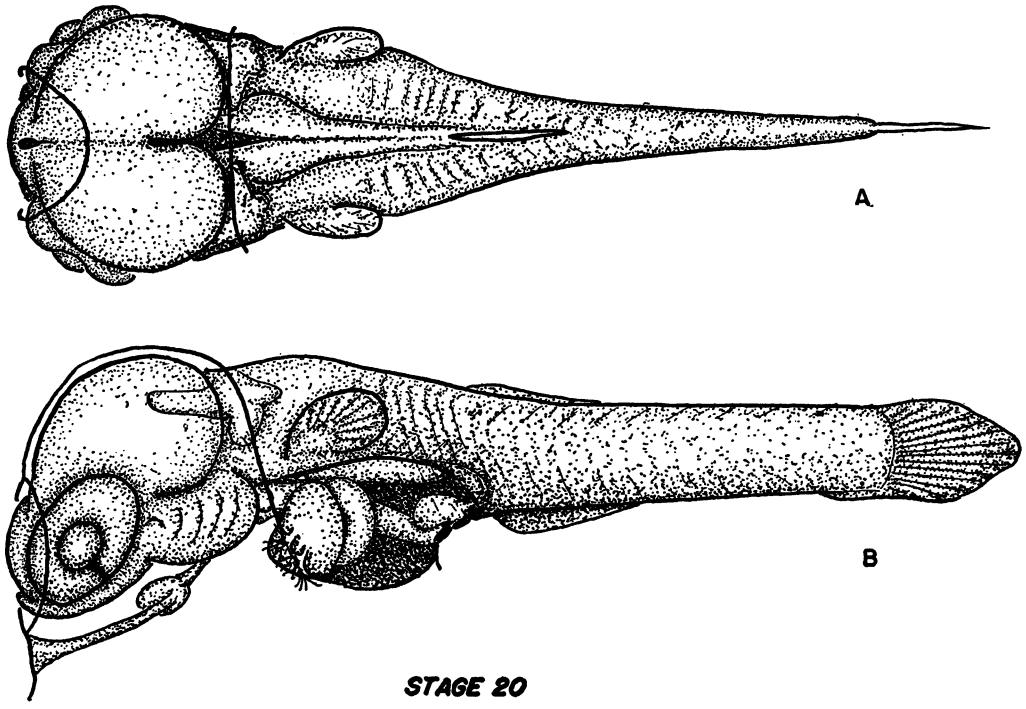

FIG. 36. Stage 20. A. Dorsal view. B. Lateral view. (Labels as in figure 35.) ×30.

skeletal systems are well developed, and embryos of this stage, when removed from the ovarian follicles, swim about rapidly and will survive in conditioned aquarium water.

The telencephalon is short, and the lateral vesicles are solid and poorly distinguishable. The olfactory bulbs are solid masses of tissue attached lateroventrally to the telencephalon (fig. 25A). The diencephalon underlies the optic lobes of the mesencephalon (fig. 25B). At the level of the optic chiasma, a small middorsal extension of the diencephalon projects through the cleft between the optic lobes, i.e., the epiphysis (fig. 26A). The large hypothalamus extends ventrad and caudad to the level of the medulla (fig. 26B). The metencephalon is short, overlain in part by the optic lobes and in part by the myelencephalon.

Three layers of the sensory layer of the retina are visible, the innermost fibrous layer, a thick ganglionic layer, and the outermost nuclear layer (fig. 25B). A thin retinal pigment layer coats the sensory layer (fig. 25B). The choroid coat of the eye consists only of a pigment layer one or two cells in thickness (fig. 26B). The optic nerve leaves the retina from the posterior ventral quadrant and runs mesiad to form the optic chiasma (fig. 26A).

The otocyst consists of a large anterior vertical canal primordium, and smaller lateral and posterior vertical primordia. A prominent ventral saccular region and a dorsal medial saccus endolymphaticus are present (figs. 24A, 26A, B, 27A, B).

The mandibular arch possesses a set of small cartilages, most prominent of which are a pair of lateral primordia of the palatoquadrates with ventral extensions, i.e., Meckel's cartilages (fig. 25B). The hyoid arch and in part the mandibular form the operculum enclosing four pairs of branchial arches (i.e., the third, fourth, fifth, and sixth visceral arches; figs. 24B, 27A, B, 28A, 32). The opercula are separate at the midventral line from the level of the fifth visceral arch, where the ventral aorta enters the base of the gill arches. Each of the branchial arches is supplied by a large, unbranched aortic arch, and blunt, rounded gill filament primordia

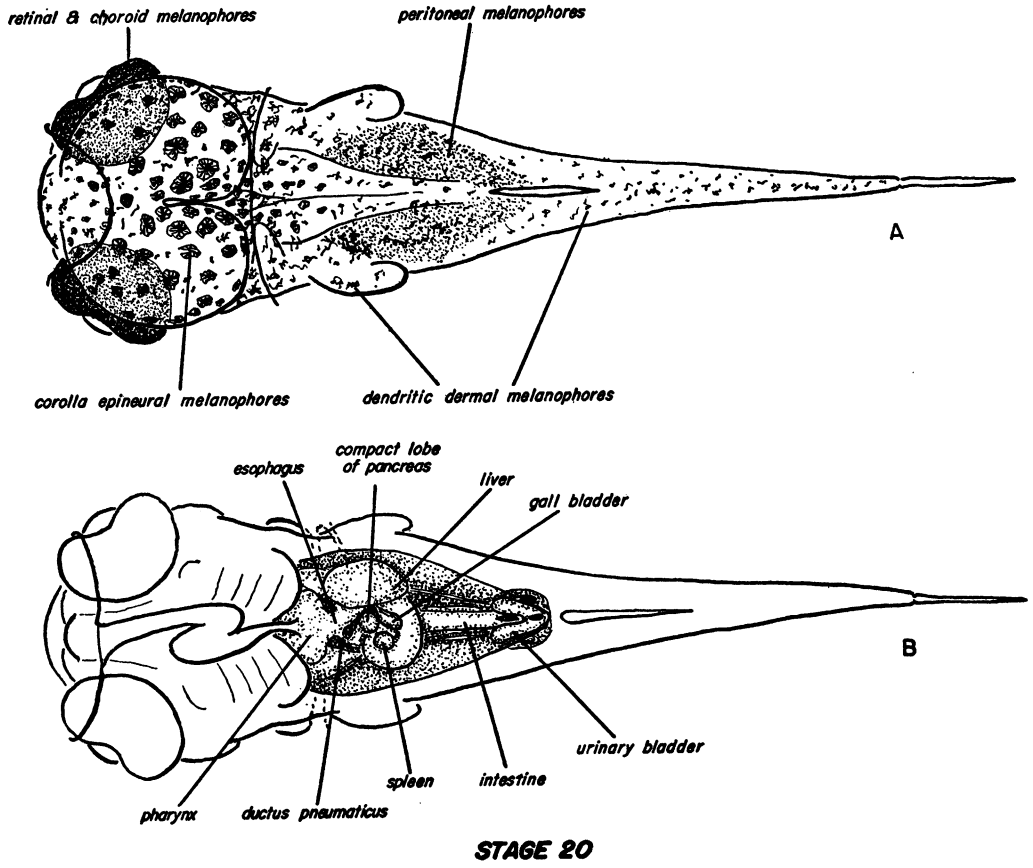

FIG. 37. Stage 20. A. Dorsal view, showing distribution of melanophores. B. Ventral view, showing viscera. ×30.

are present on the external surfaces of the gill bars (fig. 27A, B). In the posterior region of the pharynx, the roof, at the level of the third gill bar (fig. 27B), and the floor, at the level of the fourth gill and back (fig. 28A), possess rows of enamel organs which will form the pharyngeal teeth. Posterior to the fourth gill bar (sixth visceral arch), the pharynx possesses a pair of lateral evaginations which are presumed to be vestigial seventh visceral pouches (fig. 28B).

The esophagus is short, lined by cuboidal cells. This lining changes abruptly into a vacuolated columnar type at the level of the ductus pneumaticus (fig. 29B, C). The latter is a narrow duct with a fine lumen (fig. 30A). The basal portion of the swim bladder, where the duct enters, is lined by a high columnar epithelium which is greatly vacuolated and glandular in appearance (fig. 30A, B). The remainder of the swim bladder, extending to the right side and caudad almost as far as the anus, is retroperitoneal and possesses a squamous lining (figs. 30C, 31A, 32).

The gall bladder projects ventrad and craniad in the mesentery mesiad to the liver (figs. 29C, 32). The exocrine portion of the pancreas may be found in irregular masses and lobules throughout the mesentery, scattered among the coils of the intestine, and embedded in the surface of the liver (figs. 29B, C, 30B, C, 32). The compact lobe of the pancreas is located in the mesentery at the level of the spleen, situated between the spleen and the liver (figs. 30A, 32). The cells of this lobe are tightly packed and possess large, darkly staining nuclei, basophilic cytoplasm, and small, slightly basophilic granules.

The intestine, with a small circular lumen and tall columnar epithelium, possesses a

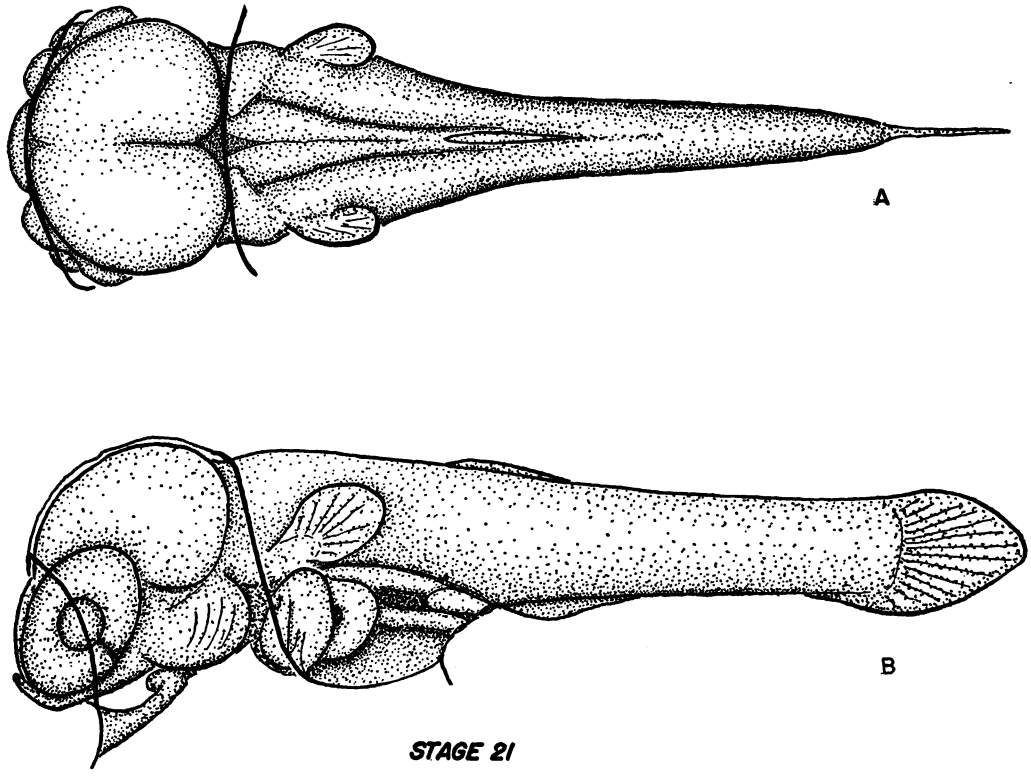

FIG. 38. Stage 21. A. Dorsal view. B. Lateral view. ×30.

single loop extending craniad, ventrad, and somewhat to the right of the midline (figs. 29B, C, 30A, C, 31A–C, 32). The character of the epithelium does not change throughout its length. The anus, at the level of the sixth myomere, has a longitudinally oriented, slit-shaped opening (figs. 31C, 32).

The anterior tip of the notochord is situated at a level just posterior to the auditory vesicle. The notochord is laterally compressed throughout its length (figs. 28A, 30C). Neurocranial cartilages are forming in the region ventral to the hind brain. Cartilage partially envelops the otocyst. Sclerotomal cartilages extend laterad from the notochord, forming the initial stages in the development of neural arches. The bases of the pectoral fins also contain cartilaginous plates.

The heart extends forward within the pericardial sac located under the head (figs. 24B, 25–27). The elongate sinus venosus drains the blood vessels of the yolk sac and the pericardial serosa. The atrial region is poorly distinguished from the sinus. The ventricle protrudes to the right of the sinu-atrium. The conus arteriosus region is not distinguishable, and the long ventral aorta curves dorsally to enter the base of the gill arches at the level of the fourth branchial arch (sixth visceral arch). The ventral aorta turns anteriorly here and gives off, in the following order, the common bases for the fifth and sixth aortic arches, the fourth arch, the third arch, and the smaller second and first arches (fig. 33A, B). The median continuation of the ventral aorta forms the external carotid. The internal carotids originate from the third aortic arches. The third and fourth aortic arches enter the dorsal aorta separately from the fifth and sixth arches (fig. 33A, B). At this point, the mesonephroi surround the dorsal aorta, and numerous renal arteries are given off (fig. 28B). Caudad, a pair of large subclavian arteries are present, and a single, ventral coeliac artery (figs. 28B, 33A, B). The latter is relatively short, ramifying out to supply the viscera. The dorsal aorta continues caudad to become the caudal artery (figs. 31A, D, F, 33A, B).

The caudal veins drain the tail region (figs.

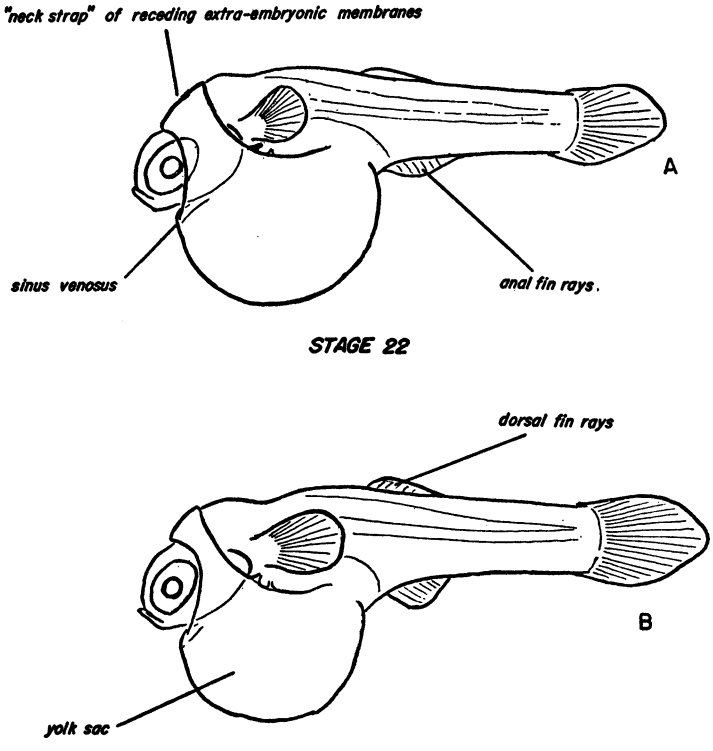

FIG. 39. A. Stage 22, lateral view. B. Stage 23, lateral view. ×15.

31D, E, F, G, 34A, B). The dorsal caudal vein runs along the dorsal aorta and in contact with it. The ventral caudal vein passes through the anal fin primordium (fig. 31G). The ventral caudal curves around craniad to the urinary bladder and runs ventrad to the right side of the intestine to form the vitello-caudal vein (figs. 31A–D, 34A, B). The long, fine, posterior intestinal vein drains into this vessel (fig. 34B). This vessel eventually becomes part of the hepatic portal system, but retains its connection with the ventral caudal vein. Three vertical cross connections are present between the dorsal and ventral caudal veins. The anteriormost is at the level of the urinary pore (figs. 31D, 34B), the second at the level of the anal fin (fig. 31F), and the third at the base of the caudal fin. The dorsal caudal vein splits anteriorly to form two postcardinals (fig. 30B), the left one being much the smaller of the two (fig. 34A, B). The dorsal caudal and postcardinal veins actually form the renal portal system, draining into the numerous renal vessels. The subclavian veins and the anterior cardinal branches also drain into the renal plexus. Two large ducts of Cuvier collect the blood from the renal plexus (fig. 34A, B). A yolk sac portal sinus forms a ring around the trunk of the embryo, extending over the head as the posterior margin of the pericardial serosa. The vessel drains the vitellocaudal vein at its anal margin (figs. 31A, B, 34B). Laterally it drains the two ducts of Cuvier and a single hepatic vein entering the portal sinus on the left side (figs. 29A, B, 34A, B).

The hepatic portal vein forms a large sinus in the mesentery at the level of the spleen (figs. 30A, 34A, B).

The mesonephroi are limited to regions lateral to the notochord at the level of the base of the pectoral fin buds (fig. 28A, B). They are highly vascularized, partially enveloping the fork of the dorsal aorta. The mesonephric ducts become distinguishable

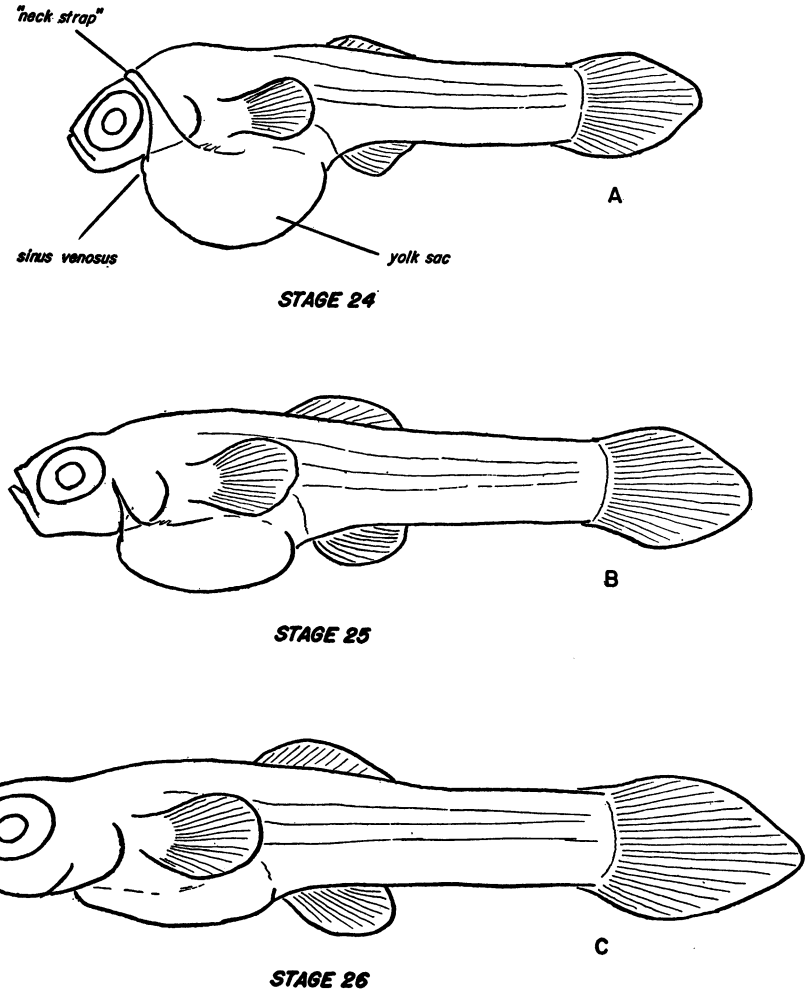

FIG. 40. A. Stage 24, lateral view. B. Stage 25, lateral view. C. Stage 26, lateral view. ×15.

near the caudal margins of the mesonephroi (fig. 29B). Here a small dorsal branch is given off by each of the ducts (fig. 29B, C). These accessory Wolffian ducts run caudad, closely appressed to the sides of the notochord. They possess a lumen, and an epithelium similar to that of the definitive ducts, and extend posteriorly to the level of the base of the swim bladder, where they end blindly.

The mesonephric (Wolffian) ducts continue posteriorly, curving ventrad in the postanal region of the coelom, and empty into the base of a somewhat bilobed urinary bladder. The elongate urinary pore is situated posterior to the anus (fig. 31A, D, E).

The gonadial ridges become evident attached to the peritoneum undercoating the membranous portion of the swim bladder (fig. 30B, C). They extend caudad as far back as does the swim bladder (fig. 31A, B). No evidence of sexual dimorphism in the gonads is visible at this stage.

The two lobes of the pituitary gland are completely separate. The infundibulum has moved back to a position posterior to the hypophysis and is poorly distinguishable from the hypothalamus. The hypophysis is detached from the stomodeal ectoderm and exhibits no differentiation into transitional, intermediate, or anterior lobes (fig. 27A). A plexus of blood vessels derived from the

"circle of Willis," described for stage 12, supplies the pituitary.

The epiphysis is small, saccate, and lodged between the optic lobes, and the connection with the diencephalon is narrowed down considerably (fig. 26A).

The thyroid makes its first appearance in this stage or in stage 17. It is present as a diffuse group of small follicles around the ventral aorta at the level of the third and fourth aortic arches (figs. 26B, 27A). In later stages it becomes increasingly difficult to locate, as it migrates caudad in individual lobules or follicles.

Stage 19

Figure 35

Age, 9.6 days.
Standard length, 3.68 mm.
Length of caudal fin, 0.32 mm.
Mesencephalon width, 1.00 mm.
Depth of yolk, 1.42 mm.

This stage is characterized by the appearance of fin rays in the pectoral fin buds. The pericardial extra-embryonic membranes begin to split here in the region in front of and between the eyes. This is the first step in the regression of these membranes.

Stage 20

Figures 36 and 37

Age, 10.9 days.
Standard length, 3.87 mm.
Length of caudal fin, 0.47 mm.
Mesencephalon width, 1.03 mm.
Depth of yolk, 1.39 mm.

The anterior margin of the pericardial serosa forms a small circle with the mouth and the front of the head protruding (fig. 36A, B). The number of melanophores has increased considerably, accompanied by the first appearance of corolla-type melanophores on the head (fig. 37A). Since these were present in all the strains of platyfish, swordtails, and hybrids studied, they may be identified as the micromelanophores.

The intestine possesses a single complete coil. The urinary bladder is large, bilobed, and opens to the exterior by a slit-shaped urinary pore. The mesonephric ducts communicate with the bladder at its most posterior margin, near the urinary pore (fig. 37B).

Stage 21

Figure 38

Age, 11.5 days.
Standard length, 3.95 mm.
Length of caudal fin, 0.63 mm.
Mesencephalon width, 1.03 mm.
Depth of yolk, 1.33 mm.

Internally, there is little difference between this stage and the previous one. The head protrudes out of the extra-embryonic membranes so that the anterior margin of the pericardial serosa encircles the head at the level of the lens.

Stage 22

Figure 39A

Age, 13.4 days.
Standard length, 4.00 mm.
Length of caudal fin, 0.79 mm.
Mesencephalon width, 1.05 mm.
Depth of yolk, 1.19 mm.

The yolk mass is further reduced, and there is a concomitant regression of the extra-embryonic membranes to form a "neck strap," covering the posterior one-third of the eye and extending posteriorly to cover most of the mesencephalic region. Fin rays in the anal fin make their first appearance here.

Stage 23

Figure 39B

Age, 15.7 days.
Standard length, 4.18 mm.
Length of caudal fin, 0.92 mm.
Mesencephalon width, 1.08 mm.
Depth of yolk, 1.14 mm.

The "neck strap" and yolk are reduced, and the former is about one-half the width of the eye and situated posterior to it. The fin rays are more distinct in the anal fin, and rays can be distinguished in the dorsal fin bud. Corolla-type melanophores are scattered thickly in the epidermis and dermis. Meningeal melanophores are smaller and stellate. Punctate melanophores are most frequent in the peritoneum and notochordal sheath, forming almost solid black sheets in the dorsal coelomic region.

Stage 24

Figure 40A

Age, 17.2 days.
Standard length, 4.45 mm.

Length of caudal fin, 1.05 mm.
Mesencephalon width, 1.11 mm.
Depth of yolk, 0.95 mm.

The "neck strap" is narrow, less than one-quarter the width of the eye, and it is sometimes broken in the middorsal region. The cephalic flexure is slightly straightened, with the tip of the lower jaw moving into a more dorsal position.

STAGE 25
Figure 40B

Age, 19.7 days.
Standard length, 5.00 mm.
Length of caudal fin, 1.34 mm.
Mesencephalon width, 1.15 mm.
Depth of yolk, 0.52 mm.

Remnants of the "neck strap" are still visible, the yolk mass is greatly reduced and flattened, and the cephalic flexure is almost completely absent.

STAGE 26
Figure 40C

Age, 21.9 days.
Standard length, 5.69 mm.
Length of caudal fin, 1.76 mm.
Mesencephalon width, 1.18 mm.

Birth usually takes place at this stage, as the embryos rupture the follicle walls and move into the ovarian cavity and into the gonoduct. The remaining yolk is completely enclosed within the abdominal cavity, but is still visible through the thin belly epidermis. The heart has now assumed its definitive position, with the sinu-atrium situated posterior to the conus and ventral aorta. Growth after birth is rapid, and the larval fish increases to almost 7 mm. within 24 hours after parturition. Macromelanophores in the wild stock of platyfish do not appear until one or more days after birth, so that only micromelanophores are present at stage 26.

REPRODUCTIVE CYCLE AND EMBRYONIC GROWTH IN *PLATYPOECILUS*

Normal *Platypoecilus* females, having attained sexual maturity (four to six months of age), begin producing broods at fairly regular intervals. The intervals between the first few broods may be irregular and vary between 26 and 90 days, but once sexual maturity is reached, if environmental conditions remain unchanged, the intervals between broods vary little from the characteristic 28 days. In young and very old females, the intervals are less regular and the numbers of young per brood are reduced. The average number of young per brood for a female in her prime is 30 to 40 and is often over 60. The reproductive cycle of *P. maculatus* is similar to that described for *X. hellerii* (Bailey, 1933), *Lebistes reticulatus* (Purser, 1938), and *Gambusia patruelis* (Ryder, 1882).

Insemination of a female is effected by means of the modified anal fin of the male. This gonopodium is a sex-hormone influenced structure, as has been shown by Cohen (1946) and M. C. Tavolga (in press). Females once inseminated will produce as many as four or more broods at twenty-eight-day intervals without further contact with males. There is evidence that sperm are stored by the female in the folds of the oviduct for periods up to seven months (Gerschler, 1914, Winge, 1922, for *Lebistes;* van Oordt, 1929, for *Xiphophorus*), and whenever successive complements of ova mature there are sperm available.

The latter fact gives rise to considerable variation in the ages of members of the same embryonic brood. Hopper (1943) described the existence of a seven-day interval between the birth of one brood and the fertilization of the next complement of eggs. During this interval, yolk is deposited and maturation of the egg takes place. Apparently all the ova of a given complement do not mature at the same rate, and therefore fertilization and the start of development are staggered over a period of 24 to 48 hours. Consequently, the ages of embryos within a single ovarian sac may vary considerably during early development. Since development is slower during the latter portion of the gestation period, the initial differences become insignificant, and

parturition of an entire brood is accomplished over a period of an hour or two.

Fertilization of the ova takes place through a follicular canal leading from the ovarian cavity to each egg. This structure was described by Bailey (1933) for *Xiphophorus* and by Purser (1938) for *Lebistes*. The fertilized ova are retained within the follicles, and all embryonic development takes place there. The follicle ruptures just before parturition, and the larval fishes find their way from the ovarian cavity through the oviduct and out through the urinogenital pore. Towards the end of the gestation period, no young embryos of the next brood are present, nor are there any mature ova. Immediately after birth of a brood, all the ova are small and contain little yolk. There is no evidence of superfoetation in this group of xiphophorin fishes, although superfoetation is common in related poeciliids (Scrimshaw, 1944a, 1944b; Turner, 1937, 1940).

It was recognized that because of the viviparous type of reproduction of the platyfish, the determination of the intra-ovarian growth rate would be difficult. An attempt to make this determination was made by Tavolga and Rugh (1947), but the quantity of material was insufficient.

The following terms were introduced by the above authors and are retained: *theoretical age*, the value, in days, determined from the date the previous brood was born, less seven days; *morphological age*, given in terms of stage numbers, established for each embryo by comparison with the graded series; *chronological age*, a calculated value representing the actual developmental time for each stage. It should be noted that the seven-day interval between birth of a brood and fertilization of the next brood is only an average value, since maturation and fertilization of a complement of ova may be spread over a period of up to 48 hours (Hopper, 1943). Actually the calculated mean value for the time of fertilization is 6.8 days, as will be shown later.

In a given embryonic brood, the frequency distribution of morphological ages approaches a normal curve of probability. Consequently, mean values of morphological ages for a given theoretical age would help to determine the chronological age. In graphic construction, plotting the arrays and means of theoretical ages against morphological age proved to be more effective. Such a graph is shown in figure 41, based upon examination of 2425 *P. maculatus* embryos. In this graph, the extremes for each morphological age group are shown, and it is obvious that there would be considerable difficulty in attempting to predict what stage of development would be present in the gravid female at any given day of its cycle. Despite the large variation, the correlation is high, with the correlation coefficient r being equal to .89 and the curvilinear correlation coefficient (correlation ratio, *eta*) being equal to .91 (calculations according to Simpson and Roe, 1939).

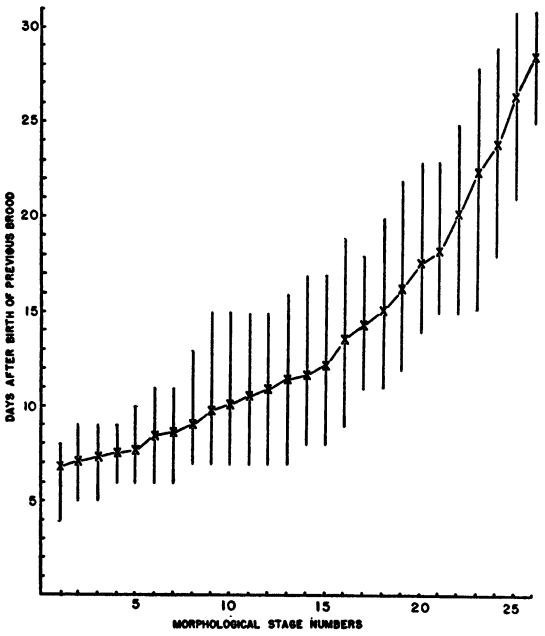

FIG. 41. Graph showing correlation between morphological age and theoretical age of *Platypoecilus* embryos. Vertical bars represent extreme range with crosses marking the mean age for each morphological stage. (See text.)

The regression curve resulting from the plotting of data given in table 2 gives a reliable estimate of the time lapse between any two embryonic stages.

The above values were used in plotting the growth curves (fig. 42). The time abscissa, in days, represents the mean values taken from the graph in figure 41, after subtracting

TABLE 2

Stage Nos.	Number of Days After Birth of Previous Brood			Mean Theoretical Age (in Days)
	Means	Standard Error	Extremes	
1	*6.8*	±0.21	4– 8	0.0
2	*7.1*	±0.20	5– 9	0.3
3	*7.3*	±0.20	5– 9	0.5
4	*7.6*	±0.18	6– 9	0.8
5	*7.7*	±0.21	6–10	0.9
6	*8.5*	±0.21	6–11	1.7
7	*8.7*	±0.20	6–11	1.9
8	*9.1*	±0.22	7–13	2.3
9	*9.8*	±0.24	7–15	3.0
10	*10.2*	±0.23	7–15	3.4
11	*10.7*	±0.22	7–15	3.9
12	*11.0*	±0.21	7–14	4.2
13	*11.6*	±0.25	7–16	4.8
14	*11.8*	±0.24	8–17	5.0
15	*12.3*	±0.22	8–17	5.5
16	*13.7*	±0.23	9–19	6.9
17	*14.5*	±0.17	11–18	7.7
18	*15.2*	±0.19	11–20	8.4
19	*16.4*	±0.17	12–22	9.6
20	*17.7*	±0.19	14–23	10.9
21	*18.3*	±0.16	15–23	11.5
22	*20.2*	±0.17	15–25	13.4
23	*22.5*	±0.14	15–28	15.7
24	*24.0*	±0.13	18–29	17.2
25	*26.5*	±0.12	21–31	19.7
26	*28.7*	±0.09	25–31	21.9

the seven-day interval so that fertilization time is zero. Actually, the more accurate 6.8-day value was subtracted, since this was the calculated average time of fertilization after the birth of a previous brood.

Three curves are plotted against the same abscissa in figure 42. The standard length of the embryos is shown on the left ordinate, and the width of the mesencephalon and depth of yolk are plotted against the right ordinate. The data for the graph in figure 42 are given in the descriptions of the individual stages.

The standard length measurements were made with the aid of a camera lucida, and in stages where a cephalic flexure was present, the length was taken along the curvature of the body axis. Determinations were begun with stage 5, at which time a measurable germinal shield first appears. Up to stage 15, standard length is equivalent to total length, but in subsequent stages the caudal fin begins to form and is not included in this series of measurements.

Head width is given in terms of the maximum width of the mid-brain. These measurements were begun at stage 9, at which stage a mesencephalon first became distinguishable. This was considered a more accurate determination of growth in width than the distance across the eyes, since the latter are pushed laterad and craniad by the growth of the optic lobes.

The diameter of the yolk remains substantially constant up to about stage 17, when utilization of yolk material is apparently accelerated. The longitudinal axis of the yolk, i.e., the one parallel to the long

axis of the embryo, changes little, even by stage 25 when most of the yolk is gone. The depth of the yolk, however, is a measurement more accurately expressing the change in yolk volume. This distance is taken from the point of entry of the duct of Cuvier into the portal system directly ventrad, perpendicular to the long axis of the embryo. In stages before the formation of any circulatory system, the yolk mass is spherical so that all axes would be equal in length.

The growth curves for both standard length and head width exhibit a roughly sigmoid shape, with a considerable reduction in slope at about the eighth and ninth day, with some recovery after the fourteenth day (fig. 42). This change in slope corresponds in time to about stage 18 in terms of morphological age. When these growth curves are compared to a curve showing the change in the size of the yolk mass (fig. 42), it is seen that the sharp reduction in yolk volume begins at stage 18 (eighth day of development). This stage also marks the most extensive development of the vascularized extra-embryonic membranes, and in subsequent stages these structures regress rapidly. A temporary "neck strap" structure, such as was described by Turner (1940), is formed during this regression.

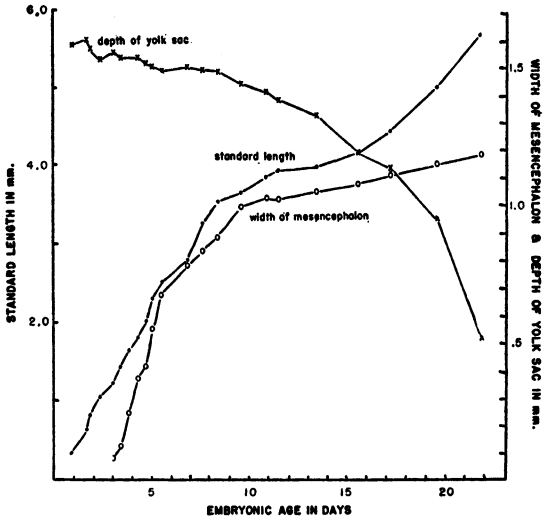

FIG. 42. Graph showing growth rates of *Platypoecilus* embryos in terms of standard length (left ordinate) and width of mesencephalon (right ordinate). The regression of the yolk mass is plotted against the right ordinate. The time scale (abscissa) was determined from data in figure 41.

DISCUSSION OF ORGANOGENESIS IN *PLATYPOECILUS*

EXTRA-EMBRYONIC MEMBRANES

The development of the pericardial amnion and the pericardial serosa, as described here and by Tavolga and Rugh (1947) for *Platypoecilus*, exhibits a remarkable similarity to the development of the amnion and serosa of avian embryos. Three important differences should be noted. One such difference lies in the initial formation of these membranes from a single layered periblastic ectoderm in the platyfish (stage 7), with a later invasion by mesenchyme (stage 11) to form a typical double-layered sac, i.e., an inner amnion and an outer serosa, both somatopleural. Second, there is the presence of a highly developed vascular plexus in the platyfish serosa. Third, the membranes enfold only the head region, and no caudal amniotic fold is present, as in avian embryos.

The function of these membranes is problematical, but it has been proposed that they possess an accessory respiratory function by Turner (1940), whose descriptions for *Platypoecilus* covered only late "neck strap" stages. Tavolga and Rugh (1947) suspected that the pericardial serosa has a nutritive, as well as a respiratory and excretory function. Support to this view is given here, since it has been shown that the regression of the membranes occurs concomitantly with an acceleration in the utilization of embryonic yolk. In addition, the work of Scrimshaw (1944b, 1945) demonstrated that closely related species of Poeciliidae, including *Xiphophorus hellerii*, are truly viviparous and gain nourishment, probably as amino acids and carbohydrates, from maternal tissue, thus giving support to the contention that the vascular pericardial serosa is a placental organ.

If the above is assumed to be true, the

simultaneous drop in the slope of the growth curve leads one to suspect that this is a rather critical period of development during which a new set of enzyme systems is brought into play and the entire nutritive pattern of the embryo is altered. Investigations concerning any possible physical and chemical changes in the yolk and in the nutritive requirements of the embryo have been planned, and results will be reported at a later date.

The nomenclature of the extra-embryonic membranes in the platyfish is that of Tavolga and Rugh (1947), rather than that of Turner (1940), for this and related species. The term pericardial amnion is used for the inner membrane, which is non-vascular and closely envelops the head. The outer pericardial serosa is thicker and highly vascularized. The cavity between the two membranes is confluent with the pericardial cavity and is termed the extra-embryonic pericardium. These terms are used in preference to Turner's "pseudoamnion" and "pseudochorion" (1940).

A similar, but less extensive, pericardium is present in the oviparous relatives of the xiphophorins. In *Fundulus* (Oppenheimer, 1937) and in *Oryzias* (Kamito, 1928; Rugh, 1941) the pericardial sac is expanded anteriorly, and the head is flexed and partially enveloped. Here, too, the pericardial membranes are vascularized and may serve as an accessory respiratory organ.

The origin of the syncytial membrane (periblast) adhering to the yolk was accurately described by Wilson (1889), as derived from the peripheral zone of junction of the early blastula. Both Wilson and Price (1934a) depicted the periblast as a thin membrane, of little morphogenetic significance, covering the entire yolk and extending under the embryonic region.

In this report the distinction between the periblast and the closely applied extra-embryonic ectoderm was not possible. In the stage descriptions, therefore, the term periblastic ectoderm was used to include the entire thin extra-embryonic tissue, and it is this tissue, in front of the head, which gives rise to the primordium of the extra-embryonic pericardial membranes. The extent to which the syncytial periblast plays a role in the formation of the definitive extra-embryonic membranes is not known.

Cleavage and Gastrulation

Platypoecilus possesses a relatively small blastodisc on the animal pole and cleavage cells that are broad and flat without protruding beyond the circumference of the yolk sphere. The more typical situation, with large, globular blastomeres, is that described for oviparous fishes such as *Fundulus* (Oppenheimer, 1937), *Coregonus* (Price, 1934a), *Serranus* (Wilson, 1889), *Carassius* (Battle, 1940), and others.

The late blastula (stage 4) begins to spread over the surface of the yolk as a result of the proliferative activity of the peripheral germ ring. As one segment of the germ ring differentiates to form the germinal shield, the remainder of the germ ring migrates over the surface of the yolk, passing through a "yolk plug" stage, and eventually terminating in a small, transient blastopore. In *Platypoecilus*, the closure of the blastopore is accomplished after stage 11, with the lateral lips closing into a temporary lineolate raphe (evidently homologous to the primitive streak of avian embryos).

The posterior margin of the embryonic shield is considered homologous to the dorsal lip of the blastopore. It is a region of highly active, proliferating, undifferentiated tissue. One of the early descriptions of this structure (Agassiz and Whitman, 1885) called attention to its probable functional significance, but the potencies of this region were not demonstrated until mapping and grafting techniques came into use. The work of Pasteels on *Salmo* (1933, 1934, 1936) and the vital staining and transplanting techniques of Oppenheimer on *Perca* (1934a, 1936b), *Fundulus* (1934b, 1935, 1936a, 1936b, 1936c, 1947), and *Epiplatys* (1938) showed that the posterior margin of the embryonic shield of teleosts has potencies in common with those of the amphibian dorsal lip organizer. Little is actually known of the mechanics of endoderm and notochord formation, and whether gastrulation takes place by an involutory movement as described by Wilson (1889) or simply by a cell proliferation at the dorsal lip.

Blastopore Closure

The typical situation in teleost fishes is similar to that of the Amphibia, in that the closure of the blastopore is accomplished by a concrescence of the blastoporal lips and an eventual inclusion of the blastopore into the neurocoele during neurulation. Since neurulation in the teleosts takes place by an invagination of a solid neural keel, a neurenteric canal, as such, is never present. This sequence of events, followed by tail bud formation, has been described for teleosts in general by Morgan (1893, 1895) and Brachet (1921), and specifically for *Coregonus* (Price, 1934a), *Fundulus* (Oppenheimer, 1937), *Serranus* (Wilson, 1889), and numerous other forms.

The closure of the blastopore in *Platypoecilus* occurs considerably later than the development of a tail bud. At stage 12, the blastopore lips concresce into a lineolate raphe (or primitive streak) somewhat behind and under the well-developed tail. The only other report of this phenomenon in a teleost is that of Clapp (1891) on the toad-fish (*Batrachus tau*), and Balfour (1878) described the post-caudal blastopore as common in the elasmobranchs.

Notochord Formation

The notochord in the platyfish is described here as originating from a longitudinal split in the chorda-endoderm, a tongue of tissue arising from the dorsal lip and growing craniad along the ventral midline (stages 7 and 8).

The simultaneous origin of notochord and endoderm is apparently typical of the teleost fishes. Wilson (1889) described the formation of two lateral endodermal wings with a median notochordal primordium under which the endoderm later fuses into a single sheet. Price (1934a) reported essentially the same for the whitefish, with the additional observation that the endoderm is initially a median cord of cells which later flattens out into the two lateral sheets and the median notochord. The derivation of the notochord in *Platypoecilus* by delamination is similar to that described for the trout by Henneguy (1888).

Ectodermal Derivatives

The early development of the nerve cord is similar to that described by Wilson (1889) for the sea bass (*Serranus*). The formation of a solid neural keel is characteristic of teleost fishes. The mesencephalon is first to differentiate and remains the broadest part of the head in the form of a pair of optic lobes, as in most other teleosts. The telencephalon is small and scarcely distinguishable from the diencephalon at all stages. The hypothalamic region of the diencephalon is the largest, beginning to enlarge as early as stage 12. In later stages it projects ventrad and caudad, pushing the infundibulum into a position posterior to the hypophysis. The epithalamus possesses a tela choroidea after stage 11, and an anterior choroid plexus after stage 15. Projecting dorsad between the optic lobes is the epiphysis, originating from the posterior margin of the diencephalon. This structure becomes visible at stage 14 as a small conical projection. At stage 16 the epiphysial stalk loses its lumen. The metencephalon (cerebellum) is small and scarcely distinguishable. It becomes hidden by the expanding optic lobes. The medulla possesses a characteristic tela choroidea after stage 10 and a posterior choroid plexus at stage 14.

The appearance of a neurocoele first takes place at stage 8, simultaneously with the formation of the optic vesicles. The latter are initially solid buds, as demonstrated for *Fundulus* (Oppenheimer, 1937). By stage 9 the opticoele is fully developed and lens placodes are present. Invagination of the lens is complete at stage 11. The distinction between the thicker, columnar sensory layer and the thinner pigment layer of the retina is present at stage 10. Pigment formation does not take place until stage 13.

Pigment Formation

DuShane (1943, 1948) reviewed the experimental work demonstrating the origin of pigment forming cells from neural crest. This derivation has been shown to be common to the Amphibia, birds, and mammals. The only evidence for neural crest origin in the teleosts is an early report by Borcea (1909), in which the claim is made that in *Uranoscopus*,

Fierasfer, and *Labrax*, pigment develops in the early neural crest stage, and its subsequent migrations can be followed. The paper is very brief and gives no description of the techniques used. The problem of pigment cell origin in teleosts, then, is badly in need of clarification and confirmation.[1]

Neural crest, as such, was observed here only as cranial and spinal nerve primordia, making its first appearance as the first cranial placode in stage 9.

It is noteworthy that, in contrast to the situation in most oviparous teleosts, the initial site of pigment formation in the platyfish is the retina (stage 13), followed closely by pigment differentiation in the optic choroid layer and the epineural region of the hind-brain (stage 15). The initial epineural melanophores are the dendritic type, and the definitive corolla-type micromelanophores do not appear until stage 20. These melanophores have been interpreted as the micromelanophore type on the basis of genetic data both here and previously by Gordon (1931b). The macromelanophores do not appear normally until some time after birth. Punctate peritoneal melanophores first become visible in the lateral peritoneum at stage 17.

These melanophores are greatly affected by the presence of the "golden" gene (*st*). Initial pigment development still takes place in the retina at stage 13, but subsequent appearance of melanophores is delayed until stage 20 or 22. The number and size of the latter are greatly reduced, but a large number of xanthophores and leucophores are visible as early as stage 18.

Pigment formation in other teleosts is usually initiated on the yolk and around the heart. In *Fundulus* this occurs at a stage approximately matching stages 10 to 13 of the platyfish (Oppenheimer, 1937). In *Carassius* eye and head pigment also develop initially, but at a relatively late stage of development (Battle, 1940).

Endodermal Derivatives

In the platyfish the gut is first a solid core of cells that develops a lumen from the esophageal region caudad, by excavation rather than by invagination as described by Agassiz and Whitman (1885) and Wilson (1889). This lumen first appears in stage 10, with an intestinal portal at a level just posterior to the pharyngeal region. The pharyngeal pouches begin to invaginate at stage 11, but the body of the pharynx does not invaginate until stage 15, when the stomodaeum is well formed. This is in agreement with the observations of Wilson (1889).

The first pharyngeal pouch, although initially the largest, becomes greatly reduced by stage 15, i.e., a vestigial spiracle. Five gill clefts, representing five pharyngeal pouches, are formed by stage 15, separated by four functional branchial arches. Posterior to the last cleft, a pair of lateral evaginations from the pharynx begin to form at stage 17 and reach their maximum at stage 19, after which regression of these structures occurs. It is presumed that the latter represent the vestigial pair of seventh pharyngeal pouches.

Garman (1895) stated that many of the cyprinodonts possess small enlargements of the gut just posterior to the origin of the ductus pneumaticus and that these swellings represent poorly developed stomachs. The order as a whole, then, is characterized by the occurrence of vestigial stomachs. A similar situation was reported for a minnow (*Campostoma*) by Rogick (1931), in which the histology of the gut was described.

In ontogeny, the platyfish is shown to have a transient gastric region at one stage in its development (stage 14). This vestigial segment of the gut loses its identity in subsequent stages.

The post-anal gut (Kupffer's vesicle) arises early (stage 7), similar to its development in the whitefish (Price, 1934a). It remains shallow and groove shaped until stage 13 when it begins to invaginate further and becomes vesicular. Eventually Kupffer's vesicle contributes to the formation of the urinary bladder in *Platypoecilus*. At stage 15, the Wolffian (nephric) ducts empty into the base of the post-anal (urinary) vesicle. The vesicle is slightly bilobed and extends craniad and dorsal to the anal portion of the gut. In subsequent stages, up to stage 26, the bilobed nature of the urinary vesicle becomes

[1] The writer's attention was directed recently to a report by G. V. Lopashov (1944, Compt. Rendus (Doklady) Acad. Sci. U.R.S.S., vol. 44, pp. 169–172) in which transplantation experiments indicated a neural crest origin of pigment in teleost fishes.

more evident, the cranial end of each of the lobes coinciding with the caudal end of the gonadial ridges.

In his original description, Kupffer (as reported by Wilson, 1889) compared this early endodermal invagination (now called Kupffer's vesicle) to the allantois in the reptiles and birds. Wilson (1889) and Sumner (1904) considered this structure as a post-anal gut which represents the site of a "neurenteric streak." The homology of the latter to the neurenteric canal of the Amphibia has been maintained more recently by Rugh (1943). Price (1934a), however, stated that his observations did not confirm the above view. Oppenheimer (1937), in her description of *Fundulus* development, described the urinary vesicle as forming early in the embryo and giving rise to the bilobed urinary bladder, but she made no mention of the contribution of Kupffer's vesicle to this structure.

The first indications of thyroid tissue were found at stage 17, appearing as a loosely arranged group of follicles around the ventral aorta at the level of the third and fourth aortic arches. The follicles possess a cuboidal epithelium whose cells are basophilic (haematoxylin and eosin stain). Most of the follicles are solid until stage 18 or 19, when a lumen appears containing a small amount of colloid typical of thyroid tissue. In subsequent stages the follicles subdivide and may be found scattered in the pharyngeal tissues. The thyroid is not normally encapsulated in teleost fishes, except in the case of the sea catfish (*Galeichthys felis*) (Fowler, 1942) and the parrot fishes (Matthews and Smith, 1947).

Liver tissue begins to form at stage 14, initially by a series of solid cords of tissue ramifying from the left side of the intestine to surround and invade, in part, the left duct of Cuvier. The liver cords soon develop lumina and form a consolidated mass of tubules, with a mesodermal reticulum, drained by a single ductus choledochus (stage 15). At stage 17 a ventral diverticulum from the base of the ductus forms the gall bladder.

Pancreas tissue begins to differentiate from the intestine at stage 16, by a large number of budding cords of cells. The pancreas lobules possess lumina by stage 18, and these can be traced back to the intestine via a number of fine pancreatic ducts, all of which empty into the intestine around the base of the ductus choledochus. A single large pancreatic lobe, located anterior to the ductus choledochus and first distinguishable in stage 17, possesses no ductules and is composed of strongly basophilic cells. This structure, on the basis of its origin and position, may be the homologue of islets of Langerhans tissue.

The swim bladder formation is pre-indicated in stage 14 by a vascular plexus on the right of the intestine at the level of the vestigial stomach. At stage 15 a short duct extending to the right of the esophagus and intestine into this plexus represents the swim bladder primordium. At stage 16 the swim bladder is well formed, extending retroperitoneally, dorsal to the intestine. By stage 18 it reaches the level of the anus. The initial epithelium of the duct and that of the bladder at stage 16 consist of high columnar cells with basal nuclei and large distal vacuoles. This epithelium is retained in subsequent stages only by the duct and the basal (anterior) portion of the bladder. The lateral and caudal expansion of the bladder consists of a one- or two-layered squamous epithelium. The duct closes and degenerates shortly after birth.

Mesodermal Derivatives

Non-segmented epimere first appears in stage 8, and occasionally as many as three relatively diffuse pairs of somites may be present at this stage. Seven or eight pairs of compact somites can be distinguished at stage 9. Thirteen somites is the average number for stage 10, 19 for stage 11, and 20 to 21 for stage 12. In the latter, striated muscle fibers differentiate, and the embryo exhibits slow, twitching movements of its body and tail. Twenty-four to 25 pairs of somites are visible at stage 14, these approaching the shape of typical myotomes. The full complement of 26 myomeres is present at stage 15, and the caudal fin primordium appears concomitantly with the last myomere.

The spleen first forms from a vascular plexus originating in part from the plexus around the ductus pneumaticus and in part from the hepatic portal plexus, becoming a highly vascularized lymphoid organ. The spleen is distinguishable as a discrete organ at

stage 17, and changes little in character in subsequent stages.

The diffuse heart primordium is evident first in stage 9. Whether or not the heart primordium in the platyfish is originally a paired structure (as in *Coregonus*, Price, 1934b) is not known, since the endocardial anlagen are too diffuse to be properly interpreted. By stage 12 the vascular circuit is complete and the heart possesses an elongate sinu-atrial portion projecting craniad, a shorter bulbous ventricle protruding towards the right side, and a short ventral aorta with no distinguishable conus region. At this stage the heart is beating quite regularly, and very light pinkish-colored blood is present.

The first blood vessel to develop is the dorsal aorta, which forms in stage 10 along the midline, compressed closely between the notochord and the gut primordium. It is here that the cellular elements of the blood first appear, similar to the description given for *Coregonus* (Price, 1934b).

The nomenclature of the blood vessels as used here was interpreted from the following sources: E. S. Goodrich (1930), Bridges (1904), Sayles (1938), Hyman (1942), and Allis (1908).

The third aortic arch is first to develop and forms the base for the internal carotid artery (fig. 12). The latter initially supplies only an extensive optic plexus. As shown in figure 14, the fourth, fifth, and sixth aortic arches develop next. The last to form are the second and first arches and the external carotid, in that order. The second arch (hyoidean artery) apparently functions as an afferent spiracular (or pseudobranchial) artery, and the first arch as the efferent spiracular (or pseudobranchial), this conclusion being based on the observed direction of blood flow and flow of injection material (India ink) in living embryos.

The development of the ventral aorta, as shown in figure 14 and described for stages 13, 14, 15, 16, 17, and 18, exhibits a longitudinal splitting so that in essence the blood flow in that vessel changes from caudad to craniad. It is noteworthy that the establishment of the definitive ventral aorta coincides with a stage in development (stage 18) subsequent to which the yolk volume becomes rapidly reduced. With this reduction in yolk volume, the locus of the sinus venosus describes an arc extending caudad and dorsad until the heart eventually takes up its final position in the intra-embryonic pericardium with no intervening yolk sac portal circulation between the ducts of Cuvier and the sinus venosus.

The development of the gonads was traced up to parturition in this work and was found to agree in every particular with the description of Wolf (1931). No evidence of sexual dimorphism was observed up to birth, nor was there any sign of transformation of somatic cells into primordial germ cells.

In the development of the kidneys, the nephric duct is the first structure to form in the mesomere region (stage 11) and may be called the pronephric duct at this stage. Mesonephric tubules, occupying a limited region, appear somewhat later in stage 15, at which time the nephric ducts possess a lumen throughout and empty into the urinary bladder. At stage 17 or 18 a pair of small accessory nephric ducts arise near the caudal margin of the tubule region. These structures extend caudad for several segments and end blindly, and they have been found unchanged in form in adult *Platypoecilus* and *Lebistes*. The functional significance of the accessory nephric ducts is unknown, but it may be possible that they represent vestigial homologues of true vasa deferentia of other vertebrates, particularly elasmobranchs.

The location and origin of adrenal tissue were not detected in this work, and the solution to this question will await future work involving the utilization of special techniques for detection of chromaffin and cortical tissues. However, it was noted that most of the visceral blood vessels (stages 18 ff.), and particularly the veins, were coated by three or four layers of lenticular cells. Whether or not this represents adrenal tissue remains to be seen.

The development of the corpuscles of Stannius was found to agree with the description of Garrett (1942). Preluminal stages were found in stage 15 embryos, luminal stages at stage 17 or 18, and post-luminal stages as early as stage 19 or 20.

COMPARISON OF *PLATYPOECILUS* WITH *XIPHOPHORUS* AND HYBRIDS

WHEN SIMILARLY COLLECTED EMBRYONIC stages of *Xiphophorus hellerii*, *Platypoecilus*, and their hybrids were compared, only three points of difference were observed, namely, time of initial pigment formation, rate of growth, and rate of caudal fin development. In all other respects organogenesis in the two genera was found to be the same, the figures and descriptions for *Platypoecilus* stages being applicable to *Xiphophorus* and *Xiphophorus-Platypoecilus* hybrids, aside from the differences mentioned above.

The laboratory-bred stock of *Xiphophorus hellerii* (described in the Materials and Methods section) was used in all of this work, and this was the same stock that was used in producing the hybrids. Some additional observations are included on a collection of swordtails representing a different strain (collected at L'Encero, near Jalapa, Mexico, in 1948), but these data were kept separate since no living material of this strain was available.

The average interval between broods for *Xiphophorus hellerii* was reported as 30 days by Bailey (1933) for a domesticated stock of unknown origin and purity. In the present report, the variation in brood intervals was high (27 to 43 days, average 29.2 days), and too few females were available for a reliable determination of an average value. However, the variations were well within the limits of variability for the platyfish, so that swordtail embryonic growth stages could be plotted against the scale determined for the platyfish. In the case of the hybrids, the brood intervals were 25 to 34 days, averaging 28.6. The hybrid growth stages, then, could also be plotted against the same time scale.

TIME OF INITIAL PIGMENT FORMATION

As was shown previously for *Platypoecilus*, pigment is first visible at stage 13 in the outer retinal layer. At stage 15 iridiocytes and additional melanophores are present in the secondary choroid coat of the eye, and stellate epineural melanophores first appear (fig. 20A).

In the swordtail, however, pigment appears slightly later. Stage 13 exhibits no pigment, whereas stages 14 and 15 possess pigment granules only in the outer retinal layer. Not until stage 16 does any extraocular pigment appear. By stages 19 ff. the embryos of the two forms are indistinguishable with regard to pigmentation.

In all of the hybrids the time of initial pigment appearance and its future differentiation follow the time sequence of the platyfish parent, i.e., first in the retina at stage 13, then epineural melanophores at stage 15. In about 12 per cent of stage 12 embryos resulting from a backcross of an F_1 hybrid to *Platypoecilus*, some pigment was evident in the retinal layer. Occasional embryos of stage 14 were found with choroid and epineural pigment. Corolla-type melanophores were distinguishable as early as stage 19 in these backcross hybrids. The stages at which the various types of pigment first appear in the several strains of fish are shown in table 3.

The initial pigmentation is apparently of the micromelanophore type, since its amount and distribution are affected only by the presence of the recessive *st* gene in a homozygous condition, i.e., in the "golden" strain of the platyfish. The macromelanophore producing genes are not expressed prenatally in the platyfish, F_1, and F_2 hybrids, and the wild stock swordtail does not possess any of these genes. However, the embryos resulting from a backcross to a platyfish exhibit very few prenatal macromelanophores. The backcross to swordtails has been shown to have an intensifying effect on melanosis over that exhibited by F_1 and F_2 hybrids (Gordon, 1937; Gordon and Flathman, 1943; Gordon and Smith, 1938a). In the hybrid embryos studied here, the intensification resulted in the appearance of occasional macromelanophores on the sides of the body in stages 25 and 26, and this occurred only if the F_1 hybrid parent possessed the *Sp* factor.

TABLE 3

APPEARANCE OF PIGMENT GIVEN IN TERMS OF MORPHOLOGICAL STAGE NUMBERS

	P. maculatus	*X. hellerii*	F_1 Hybrids	F_2 Hybrids	$F_1 \times X.$ *hellerii* Hybrids	$F_1 \times P.$ *maculatus* Hybrids
Retinal pigment	13	14	13	13	13	12–13
Choroid pigment	15	16	15	15	15	14–15
Dendritic epineural melanophores	15	16	15	15	15	14–15
Punctate peritoneal melanophores	17	18	17	17	17	17
Dendritic dermal melanophores	17	18	17	17	17	17
Corolla-type melanophores	20	20	20	20	20	19–20

GROWTH RATES

Figure 43 shows the mean standard lengths of embryos of *Platypoecilus* and *Xiphophorus* plotted against time. After about the ninth day (stages 19 ff.) the growth rate of the swordtail is somewhat faster, and the larval fish are usually about 1 mm. longer at birth than the platyfish. The change in the slope of the curve from stage 18 is less well defined than that of *Platypoecilus*. The differences between the terminal segments of the two curves are considered significant, since there is very little or no overlap in the distribution of points about the means.

When the above growth rates were compared with those of *Platypoecilus-Xiphophorus* hybrids, it was found that, past stage

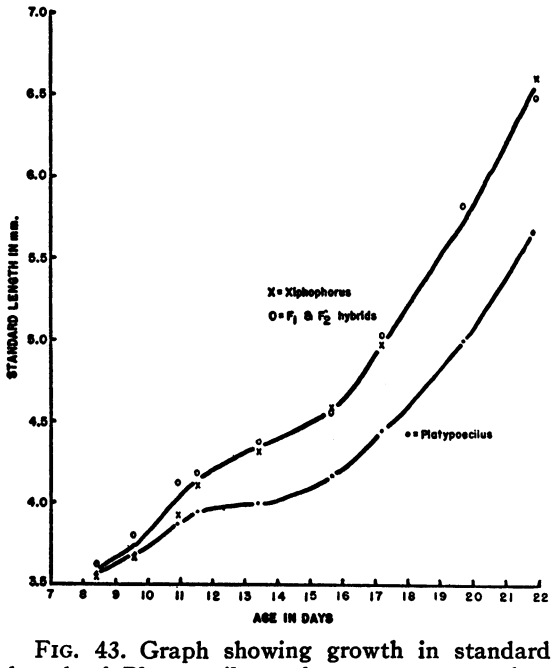

FIG. 43. Graph showing growth in standard length of *Platypoecilus* embryos, as compared to that of *Xiphophorus*, and of F_1 and F_2 hybrid embryos.

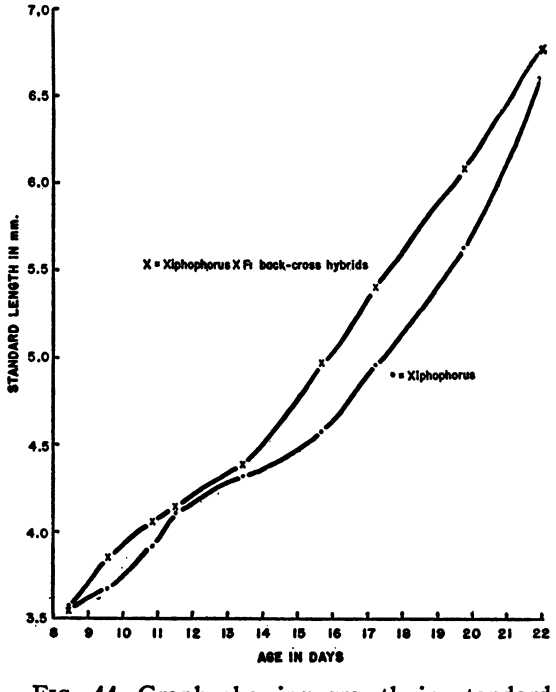

FIG. 44. Graph showing growth in standard length of *Xiphophorus* embryos, as compared to that of embryos resulting from a backcross of F_1 hybrids to *Xiphophorus*.

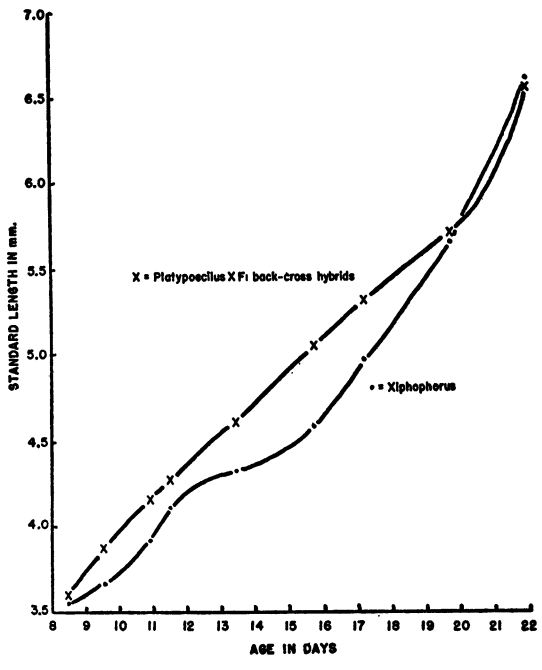

FIG. 45. Graph showing growth in standard length of *Xiphophorus* embryos, as compared to that of embryos resulting from a backcross of F_1 hybrids to *Platypoecilus*.

18, all the hybrids either coincided with or exceeded the growth rate of the swordtail (figs. 43, 44, 45). The distinction between the hybrids and the platyfish, therefore, is very sharp.

The F_1 and F_2 embryos followed the growth curve of the swordtail very closely, although the variability in the hybrids was somewhat greater. Whether or not the latter difference is statistically significant is unknown, since insufficient data were available for a comparison of variabilities. Figure 43 shows a single curve for combined data on *Xiphophorus*, F_1, and F_2 hybrids.

The backcross hybrids (both types) ex-

TABLE 4

MEAN STANDARD LENGTHS IN MILLIMETERS

Stage Nos.	*P. maculatus*	*X. hellerii*	F_1 Hybrids	F_2 Hybrids	$F_1 \times X.$ *hellerii* Hybrids	$F_1 \times P.$ *maculatus* Hybrids
5	.35	.35	.35	.34	.35	.34
6	.64	.62	.64	.64	.65	.65
7	.82	.83	.80	.80	.81	.82
8	1.06	1.08	1.06	1.04	1.04	1.06
9	1.23	1.22	1.22	1.23	1.24	1.25
10	1.45	1.45	1.47	1.43	1.48	1.46
11	1.67	1.64	1.64	1.68	1.70	1.67
12	1.81	1.78	1.79	1.84	1.81	1.83
13	2.02	2.07	2.05	2.01	1.97	2.05
14	2.31	2.28	2.28	2.30	2.33	2.30
15	2.52	2.58	2.53	2.50	2.49	2.51
16	2.80	3.13	2.95	2.89	2.96	2.88
17	3.29	3.31	3.24	3.37	3.29	3.33
18	3.57	3.55	3.61	3.62	3.54	3.58
19	3.68	3.67	3.79	3.81	3.85	3.87
20	3.87	3.92	4.13	4.13	4.05	4.16
21	3.95	4.11	4.17	4.19	4.14	4.27
22	4.00	4.32	4.40	4.39	4.38	4.60
23	4.18	4.58	4.56	4.55	4.96	5.04
24	4.45	4.96	5.01	5.02	5.40	5.30
25	5.00	5.64	5.80	5.83	6.08	5.69
26	5.69	6.60	6.47	6.49	6.78	6.54
Correlation coefficients	.91	.90	.89	.87	.91	.91

ceeded the growth rate of the swordtail in part (figs. 44, 45), but the differences here are of a low order of significance.

The correlation coefficients for the individual curves ranged from .87 to .91, all of a high order of significance. The mean values for standard lengths of embryonic stages of the pure species and the hybrids are given in table 4.

A group of embryos was obtained from *Xiphophorus* females collected by Gordon, Atz, and Wood at L'Encero, in 1948. Although this group of females did not appear to exceed laboratory-raised animals in size, the dimensions of the embryos were considerably larger than those of the laboratory strain. The disparity in size is evident in very early stages. There was also a difference in egg size between the two strains. The egg diameter for the laboratory-bred Zacatispan strain averaged 1.6 mm. and for the L'Encero strain 2.3 mm. Table 5 shows a comparison between the L'Encero strain and the laboratory-bred *Xiphophorus hellerii*. The comparison cannot be made graphically since no living L'Encero females were available and nothing is known of their developmental rate and the length of the brood intervals. In addition, it is not known whether the differences may be ascribed to genetic diversity or to environmental conditions.

TABLE 5

MEAN STANDARD LENGTH MEASUREMENTS IN MILLIMETERS OF *Xiphophorus hellerii*

Stage Nos.	Zacatispan Strain (Laboratory Bred)	L'Encero Strain (Field Bred)
7	.83	.79
8	1.08	1.11
9	1.22	1.32
10	1.45	1.58
11	1.64	1.82
12	1.78	2.10
13	2.07	2.45
14	2.28	2.61
15	2.58	2.95
16	3.13	3.87
17	3.31	4.63
18	3.55	5.02
19	3.67	5.27
20	3.92	5.79
21	4.11	6.32
22	4.32	6.61
23	4.58	7.10
24	4.96	7.89
25	5.64	8.68

GROWTH OF THE CAUDAL FIN

As was described in the previous section on *Platypoecilus*, the caudal fin begins to differentiate at stage 15 (eight days; fig. 19B) and fin rays appear at stage 16 (fig. 21B). This occurs just after the full complement of myomeres is attained, the normal number being 26. (The numbers of somites, myotomes, myomeres, and vertebrae are

considered equal.) The normal number of body and tail segments in *Xiphophorus* is 28 (Gordon and Benzer, 1945), and the last two segments are not formed until stage 16, one stage later than in the platyfish. The initial differentiation of the caudal fin in *Xiphophorus* is also one stage later, i.e., stage 16

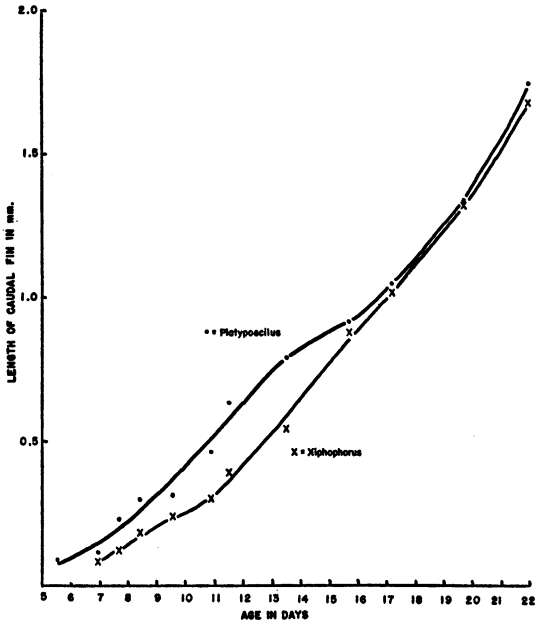

FIG. 46. Graph comparing rate of embryonic caudal fin differentiation in *Platypoecilus* to that of *Xiphophorus*.

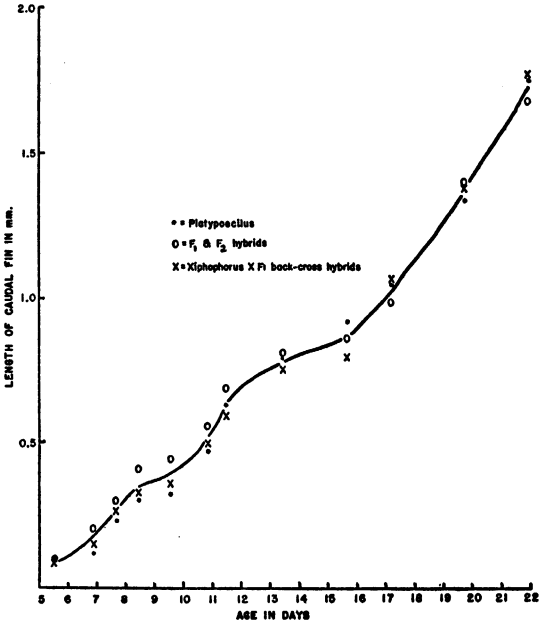

FIG. 47. Graph showing similar rate of embryonic caudal fin differentiation in *Platypoecilus*, F_1 and F_2 hybrids, and embryos resulting from a backcross of F_1 hybrids to *Xiphophorus*.

TABLE 6

LENGTH OF CAUDAL FIN IN MILLIMETERS

Stage Nos.	*P. maculatus*	*X. hellerii*	F_1 Hybrids	F_2 Hybrids	$F_1 \times X.$ *hellerii* Hybrids	$F_1 \times P.$ *maculatus* Hybrids
15	.09	—	.09	.09	.08	.07
16	.12	.08	.20	.21	.15	.14
17	.23	.12	.31	.30	.27	.24
18	.30	.18	.41	.41	.33	.29
19	.32	.24	.43	.44	.36	.36
20	.47	.30	.57	.56	.50	.69
21	.63	.39	.66	.69	.59	.82
22	.79	.54	.82	.81	.76	.91
23	.92	.88	.86	.86	.80	1.01
24	1.05	1.02	.97	.99	1.07	1.23
25	1.34	1.33	1.42	1.41	1.38	1.61
26	1.76	1.69	1.70	1.69	1.78	1.88
Correlation coefficients	.79	.85	.86	.87	.83	.80

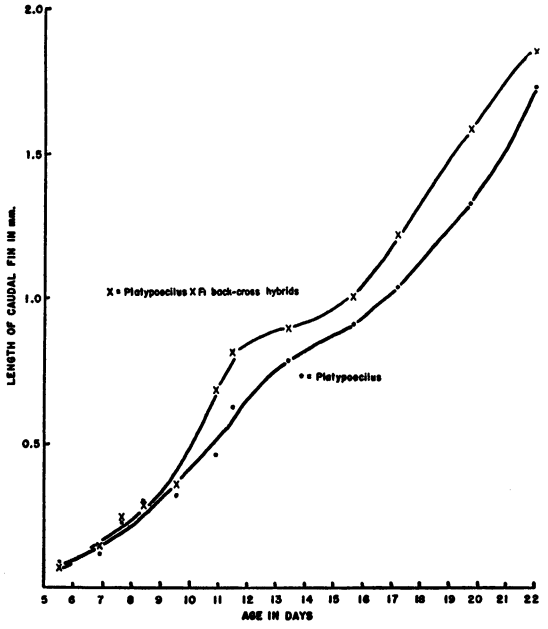

FIG. 48. Graph comparing rate of embryonic caudal fin differentiation in *Platypoecilus* to that of embryos resulting from a backcross of F_1 hybrids to *Platypoecilus*.

(about nine days), with fin rays appearing at stage 17. This is shown by figure 46, which also shows that, although initial differentiation of this structure in the swordtail is delayed, at birth it is not significantly different in size from that of the platyfish.

In a comparison of the rate of caudal fin differentiation in the pure species with that of the hybrids, it was seen that initial differentiation occurs at stage 15, as in the platyfish, and this is true even among the embryos resulting from a backcross of an F_1 hybrid to a swordtail. The latter embryos and the F_1 and F_2 embryos follow the platyfish very closely in terms of rate of caudal fin growth and its final dimensions (fig. 47). The group resulting from a backcross to a platyfish exceeds the parental type in caudal fin growth rate and reaches dimensions above the average for the platyfish and the other hybrids (fig. 48).

Table 6 summarizes the data upon which the graphs in figures 46, 47, and 48 were based.

FECUNDITY OF HYBRIDS

Among all the *Platypoecilus* embryonic broods examined in this work, occasional abnormalities were found. The most common of these were the occurrence of over-ripe, unfertilized ova and degenerate gastrulae or blastulae (described under stage 1). Abnormalities in later stages were exceedingly rare, represented by a total of nine partially disintegrated embryos of stage 13, 16 embryos with curved and retarded tails found at the rate of one or two in a brood, one acephalic embryo, and one two-headed embryo of stage 16. The average frequency of abnormalities of all previously mentioned types was 4.2 per cent per embryonic brood.

The frequency of occurrence of anomalies was distinctly higher in the "golden" strain of platyfish, and as many as 23 per cent of the embryos of stages 18 to 26 were found to be dead and degenerating.

Anomalies in embryonic broods of *Xiphophorus* were found at a slightly lower frequency than in the platyfish, i.e., 3.4 per cent per embryonic brood.

The same types of abnormalities were found in the embryonic broods of the various types of hybrids used in this work, but the most frequent types were delayed or anomalous gastrulae and later stages with curled or retarded tails. The abnormal shapes of the tails were the result of an unevenly developed notochord which often assumed a spiral shape. The frequency of occurrence of the anomalies was found to be correlated with the particular pattern genes involved in the cross (table 7). As described in the Materials and Methods section, the F_1 hybrids possessed either of two genes for macromelanophores, *Sp* (spots on the sides) or *Sd* (spot on the dorsal fin). The expression of these genes in the hybrids results in a melanotic or melanomatous condition (as described and defined by Gordon and Smith, 1938a). Anomalies among F_1 embryos were infrequent. Out of 33 F_1 females of the *Sp* type, only two females proved to be completely sterile, and three possessed aberrant broods, with over 30 per cent anomalous embryos. The total frequency of anomalies in the latter was 8.7 per cent per embryonic brood.

TABLE 7

FERTILITY AMONG FEMALES OF *Platypoecilus*, *Xiphophorus*, AND THEIR HYBRIDS

Strains or Species	Total No.	No. Sterile	No. with Aberrant Embryonic Broods (i.e., with Over 30% Anomalies)	No. Producing Abortive Broods (i.e., Less than 6 Fish per Brood)	Average Frequency of Anomalous Embryos per Embryonic Brood
Pure species					
P. maculatus, wild stock, inbred	89	2	2	2	4.2%
P. maculatus, golden strain	10	0	1	3	23 %
X. hellerii, wild stock, inbred	23	0	0	0	3.4%
Platypoecilus-Xiphophorus hybrids					
P. maculatus ♀ × *X. hellerii* ♂	12	0	0	0	1.1%
F_1 *Sp* ♀ × F_1 *Sp* ♂	10	1	1	1	
F_1 *Sp* ♀ × F_1 *Sd* ♂	4	0	0	1	8.7%
F_1 *Sp* ♀ × *X. hellerii* ♂	12	0	0	1	
F_1 *Sp* ♀ × *P. maculatus* ♂	7	1	0	0	
F_1 *Sd* ♀ × F_1 *Sp* ♂	11	3	3	1	
F_1 *Sd* ♀ × F_1 *Sd* ♂	6	3	2	0	31 % 47%
F_1 *Sd* ♀ × *X. hellerii* ♂	9	4	2	0	
F_1 *Sd* ♀ × *P. maculatus* ♂	8	5	2	1	82 %
P. maculatus ♀ × F_1 *Sd* ♂	5	0	0	0	0

This held for all types of crosses, backcross or inbred, using both *Sp* and *Sd* hybrid males. An embryonic brood possessing a 30 per cent or higher incidence of anomalous stages is considered aberrant.

Out of 34 *Sd* hybrid females, 15 were completely sterile and 11 possessed aberrant broods or gave birth to abortive broods of one to five individuals. The embryonic anomalies occurred with a frequency of 47 per cent per embryonic brood. *Sd* females crossed to hybrid males or swordtail males exhibited an average of 31 per cent anomalies per embryonic brood, and when backcrossed to platyfish males the frequency was 82 per cent. In the reciprocal cross, using *Sd* males, no anomalies were found.

See table 7 for list of crosses used, with total number of females, number of sterile females, and those females that produced aberrant or abortive broods.

Part of the records on sterility were kindly supplied by Miss Eugenie Clark of the Department of Animal Behavior of the American Museum of Natural History from unpublished data, and all her records on sterile female hybrids indicated that motile sperm were recovered from the oviducts after copulation.

DISCUSSION OF THE EFFECTS OF HYBRIDIZATION ON DEVELOPMENT

In 1948 Myron Gordon reviewed a series of his papers on the genetics of melanomas in fishes. He showed how melanosis may be induced in *Platypoecilus-Xiphophorus* hybrids if certain pattern genes are present in the platyfish parent. In all cases the genes necessary were those producing patterns of macromelanophores. The melanosis in F_1 hybrids frequently developed into a melanomatous condition, which could be further intensified by backcrossing the hybrid to the swordtail. The site of the melanoma could be predicted

on the basis of which of the several genes was used, i.e., members of the sex-linked, dominant, allelic series—*Sp* (spots on the sides), *Sd* (spot on the dorsal fin), *Sb* (spotted belly), *N* (broad black lateral band), and *Sr* (stripes on the sides). The genes *Sp*, *Sb*, and *N* produce the most intense melanosis and the most destructive melanomas. The genes *Sd* and *Sr* were expressed later in life and produced a more localized melanotic condition in hybrids (Gordon, 1948; Levine, 1948).

In 1943 Gordon and Flathman showed how the intensified melanosis produced by a backcross to *Xiphophorus* was expressed in late embryonic stages. The pattern gene utilized was *N*, forming a broad, black, lateral band of macromelanophores. A similar prenatal melanosis was described by Gordon and Smith (1938a), in which case the *Sp* gene was used. Gordon (1946) showed that the stock fishes used previously were "domesticated" and consequently were not pure *Platypoecilus* but possessed swordtail genes acquired by introgressive hybridization. The *N* and *Sp* genes used earlier may have been associated with some intensifying modifiers inherited from the swordtail. It is not surprising, therefore, that no such effects were observed in the present paper, since exclusively wild-type macromelanophore genes were used.

The effect of hybridization on embryonic growth rate somewhat paralleled the production of melanosis. The hybrids all fell in with the more rapidly developing of the two parental species, at least with respect to growth and caudal fin differentiation.

One possible genetic explanation of hybrid melanosis was that offered by Gordon (1948), which involved the assumption that the swordtail possesses dominant modifiers *A* and *B*. Either of these genes combined with a platyfish macromelanophore factor would produce melanosis, and when, by backcrossing, both *A* and *B* are present, the melanosis is further intensified. A somewhat similar explanation may be applied to results described here.

In the case of the body growth rate, the growth modifiers of the swordtail appear to be dominant, since both F_1 and F_2 hybrids followed the growth rate of *Xiphophorus*. A slight intensification was achieved by backcrossing to *Xiphophorus*. The fact that the same result was obtained in *P. maculatus* backcross hybrids seems to indicate that not only were a large number of dominant genes involved but that a reassortment with certain platyfish genes exhibited the effects of heterosis.

With regard to the growth of the caudal fin, the reverse situation obtained. The F_1 and F_2 hybrids developed a caudal fin at a rate coinciding with that of the platyfish parent. Backcrossing to *P. maculatus* distinctly intensified the development of this structure, indicating the accumulation of more platyfish modifiers.

It was shown here that the swordtail initially develops pigment at a slightly later stage than does the platyfish. All the hybrids formed pigment at the same stage the platyfish did and often earlier. This was particularly true of the *P. maculatus* backcross hybrids, indicating again that the one parental species possessed numerous dominant modifiers, in this case the platyfish having genes for earlier melanin formation. This has no apparent direct bearing on hybrid melanosis, since the effect is primarily on the micromelanophores, and the macromelanophores do not differentiate until after birth. It is quite likely that the site of origin of micromelanophores and macromelanophores is the same, but it is not known just when a pigment cell acquires the specific potency for either one or the other of the two types, or if non-pigmented micromelanophores are the direct source of macromelanophores. In 1937 Gordon reported the effect of the golden gene (*st*) on the expression of the macromelanophore genes. The *st* gene is to be found only in domesticated stocks. It is a recessive mutant, producing a great reduction in the number of micromelanophores. This mutation was traced back by Gordon (1935) as probably occurring during the early years of tropical fish culture and later introduced into the swordtail by introgressive hybridization (1946b). Although the *st* gene affects the micromelanophores primarily, Gordon (1927, 1937) showed that it also produced a reduction in the numbers of macromelanophores. There is, then, some interaction between the two kinds of melanophores and the factors controlling their expression.

In *Platypoecilus* certain genes have been

found to reduce viability. The behavior of two such genes has been described by Gordon (1948). The albino gene, arising as a mutant in domesticated stocks of swordtails, produced aberrant Mendelian ratios as a result of embryonic lethal effects (Gordon, 1942). The gene for golden, also arising during domestication, is described here as being associated with poor viability among embryos. However, hybridization produced not only embryonic death but complete sterility, as shown by Gordon (1946a).

Gordon (1946a) reported that F_1 hybrid fishes exhibited a large percentage of sterility and highly aberrant sex ratios. The cross originally was between a *Xiphophorus hellerii* female and a *Platypoecilus maculatus* male, the latter possessing the *Sr* gene on the X-chromosome and the *Sd* gene on the Y-chromosome. As expected, 50 per cent of the offspring were of the *Sr* type and were all fertile females. Of the remaining hybrids, possessing the *Sd* factor, only about 8 per cent were fertile males and females, and 92 per cent were sterile. Both the sterility and the aberrant sex ratio were explained on the basis of a multifactorial sex-determining mechanism of the swordtail as opposed to the digametic type in the platyfish, the sterility being associated in the hybrids with the presence of the platyfish Y-chromosome.

It should be noted that in the present work the fundamental cross was the recriprocal of the above. The female was a platyfish with one X-chromosome marked by the *Sd* gene, and the other by *Sp*. No platyfish Y-chromosome was involved, and yet sterility and poor viability were of frequent occurrence and associated almost entirely with the *Sd* gene. The sex ratio was aberrant, with females predominating. The same cross was reported by Gordon in 1948, but the results given at that time were based on incomplete data. Additional data have tended to corroborate the observations made here (Gordon, personal communication).

Two possible explanations are presented here. The *Sd* factor itself may possess some lethal effect which is expressed when swordtail modifiers are present. On the other hand the lethal factor may be linked to the *Sd* gene by virtue of its being on the same chromosome, and be expressed when dissociated from its allele as a result of hybridization. The lethal effect is apparently one that is inherent in the female parent rather than in the embryos, since the use of *Sd* hybrid males in matings with *Sp* hybrid females or *P. maculatus* females produced viable offspring. The final explanation of this linkage of embryonic lethal effects and sterility with the *Sd* gene will depend upon additional crosses and analyses of sterility data.

SUMMARY

1. EMBRYONIC DEVELOPMENT of the viviparous poeciliid fish *Platypoecilus maculatus* may be conveniently divided into 26 stages for descriptive purposes.

2. The embryonic growth rate for *P. maculatus* is determined by comparison of morphological age (in terms of embryonic stage) with theoretical age (days after the birth of a previous brood). This comparison is based on a series of embryonic broods obtained by laparotomy at various times during the twenty-eight- to thirty-day reproductive cycle of this species.

3. A study of growth and organogenesis in *P. maculatus* reveals the following features:

A. The concomitant regression of the extra-embryonic membranes and the yolk mass is accompanied by a drop in the slope of the growth curve.

B. The initial formation of the extra-embryonic membranes takes place in a manner similar to that in the "amniotes."

C. Cleavage, gastrulation, and neurulation follow a course basically similar to that of other teleosts.

D. Blastopore closure occurs after tail bud formation.

E. The notochord forms directly from endoderm by delamination.

F. Pigment formation is evident first in the retina and subsequently in the choroid and meningeal coats.

G. Kupffer's vesicle (post-anal gut) contributes to the development of the urinary bladder.

H. The formation of the ventral aorta and aortic arches is described with regard to the reversal of blood flow in the ventral aorta and the change of position of the sinus venosus during yolk regression.

4. Comparisons with other species of *Platypoecilus* (*P. variatus*, *couchianus*, and *xiphidium*) reveal no significant differences in embryonic development.

5. *Platypoecilus maculatus* development, compared to that of *Xiphophorus hellerii* and *Platypoecilus-Xiphophorus* hybrids, shows the following differences:

A. Initial pigment differentiation in *Xiphophorus* occurs one stage later than in *Platypoecilus*. The hybrids form pigment at the same stage as *Platypoecilus* or earlier.

B. Over the same period of time, *Xiphophorus* embryos attain a larger size than *Platypoecilus* embryos. The growth rates of the hybrids all coincide with or exceed those of *Xiphophorus*.

C. Caudal fin differentiation is one stage later in *Xiphophorus* than in *Platypoecilus*. However, all the hybrids form a caudal fin at the same rate as *P. maculatus*, and the $F_1 \times$ *Platypoecilus* backcross hybrid embryos exceed both parental species in this respect.

6. Sterility and embryonic anomalies are frequent among hybrid females. This is particularly true of F_1 females possessing the *Sd* (spotted dorsal fin) character, indicating a linkage of lethal factors with this pattern gene.

LITERATURE CITED

AGASSIZ, L., AND C. O. WHITMAN
1885. On the development of some pelagic fish eggs. Preliminary notice. Proc. Amer. Acad. Arts and Sci., vol. 20, pp. 23–75.

ALLIS, E. P., JR.
1908. The pseudobranchial and carotid arteries in the gnathostome fishes. Zool. Jahrb., vol. 27, pp. 103–134.

BAILEY, R. J.
1933. The ovarian cycle in the viviparous teleost, *Xiphophorus hellerii*. Biol. Bull., vol. 64, pp. 206–225.

BALFOUR, F. M.
1878. A monograph on the development of elasmobranch fishes. London, Works of Francis Maitland Balfour, Macmillan and Co., 1885.

BATTLE, H. I.
1940. Embryology and larval development of the goldfish (*Carassius auratus* L.). Ohio Jour. Sci., vol. 40, pp. 82–93.

BORCEA, M. I.
1909. Sur l'origine du coeur, des cellules vasculaires migratrices et des cellules pigmentaires chez les téléostéens. Comp. Rend. Acad. Sci. Paris, vol. 149, pp. 688–689.

BRACHET, A.
1921. Traité d'embryologie des vertebrétés. Paris, Masson et Cie.

BRIDGE, T. W.
1904. Fishes, exclusive of the systematic account of Teleostei. Cambridge Natural History, vol. 8, pp. 141–537.

CLAPP, C. M.
1891. Some points in the development of the toadfish (*Batrachus tau*). Jour. Morph., vol. 5, pp. 494–501.

COHEN, H.
1946. Effects of sex hormones on the development of the platyfish, *Platypoecilus maculatus*. Zoologica, vol. 31, pp. 121–128.

DUSHANE, G. P.
1943. The embryology of vertebrate pigment cells. I. Amphibia. Quart. Rev. Biol., vol. 18, pp. 109–127.
1948. The development of pigment cells in vertebrates. *In* Biology of melanomas. Special Publ. New York Acad. Sci., vol. 4, pp. 1–14.

FOWLER, E.
1942. Embryology of the sea catfish, *Galeichthys felis*. (Abstract.) Proc. Louisiana Acad. Sci., vol. 6, p. 81.

GARMAN, S.
1895. The Cyprinodontes. Mem. Mus. Comp. Zool., vol. 19, pp. 1–179.

GARRETT, F. D.
1942. The development and phylogeny of the corpuscle of Stannius in ganoid and teleostean fishes. Jour. Morph., vol. 70, pp. 41–67.

GERSCHLER, W. S.
1914. Über alternative Vererbung bei Kreuzung von Cyprinodontiden-Gattungen. Zeitschr. indukt. Abstamm. Vererb., vol. 12, pp. 73–96.

GOODRICH, E. S.
1930. Studies on the structure and development of vertebrates. London, Macmillan and Co.

GORDON, MYRON
1927. The genetics of a viviparous top-minnow, *Platypoecilus;* the inheritance of two kinds of melanophores. Genetics, vol. 12, pp. 253–283.
1931a. Hereditary basis of melanosis in hybrid fishes. Amer. Jour. Cancer, vol. 15, pp. 1495–1523.
1931b. Morphology of the heritable color patterns in the Mexican killifish, *Platypoecilus. Ibid.*, vol. 15, pp. 732–787.
1935. Discovery of the gold platyfish. Jour. Hered., vol. 26, pp. 96–101.
1937. The production of spontaneous melanotic neoplasms in fishes by selective matings. II. Neoplasms with macromelanophores only. III. Neoplasms in day old fishes. Amer. Jour. Cancer, vol. 30, pp. 362–375.
1942. Mortality of albino embryos and aberrant Mendelian ratios. Zoologica, vol. 27, pp. 73–74.
1946a. Interchanging genetic mechanisms for sex determination in fishes under domestication. Jour. Hered., vol. 37, pp. 307–320.
1946b. Introgressive hybridization in domesticated fishes. I. The behavior of Comet, a *Platypoecilus maculatus* gene, in *Xiphophorus hellerii*. Zoologica, vol. 31, pp. 77–88.
1947a. Genetics of *Platypoecilus maculatus* IV. The sex determining mechanism in two wild populations of the Mexican platyfish. Genetics, vol. 32, pp. 8–17.
1947b. Speciation in fishes. Distribution in time and space of seven dominant multiple alleles in *Platypoecilus maculatus*. Advances in Genetics, vol. 1, pp. 95–132.
1948. Effects of five primary genes on the site of melanomas in fishes and the influence of two color genes on their pigmentation. *In* Biology of melanomas. Special Publ. New York Acad. Sci., vol. 4, pp. 216–269.

GORDON, M., AND P. BENZER
1945. Sexual dimorphism in the skeletal elements of the gonopodial suspensoria in xiphophorin fishes. Zoologica, vol. 30, pp. 57–72.

GORDON, M., AND F. FLATHMAN
1943. The genetics of melanoma in fishes. VI. Mendelian segregation of melanophore reaction types in embryos of a melanomatous mother. Zoologica, vol. 28, pp. 9–12.

GORDON, M., AND G. M. SMITH
1938a. Progressive growth stages of a heritable melanotic neoplastic disease in fishes from the day of birth. Amer. Jour. Cancer, vol. 34, pp. 255–272.
1938b. The production of a melanotic neoplastic disease by selective matings. IV. Genetics of geographical species hybrids. *Ibid.*, vol. 34, pp. 543–565.

HENNEGUY, F.
1888. Récherches sur la développement des poissons osseaux. Embryogénie de la truite. Jour. Anat. Physiol., pp. 413–502.

HOPPER, A. F., JR.
1943. The early embryology of *Platypoecilus maculatus*. Copeia, pp. 218–224.

HYMAN, L. H.
1942. Comparative vertebrate anatomy. Chicago, The University of Chicago Press.

KAMITO, A.
1928. Early development of the Japanese killifish (*Oryzias latipes*), with notes on its habits. Jour. Coll. Agric., Imp. Univ. Tokyo, vol. 10, pp. 21–38.

LEVINE, M.
1948. The cytology of the typical and the amelanotic melanomas. *In* Biology of melanomas. Special Publ. New York Acad. Sci., vol. 4, pp. 177–215.

MATTHEWS, S. A., AND D. C. SMITH
1947. Concentration of I^{131} by the thyroid gland of the Bermuda parrot-fish. (Abstract.) Anat. Rec., vol. 99, p. 36.

MORGAN, T. H.
1893. Experimental studies on the teleost eggs. Anat. Anz., vol. 8, p. 803.
1895. The formation of the fish embryo. Jour. Morph., vol. 10, pp. 419–472.

OPPENHEIMER, J.
1934a. Experimental studies on the developing perch (*Perca flavesens* Mitchill). Proc. Soc. Exp. Biol. Med., vol. 31, pp. 1123–1124.
1934b. Experiments on early developing stages of *Fundulus*. Proc. Natl. Acad. Sci., Washington, vol. 20, pp. 536–538.
1935. Processes of localization in developing *Fundulus*. *Ibid.*, vol. 21, pp. 551–553.
1936a. The development of isolated blastoderms of *Fundulus heteroclitus*. Jour. Exp. Zool., vol. 72, pp. 247–269.
1936b. Transplantation experiments on developing teleosts (*Fundulus* and *Perca*). *Ibid.*, vol. 72, pp. 409–437.
1936c. Processes of localization in developing *Fundulus*. *Ibid.*, vol. 73, pp. 405–444.
1937. The normal stages of *Fundulus heteroclitus*. Anat. Rec., vol. 68, pp. 1–15.
1938. Potencies for differentiation in the teleostean germ-ring. Jour. Exp. Zool., vol. 79, pp. 185–212.
1947. Organization of the teleost blastoderm. Quart. Rev. Biol., vol. 22, pp. 105–118.

PASTEELS, J.
1933. La gastrulation et la répartition des territoires dans la moitié dorsal du blastodisque de truite (*Salmo iridaeus*). Comp. Rendus Soc. Biol. Paris., vol. 113, pp. 425–428.
1934. Répartition des territoires et mouvements morphogénétiques de la gastrulation de l'oeuf de truite (*Salmo iridaeus*). Comp. Rendus Assoc. Anat. Bruxelles, pp. 451–458.
1936. Études sur la gastrulation des vertébrés méroblastiques. I. Téléostéens. Arch. Biol., vol. 47, pp. 205–308.

PRICE, J. W.
1934a. The embryology of the whitefish, *Coregonus clupeaformis* (Mitchell). Part I. Ohio Jour. Sci., vol. 34, pp. 287–305.
1934b. The embryology of the whitefish, *Coregonus clupeaformis* (Mitchell). Part II. Organogenesis. *Ibid.*, vol. 34, pp. 399–414.

PURSER, G. L.
1938. Reproduction in *Lebistes reticulatus*. Quart. Jour. Micro. Sci., vol. 81, pp. 150–158.

ROGICK, M. D.
1931. Studies on the comparative histology of the digestive tube of certain teleost fishes. II. A minnow (*Campostoma anomalum*). Jour. Morph. Physiol., vol. 52, pp. 1–25.

RUGH, ROBERTS
1941. Experimental embryology; a manual of techniques and procedures. New York, New York University.
1943. The neurenteric canal in the frog, *Rana pipiens*. Proc. Soc. Exp. Biol. Med., vol. 52, pp. 304–307.

RYDER, J. A.
1882. Structure and ovarian incubation of

Gambusia patruelis, a top-minnow. Amer. Nat., vol. 16, pp. 109–118.

SAYLES, L. P.
1938. Manual for comparative anatomy. New York, The Macmillan Co.

SCRIMSHAW, N. S.
1944a. Superfetation in poeciliid fishes. Copeia, pp. 180–183.
1944b. Embryonic growth in the viviparous poeciliid fish, *Heterandria formosa*. Biol. Bull., vol. 87, pp. 37–51.
1945. Embryonic development in poeciliid fishes. *Ibid.*, vol. 88, pp. 233–246.

SIMPSON, G. G., AND A. ROE
1939. Quantitative zoology. New York, McGraw-Hill Book Co.

SUMNER, F. B.
1904. A study of early fish development. Arch. Entwmech. Organ., vol. 17, pp. 92–149.

TAVOLGA, M. C.
[In press.] Differential effects of estradiol, estradiol benzoate, and pregneninolone on *Platypoecilus maculatus*. Zoologica.

TAVOLGA, W. N., AND R. RUGH
1947. Development of the platyfish, *Platypoecilus maculatus*. Zoologica, vol. 32, pp. 1–15.

TURNER, C. L.
1937. Reproductive cycle and superfoetation in poeciliid fishes. Biol. Bull., vol. 72, pp. 145–164.
1940. Pseudoamnion, pseudochorion, follicular pseudoplacenta in poeciliid fishes. Jour. Morph., vol. 67, pp. 59–89.

VAN OÖRDT, G. J.
1928. The duration of life of the spermatozoa in the fertilized female of *Xiphophorus hellerii* Regan. Tijdschr. Nederlandsche Dierkund. Vereen., ser. 3, vol. 1, pp. 77–80.

WILSON, H. V.
1889. The embryology of the sea bass (*Serranus atrarius*). Bull. U. S. Fish Comm., vol. 9, pp. 209–277.

WINGE, Ö.
1922. A peculiar mode of inheritance and its cytological explanation. Jour. Genetics, vol. 12, pp. 137–144.

WOLF, L. E.
1931. The history of germ cells in the viviparous teleost *Platypoecilus maculatus*. Jour. Morph. Physiol., vol. 52, pp. 115–153.